Lithium Complexes of Ketoimines and Novel Alkynyl Imines and Diimines: Discoveries in the Attempted Synthesis of PacNac

TWYLA MAE GIETZ
B.Sc. University of Lethbridge, 2006

A Thesis
Submitted to the School of Graduate Studies
of the University of Lethbridge
in Partial Fulfillment of the
Requirements for the Degree

MASTER OF SCIENCE

Chemistry and Biochemistry
University of Lethbridge
LETHBRIDGE, ALBERTA, CANADA

To the Magnificent Mysteries of God's Creation

Abstract

Two different methodologies were used to attempt the synthesis of a novel P-N ligand, denoted as PACNAC for the similarity to the analogous NACNAC and ACAC ligands. Although the synthesis of PACNAC was not successful, each methodology led to interesting discoveries. First, a number of lithium complexes of ketoimines were isolated and studied by X-ray crystallography and NMR spectroscopy revealing some interesting substituent based effects on the structure, solubility and solution state behaviour. The X-ray data of the two known and two related novel ketoimines were also collected and compared to the lithium complexes. Secondly, the synthesis of novel alkynyl imines along with the new alkynyl diimines by novel synthetic routes and studied by x-ray crystallography, NMR, electrochemistry, and UV-Visible spectra.

Acknowledgements

Without the support of a variety of people, within the lab and outside the lab, the completion of this research and thesis would not have been possible.

First of all, my supervisor, Rene Boeré, for the ideas which served as the jump-off point for this research, for the assistance that I required in the progress of the work that I could rely on whenever I needed an outside view, for teaching me the techniques and the equipment such as the x-ray machine so that I could fully perform my own research, and for the financial assistance which allowed me to research with little financial worry.

My office mate and fellow graduate student, Tracey Roemmele, for the general insights and sympathy for the difficulties, and for sharing in the joys that come as a part of the unique experience of being a graduate student in synthetic chemistry; also for her help in performing the electrochemistry portion of this research, both with the experiments and the analysis. Tracey's friendship, in general, has also been a great blessing in the completion of my program.

Fellow group member, Elizabeth Baker for her synthesis of some of my precursor materials during some late stages of the research, certainly helped me to be able to focus my energy on the emerging portions of the research as well as for her friendship. Other people, some that were around for the duration of the research, others which have already moved on, for their friendship, distraction, and sometimes help with the research: Maria Ksiazek (former Boeré Group member), Jared Nieboer (MSc with Michael Gerken), Steve Robbins (MSc with Peter Dibble), Dave Franz (PhD with Peter Dibble), Jennifer Przybylski (MSc with Stacey Wetmore – special mention for being my computational chemistry consultant), Karinna Yu (former Boeré Group member, most recently worked with Michael Gerken), and Ben Ireland (MSc with Paul Hayes). Kevin Johnson (MSc with Paul Hayes) was very helpful with the mass spectrometer, by teaching me to run my samples and giving me help whenever I ran into any difficulties. Craig

Wheaton (PhD with Paul Hayes) for running my samples for elemental analyses. My committee members, Michael Gerken and Ken Vos, who made the semester-ly committee meetings helpful and surprisingly enjoyable also deserve much thanks.

Many family members and friends from outside the university community also deserve much thanks for the variety of support of my life in general that they have provided: my parents Dwayne and Karolyn Gietz (who I am very thankful to still have around – one of God's big miracles in my life), my brother Merlin, my husband Scott Ellis, and my best friends Sandra Hirsche and Sarah Paquette (latter also a fellow MSc student in Biology). More recently, my curling team in the Monday Ladies have provided me with a much needed distraction from the stress of writing and an escape from science in general. The graduate students bible study which was started up Fall 2008 by IVCF has also been a great help in reconnecting myself to my spiritual beliefs and has given me much strength towards the end of my program. Thanks to Dave McMurray, Gail McKenzie, and Lindsay Wichers for the thoughtful discussion and encouraging ideas that have been a great part of that experience.

I also wish to thank all those whose prayers were heard and answered, for the praying I did not know how to do, when I was at risk of losing both my parents much too early from cancer (both) and heart disease (Dad).

Thanks also to all those who have encouraged me to come back after taking leave for the reason mentioned above. It was more difficult than most could ever understand.

Table of Contents

List of Tables

List of Figures

List of Schemes

List of Abbreviations

Abs – absorbance

AcAc – acetylacetonate

AIBN – azobisisobutyronitrile

Bn – benzyl

Bt – benzotriazolyl

Bu – butyl

CVD – chemical vapor deposition

CV – cyclic voltammogram

Cod – 1,5-cyclooctadiene

Dba – dibenzylideneacetone

DBU – 1,8-diazabicyclo[5.4.0]undec-7-ene

DFT – density functional theory

Dipp – 2,6-diisopropylphenyl

DMF – dimethylformamide

DMSO – dimethyl sulfoxide

Dppe – 1,2-bis(diphenylphosphino)ethane

Et – ethyl

GC – glassy carbon

Hmpa – hexamethylphosphoramide

HOMO – highest occupied molecular orbital

IR – infrared

iPr – isopropyl

LDA – lithium diisopropylamide

LiTMP – lithium 2,2,6,6-tetramethylpiperidine

LUMO – lowest unoccupied molecular orbital

Me - methyl

Mes or **Mesityl** – 2,4,6-trimethylphenyl

MeOH – methanol

MO – molecular orbital

Min – minutes

NacNac – β-diketoimidate

NMR – nuclear magnetic resonance

OAc – acetate

Ph – phenyl

PMP – p-methoxyphenyl

Py - pyridine

Super-mesityl – 2,4,6-tris-t-butylphenyl

Tbaf – tetra-n-butylammonium fluoride

t-boc – N-t-butoxycarbonyl

t-Bu – tert-butyl

Tbt – 2,4,6-tris[bis)trimethylsilyl)methyl]-phenyl

TD-DFT – time dependent DFT

Tf – trifluoromethane sulfonate

TFA – trifluoroacetic acid

THF – tetrahydrofuran

TMS - trimethylsilane

TMSTf – trimethylsilyltrifluoromethane sulfonate

Tol – tolyl

UV/Vis – ultraviolet/Visible

VT – variable temperature

Compound Numbering Scheme

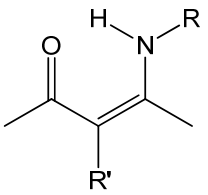

1a-d

a : R = Dipp, R' = H
b : R = Mes, R' = H
c : R = Dipp, R' = Me
d : R = Mes, R' = Me

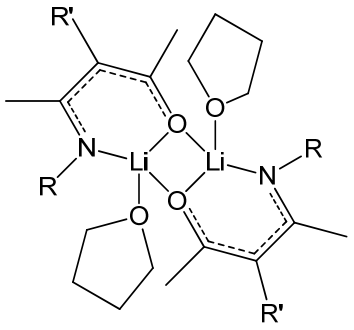

2a-c

a : R = Dipp, R' = H
b : R = Mes, R' = H
c : R = Dipp, R' = Me
d : R = Mes, R' = Me

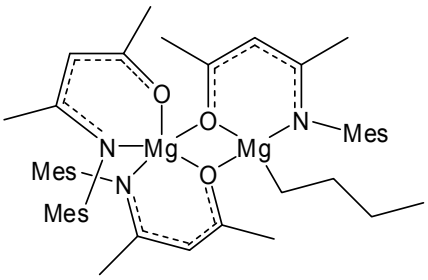

3b

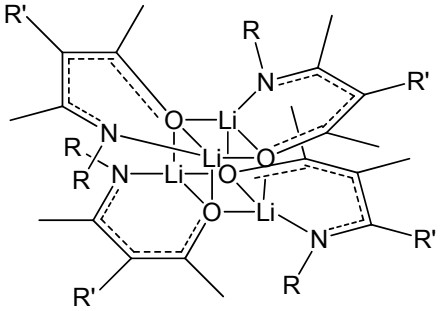

4a-d

a : R = Dipp, R' = H
b : R = Mes, R' = H
c : R = Dipp, R' = Me
d : R = Mes, R' = Me

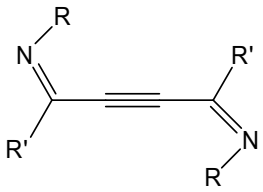

5a : R = Ph, R' = t-Bu
5b : R = Dipp, R' = p-Tol

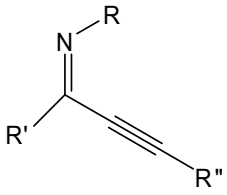

6a: R = Ph, R' = t-Bu, R" = $SiMe_3$
6b: R = Dipp, R' = p-Tol, R" = $SiMe_3$
7a: R = Ph, R' = t-Bu, R" = H
7b: R = Dipp, R' = p-Tol, R" = H

Chapter 1

Summary of the Work

1.1 Introduction

The bidentate ligands, acetylacetonate **A-1** (AcAc) and β-diketoiminate **B-1** (NacNac) and several variations thereof have been used extensively in coordination chemistry and catalysis, historically and to this date.[1,2] More recently the mixed oxygen and nitrogen analogue, β-ketoiminate ligand **C-1,** has joined the above two in such research interest.[3] In the first year of work on this project, the first examples of the β-ketophosphenato ligand **D-1** and their rhodium complexes were reported by Sasamori et al.[4] This opens the frontier of two other analogues using O, N, and P as bidentate coordination points to metals: N, P (which we have coined as PacNac) **E-1** and P, P **F-1** (Figure 1.1). The original goal of this thesis work was to isolate the first example of **E-1** as the free molecule and as a ligand to a metal. A PacNac ligand generated in situ on Ti from a NacNac ligand by phospha-Staudinger and phosphaalkene-insertion reactions has previously been reported.[5]

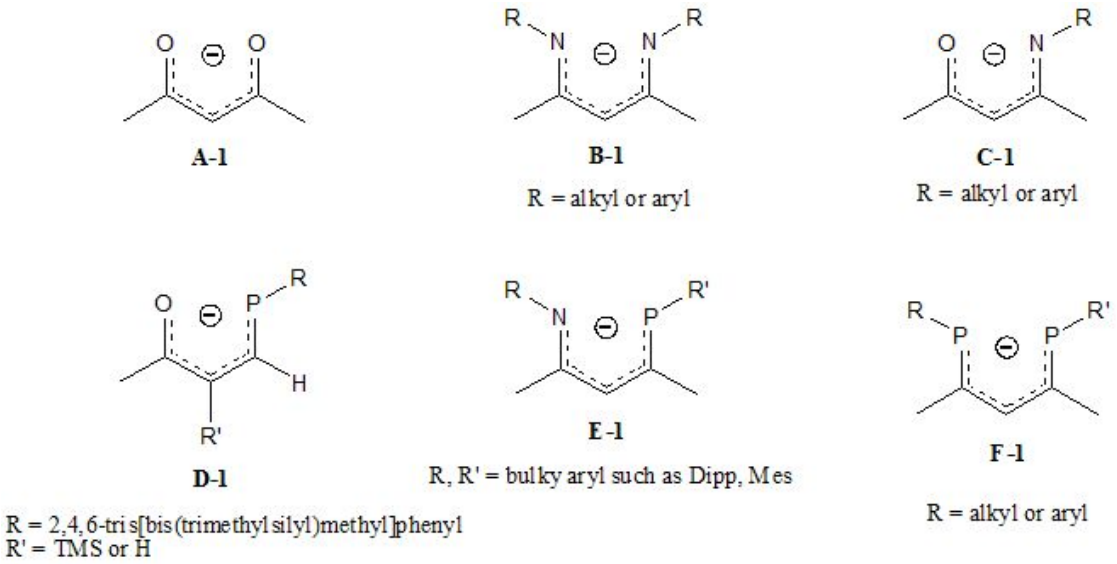

Figure 1.1 - Various analogous bidentate ligands containing O, N, and P.

A couple of other goals which branched off of each of the main routes to PacNac, which are discussed below, were introduced in the progress of the work. One was to isolate and fully characterize some s-block metal complexes of β-ketoiminate ligands because, although known and used as intermediates in several reactions in transition metal coordination chemistry,[6] few have been studied in depth themselves (see Chapter 2 for discussion of examples).[7] As well, the crystal structures of the particular β-ketoimines of interest, which are solids, had not been previously reported, and therefore were also of interest.

This chapter will briefly summarize the ideas and background literature to the research performed for this thesis. More extensive literature background will be discussed later along with the results in the respective chapters dealing with each area of the research.

1.2 Why PacNac?

NacNac acts as a monoanionic spectator ligand much like its closely related analogues, AcAc and ketoiminate. NacNac strongly binds to metals and has more extensive tunability and more extensive steric demands than ketoiminate by virtue of containing two imino groups with substituents that can be varied (whereas ketoiminate ligands only have one and AcAc cannot be tuned in this manner and does not have the any of the steric protecting properties). NacNac is therefore able to stabilize metals in unusually low oxidation states, rare geometries, and low coordination numbers better than the other two analogues. Such complexes are coordinatively unsaturated which is one of the keys to how well they function as catalysts in a variety of processes such as olefin- and oligio- polymerization and copolymerization and ring opening polymerization.[8] Ketoiminate complexes have only been found to function well in olefin polymerization although some research has gone into other areas.[9]

PacNac as a potential ligand retains many of the desirable attributes of NacNac; strong binding, tunability, and steric demands through a substituent on the imino as well as the phosphorus. The change to phosphorus may in fact enhance the tunable nature and steric demands of the molecule with the option of having different substituents on the imino and phosphorus portions of the molecule. Phosphorus is significantly different than nitrogen as a donor atom; first of all it is a much softer Lewis base compared to nitrogen. Phosphorus is a strong σ-donor and can also be a good π-acceptor (dependent on the electron withdrawing properties of the substituent) which can allow for differing levels of back-bonding from the metal to the phosphorus atom.[10] This may lead to catalysts with much different activity in comparison with the NacNac supported catalysts. In particular, strong coordination to later transition metals and to metals of the second and third period is expected for a PacNac type ligand.

1.3 Phosphaalkene Route to PacNac

The original goal of this project was to make the direct P, N analogue of NacNac, hence the name PacNac, which meant the formation of a phosphorus-carbon double bond or in other words, a phosphaalkene **A-2**. However, the tautomer, the P, N analogue of the ketoimine or the P, O ketophosphenate, **B-2** (Figure 1.2), provides an alternate route to the same anionic ligand and will be discussed later in this chapter.

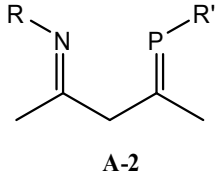

A-2

R, R' = bulky aryl such as Dipp, Mes

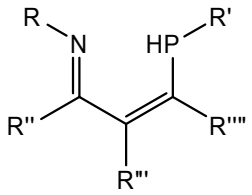

B-2

R, R' = aryl
R'' = alkyl or aryl
R''' = TMS or H
R'''' = TMS, H, or alkyl

Figure 1.2 - The two possible tautomeric molecular precursors that should give the PacNac ligand.

There are several different types of reactions that can be done to form the phosphaalkene bond. These can be broken down into a few basic different types of which there are many variations and combinations that have resulted in the detection and/or the isolation of phosphaalkenes: 1,2-elimination **A**, condensation **B**, phospha-Wittig reactions **C**, R-P transfer from phosphinidenes **D**, and double-bond migration **E** (Table 1.1).[11,12] The variations of the condensation type of reaction, in particular the phospha-Peterson reaction, done either with LiPR(TMS) **B(4)** or more rarely the base catalyzed $RP(TMS)_2$ and ketone or aldehyde substrates **B(3)**, was the most obvious of these routes to try for a few reasons. The first reason is that the disilylated phosphine of the bulky 2,6-diisopropylphenyl (dipp) and 2,4,6-tris-t-butylphenyl (super-mesityl) substituents are known compounds and had been made in the lab previously for other purposes. As well, the ketone substrate to give the desired PacNac molecule is the well known ketoimine, of which there are many well-established routes of synthesis. Lastly, the base-catalyzed phospha-Peterson reaction has been used in this group's lab to make the dipp phosphaalkene.[13] The other routes, in comparison, either require synthesis of a new substrate (many unknown and would likely take many steps) or phosphine or are limited in the phosphines that would possibly work, or some combination of the above; one of the extra difficulties here being the synthesis of the nitrogen containing part of the desired compound.

Table 1.1 - Examples of the common phosphaalkene forming reactions.

Reactions to get to: 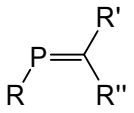

Type	Reactants	→
A	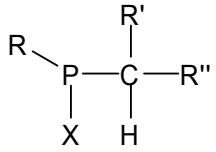	Base - HX
B	**(1)** 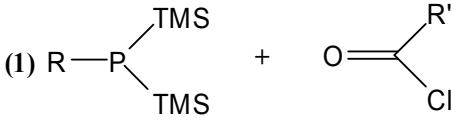	- TMSOTMS - HCl
	 R'" = H **(2)** or TMS **(3)**	- R'"$_2$O Catalyst
	(4) 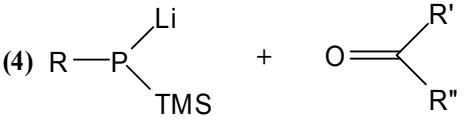	- LiOTMS
C	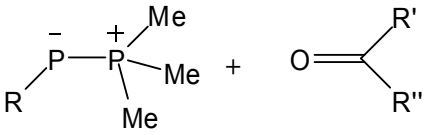	- O=PMe$_3$
D		- L$_n$M=O
E	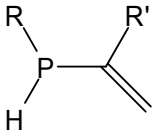	Base (cat)

The ketoimine, however, was found to be unsuitable in the phospha-Peterson reaction due to the acidic proton on the nitrogen. This proton exchanges with one of the silyl groups on the phosphine instead of the desired reaction. The t-boc (N-t-butoxycarbonyl) protecting group is a typical protecting group for the amine functional group. Therefore, attempts were made by a couple of different literature routes[14] to add it to the ketoimine but neither showed any reaction.

The alternate condensation reaction **B(2)** was also attempted with both the dipp and super-mesityl phosphines using $BF_3{\cdot}Et_2O$ as the catalyst as done in the literature.[15] This reaction was successful for super-mesitylphosphine and select ketones in the literature. Disappointingly, no reaction was observed with the ketoimine. Further reading in the literature revealed that this is likely due to the ketoimine not being a reactive enough ketone.[16] In fact, all of the phosphaalkene forming reactions from a ketone precursor are unlikely to produce the desired result with a ketoimine because ketoimines rarely react as other ketones do.[17] The phosphaalkene approach therefore really requires a different type of approach which will be discussed in detail in Chapter 4 – Future Work.

The focus changed at this point to the lithium ketoimine research, discussed further in the next section and in detail in Chapter 2. That was until reading about the recently published ketophosphenate, which gave an alternate route to give an equivalent ligand on the metal which will be introduced in section 1.4 and the results discussed in detail in Chapter 3.[4]

1.4 Bulky Ketoimines and their Main-Group Metal Complexes

During the course of the work, when difficulties with the ketoimine reactivity arose for the original phosphaalkene forming reactions, it became desirable to find alternative methods to reach the goal while still making use of the ketoimine. Through this, it was discovered that,

although transition metal complexes of ketoimines have seen considerable recent interest, the main group complexes, especially of the s-block, have been mostly neglected except for their use as a stepping stone to the transition metal complexes.[6] Therefore, it seemed a worthy pursuit to attempt the isolation and study of a large variety of such complexes.

As well, to eliminate one of the potentially problematic acidic protons on the ketoimine, the new compounds, **1c,d**, with a methyl group on the central backbone carbon (Figure 1.3) were made.[†] These and the other two ketoimines employed in this work, are fairly crystalline solids. Therefore, along with the main-group metal complexes, the crystal structures of these compounds were determined through the use of X-ray crystallography.

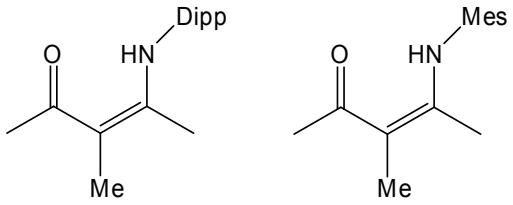

1c **1d**

Figure 1.3 - Newer ketoimines with methyl on the carbon backbone.

One interesting and unexpected result was the unsolvated lithium tetramer isolated for one of the ketoimines in the presence of 3 molar equivalents of the coordinating solvent THF. Although tetramers are known in the literature, with 59 lithium cubane structures reported containing the central lithium-oxygen cube, only 19 of those have nitrogen bonded to the lithium as well. Only one of those 19 is a ketoimine complex, **A-3**, which was isolated by excluding any coordinating solvent from the reaction and crystallization process[7] (Figure 1.4).

Following this result, the other three cubane lithium tetramers of the ketoimines **1a-c** were made and isolated in analogy to the literature synthesis reported for **A-3**.[7] Of these, two

[†] During the preparation of this thesis, **1c** was reported as a ligand on Al and Ti.[18] The lithium complex of **1c** was reportedly used as an intermediate in the latter case. The synthesis, X-ray crystal structures, and ^{1}H NMR data presented in this thesis was presented at the CSC prior to either of these being published.[19]

gave suitable crystals for X-ray data to be collected. The similarities and differences between the three structures and the literature structure will be thoroughly discussed in Chapter 2.

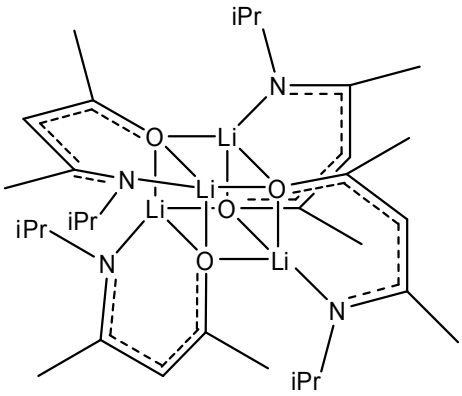

A-3

Figure 1.4 – The only previously reported cubane lithium structure of a ketoimine ligand.

1.5 The Iminophosphenate Route to PacNac

As briefly mentioned in section 1.2, there is an alternate class of potential precursors to the PacNac ligand, the iminophosphenate tautomer, or more specifically (E)-N-((Z)-4-(arylphosphino)-3-(trimethylsilylbut-3-en-2-ylidene)arylamine . There is reason to believe that the alternate desired tautomer, containing a doubly-bonded N and a singly bonded PH, could be synthesized similarly to the ketophosphenate that has been reported (Scheme 1.1).[4]

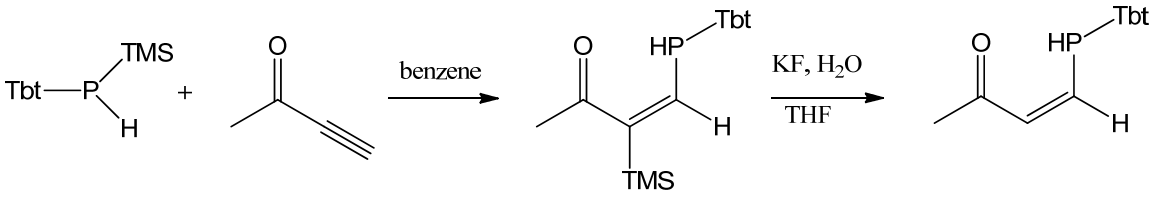

Tbt = 2,4,6-tris[bis(trimethylsilyl)methyl]phenyl

Scheme 1.1 - The synthesis of the two reported ketophosphenates.

Initial searches through the literature revealed the imino alkyne **A-4** as the closest analogue of the substrate required for this synthetic route[20] (Figure 1.5). The exact analogue

desired was 3-(dippimino)but-1-yne, which changes only the keto portion of 3-butyn-2-one to an aryl imine in the above reaction scheme.

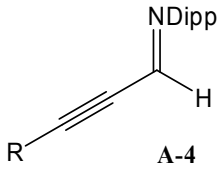

A-4

R = a variety of alkyl and aryl groups

Figure 1.5 - The closest nitrogen analogue in the literature to 3-butyn-2-one.

Better analogues do in fact exist in the literature,[21] which is a fact discovered after working through the problem of the synthesis successfully. It was first hypothesized that the imidoyl chlorides previously isolated in our lab[22] could be used in a one-step reaction with a metal acetylide to make the exact substrate analogue to react with the mono-silylated phosphine[23] (Scheme 1.2).

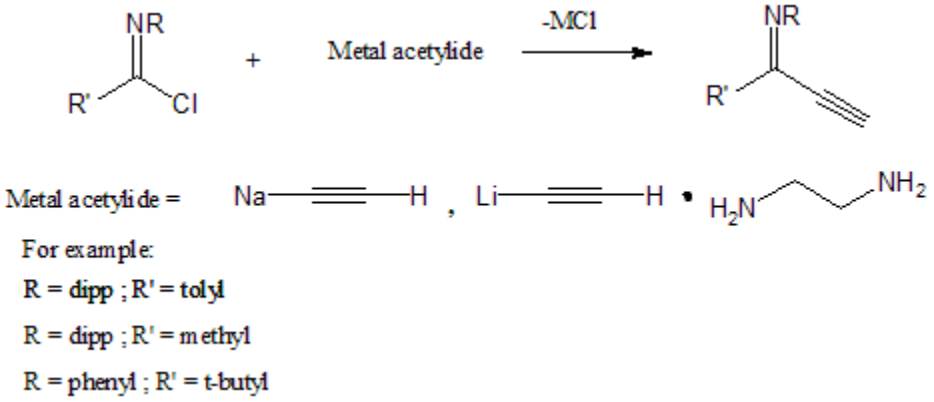

Scheme 1.2 - Metal acetylide synthesis of the nitrogen analogue of 3-butyn-2-one.

This proposed reaction instead resulted in the isolation of alkynyl diimines (Figure 1.6), which, to the best of our knowledge are a novel type of species.

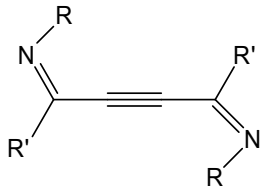

5a : R = Ph, R' = t-Bu
5b : R = Dipp, R' = p-Tol

Figure 1.6 – Novel alkynyl diimines isolated in the attempted synthesis of alkynyl imines.

An alternate scheme where the imidoyl chlorides could be reacted with bis(trimethylsilyl)acetylene and the silylated end of the alkyne removed to get the exact substrate, which is a well-established route with acid chlorides[24] (Scheme 1.3), was then attempted and was successful for R = Dipp and R′ = p-tolyl, of which both alkynyl imines are novel species, though not a novel class of species as thought initially.

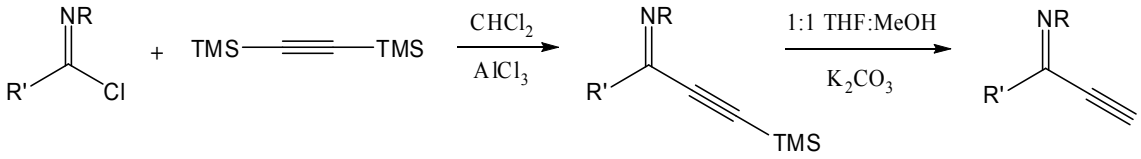

Scheme 1.3 - Synthesis of the exact analogue based on literature for acid chlorides.

The reaction conditions used to produce the ketophosphenate ligand did not in the case of the reaction of either alkynyl imine result in the desired iminophosphenate ligand.

1.6 Organization of the Thesis

The remainder of the thesis is organized as follows: Chapter 2 presents the synthesis, structure and spectroscopic characterization of ketoimines and main-group ketoiminates. Chapter 3 presents the work done on the alkynyl imines and diimines, Chapter 4 presents suggestions for ways in which the synthesis of a PacNac ligand might alternatively be achieved, and lastly Chapter 5 covers the experimental details.

References

1. For example (AcAc): a. Tonzetich, Z.J.; Jiang, A.J.; Schrock, R.R.; Muller, P. *Organometallics* **2006,** *25*, 4725. b. Schade, M.A.; Metzger, A.; Hug, S.; Knochel, P. *Chem. Commun.* **2008**, 3046.

2. For example (NacNac): a. Basuli, F.; Tomaszewski, J.; Huffman, J.C.; Mindiola, D.J. *Organometallics* **2003**, *22*, 4705. b. Bai, G.; Stephan, D.W. *Angew. Chem. Int. Ed.* **2007**, *46*, 1856.

3. For example: a. Cho, M.H.; Yoon, J.S.; Lee, I.M. *Bull. Korean Chem. Soc.* **2007,** *28*, 2471. b. Wang, L.Y.; Wu, Q. *Eur. Polym. J.* **2007,** *43*, 3970. c. Lee, D.H.; Cho, M.H.; Kwon, I.H.; Jun, I.C.; Lee, I.M.; Jin, M.J. *Catal. Commun.* **2008,** *9*, 1517. d. Lim, S.W.; Lee, J.C.; Shon, D.S.; Lee, W.I.; Lee, I.M. *Chem. Mater.* **2002,** *14*, 1548. e. Lim, S.W.; Choi, B.; Min, Y.S.; Lee, S.S. *J. Organomet. Chem.* **2004,** *689*, 224.

4. Sasamori, T.; Matsumoto, T.; Takeda, N.; Tokitoh, N. *Organometallics* **2007,** *26*, 3621.

5. Basuli, F.; Tomaszewski, J.; Huffman, J.C.; Mindiola, D.J. *J. Am. Chem. Soc.* **2003**, *125*, 10170.

6. For example: a. Jones, D.; Roberts, A.; Cavell, K.; Keim, W.; Englert, U.; Skelton, B.; White, A. *J. Chem. Soc., Dalton Trans.* **1998**, 255. b. Hsu, S.; Chang, J.; Lai, C.; Hu, C.; Lee, H.M.; Lee, G.; Peng, S.; Huang, J. *Inorg. Chem.* **2004**, *43*, 6786.

7. Brehon, M.; Cope, E.K.; Mair, F.S.; Nolan, P.; O'Brien, J.E.; Pritchard, R.G.; Wilcock, D.J. *J. Chem. Soc., Dalton Trans.* **1997**, 3421.

8. For example: a. Bourget-Merle, L.; Lappert, M.F.; Severn, J.R. *Chem. Rev.* **2002**, *102*, 3031; b. Gushwa, A.F.; Richards, A.F. *Eur. J. Inorg. Chem.* **2008**, 728; c. Spielmann, J.; Harder, S. *Eur. J. Inorg. Chem.* **2008**, 1480; d. Hadzovic, A.; Song, D. *Organometallics* **2008**, *27*, 1290; e. Prust, J.; Most, K.; Müller, I.; Stasch, A.; Roesky, H.W.; Usón, I. *Eur. J. Inorg. Chem.* **2001**, 1613; f. Prust, J.; Stasch, A.; Zheng, W.; Roesky, H.W.; Alexopoulos, E.; Usón, I.; Böhler, D.; Schuchardt, T. *Organometallics* **2001**, *20*, 3825; g. Prust, J.; Most, K.; Müller, I.; Alexopoulos, E.; Stasch, A.; Usón, I.; Roesky, H.W. *Z. Anorg. Allg. Chem.* **2001**, *627*, 2032; h. Hayton, T.W.; Wu, G. *J. Am. Chem. Soc.* **2008**, *130*, 2005; i. Tsai, Y.-C.; Wang, P.-Y.; Lin, K.-M.; Chen, S.-A.; Chen, J.-M. *Chem. Commun.* **2008**, 205; j. Lyashenko, G.; Herbst-Irmer, R.; Jancik, V.; Pal, A.; Mösch-Zanetti, N.C. *Inorg. Chem.* **2008**, *47*, 113.

9. For example: a. Cho, M.H.; Yoon, J.S.; Lee, I.M. *Bull. Korean Chem. Soc.* **2007**, *28*, 2471; b. Wang, L.Y.; Wu, Q. *Eur. Polym. J.* **2007,** *43*, 3970; c. Jones, D.; Roberts, A.; Cavell, K.; Keim, W.; Englert, U.; Skelton, B.W.; White, A.H. *J. Chem. Soc., Dalton Trans.* **1998,** 255; d. Kim, J.; Hwang, J.-W.; Kim, Y.; Lee, M.H.; Han, Y.; Do, Y. *J. Organomet. Chem.* **2001,** *686*, 1; e. He, X.; Yao, Y.; Luo, X.; Zhang, J.; Liu, Y.; Zhang, L.; Wu, Q. *Organometallics* **2003,** *22*, 4952; f. Chen, Y.; Wu, G.; Bazan, G.C. *Angew. Chem. Int. Ed.* **2005,** *44*, 1108; g. Yu, R.-C.; Hung, C.-H.; Huang, J.-H.; Lee, H.-Y.; Chen, J.-T. *Inorg. Chem.* **2002,** *41*, 6450; h. Lee, W.-Y.; Hsieh, H.-H.; Hsieh, C.-C.; Lee, H.M.; Lee, G.-H.; Huang, J.-H.; Wu, T.-C.; Chuang, S.-H. *J. Organomet. Chem.* **2007,** *692*, 1131; i. He, X.; Chen, Y.; Liu, Y.; Yu, S.; Hong, S.; Wu, Q. *J. Polym. Sci.* **2007,** *45*, 4733; j. Yu, S.; He, X.; Chen, Y.; Liu, Y.; Hong, S.; Wu, Q. *J. Appl. Polym. Sci.* **2007,** *113*, 500; k. Lee, D.-H.; Cho, M.-H.; Kwon, I.-H.; Jun, I.-C.; Lee, I.-M.; Jin, M.-J. *Catal. Commun.* **2008,** *9*, 1517; l. Sachse, A.; Mösch-Zanetti, N.C.; Lyashenko, G.; Wielandt, J.W.; Most, K.; Magull, J.;

Dall'Antonia, F.; Pal, A.; Herbst-Irmer, R. *Inorg. Chem.* **2007,** *46,* 7129; m. Xue, F.; Cai, C.; Sun, H.; Shen, Q.; Rui, J. *Tetrahedron Lett.* **2008,** *49,* 4386.

10. Spessard, G.O.; Miessler, G.L. *Organometallic Chemistry.* Upper Saddle River, New Jersey : Prentice Hall, **1997**.

11. Dillon, K.B.; Mathey, F.; Nixon, J.F. *Phosphorus: The Carbon Copy.* John Wiley & Sons Ltd.: Chichester, West Sussex, England, **1998,** 88-96.

12. Yam, M.; Chong, J.H.; Tsang, C.W.; Patrick, B.O.; Lam, A.E.; Gates, D.P. *Inorg. Chem.* **2006,** *45,* 5225.

13. Boeré, R.T.; Masuda, J.D.; Groeneweg, S. Unpublished results.

14. a. Nikolic, N.A.; Beak, P. *Org. Syn.* **1998,** *9,* 391; b. Williams, R.M.; Sinclair, P.J.; DeMong, D.E.; Chen, D.; Zhai, D. *Org. Syn.* **2003,** *14,* 18.

15. Romanenko, V.D.; Ruban, A.V.; Povolotskii, M.I.; Polyachenko, L.K.; Markovskii, L.N. *J. Gen. Chem. USSR.* **1986,** *56,* 1044.

16. Romanenko, V.D.; Ruban, A.V; Chernega, A.N.; Povolotskii, M.I.; Antipin, M.Y.; Struchkov, Y.T.; Markovskii, L.N. *J. Gen. Chem. USSR***. 1989,** *59,* 1528.

17. Greenhill, J.V. *Chem. Soc. Rev.* **1977,** *6,* 277.

18. a. Liu, B.Y.; Li, H.Q.; Ha, C.S.; Kim, I.; Yan, W.D. *Macromolecular Research* **2008**, *16,* 441; b. Lesikar, L.A.; Gushwa, A.F.; Richards, A.F. *J. Organomet. Chem.* **2008**, *693,* 3245.

19. Gietz, T.; Boeré, R.T. *Main Group Complexes of Ketoimines* **2008, May.** Poster presented at the 91st Canadian Chemistry Conference and Exhibition, Edmonton, AB.

20. Komeyama, K.; Sasayama, D.; Kawabata, T.; Takehira, K.; Takaki, K. *J. Org. Chem.* **2005,** *70,* 10679.

21. For example: a. Movassaghi, M.; Hill, M.D. *J. Am. Chem. Soc.* **2006,** *128,* 4592; b. Dong, Q.-L.; Liu, G.-S.; Zhou, H.-B.; Chen, L. Yao, Z.-J. *Tetrahedron Lett.* **2008,** *49,* 1636.

22. Boeré, R.T.; Klassen, V.; Wolmershauser, G. *J. Chem. Soc., Dalton Trans.* **1998,** 4147.

23. Daiss, J.O.; Burschka, C.; Mills, J.S.; Montana, J.G.; Showell, G.A.; Fleming, I.; Gaudon, C.; Ivanova, D.; Gronemeyer, H.; Tacke, R. *Organometallics* **2005**, *24,* 3192.

24. Morisaki, Y.; Luu, T., Tykwinski, R.R. *Org. Lett.* **2006,** *11,* 689.

Chapter 2

Bulky Ketoimines and their Main-Group Complexes

2.1 Introduction

Transition metal complexes of β-ketoimines have received considerable of recent interest in coordination chemistry and catalysis. The use of these as catalysts have been largely limited to olefin polymerization,[1] although some research has been done into other types of reactions,[2] and in general metal complexes of β-ketoimines have been widely used as precursors for metalloorganic chemical vapor depositition (CVD).[3] Many of the main group metal complexes have not been studied, however. The primary exception to this is aluminum, for which many β-ketoimine complexes have been reported.[4] A few magnesium complexes have also been studied with particular interest in their use as CVD precursors.[5] Other main group complexes such as lithium, sodium, and potassium have been used as intermediates in the synthesis of transition metal complexes,[6] but largely have not been reported as isolated species.

The exception to this is the coodinated dimer and cubane structures of 4-isopropylaminopent-3-ene-2-one complexes which were reported by Brehon et al.[7] Of particular interest is the oxygen/lithium cubane structure which was synthesized and recrystallized excluding coordinating solvent and the coodinated dimer structure which was obtained from the addition of one molar equivalent of the coordinating solvent hexamethylphosphoramide (hmpa). There are only 59 such cubane lithium structures in the Cambridge Crystallographic Database,[8] and only 19 of those have nitrogen coordinated to lithium. The cubane complex of 4-isopropylaminopent-3-en-2-one is the only cubane β-ketoimine complex among those 19.

Many of the less sterically bulky β-ketoimines are liquid in form at room temperature. However, the bulky 2,6-diisopropylphenyl (dipp) **1a** and 2,4,6-trimethylphenyl (mesityl) **1b** β-

ketoimines are crystalline solids which have not had crystal structures reported. The novel β-ketoimines – 2-dipp-3-methylpent-2-en-4-one **1c** and 2-mesityl-3-methylpent-2-en-4-one **1d** - are likewise crystalline solids of interest particularly in comparison with the unsubstituted β-ketoimines because ketoimines with R′≠H are rare in the literature.

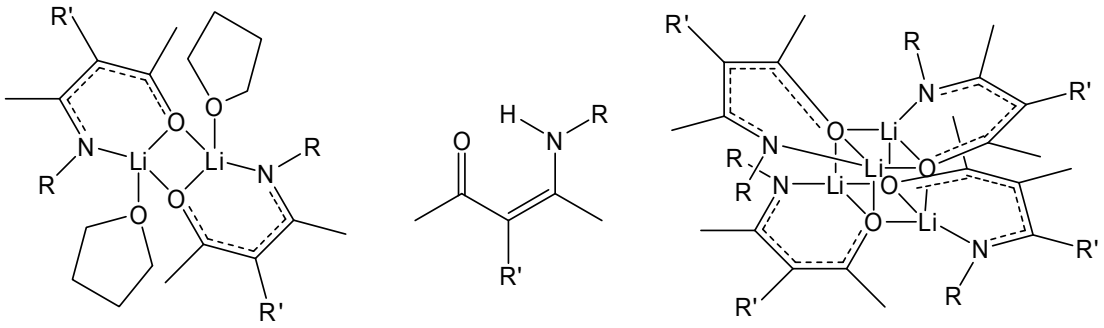

2a-c **1a-d** **4a-d**

a : R = Dipp, R' = H; b : R = Mes, R' = H; c : R = Dipp, R' = Me; d : R = Mes, R' = Me

Figure 2.1 – The ketoimines and their lithium complexes to be discussed in this chapter.

Some main group metal complexes of all four ligands were therefore made and are compared in this chapter. The crystal structures of all the β-ketoimines and the complexes were determined, along with the NMR of all the newly isolated species. All of the molecules are shown in Figure 2.1. Of particular interest is the lithium cubane structure (**4d**) of **1d** which, although synthesized in THF the same as the other lithium complexes, was recrystallized from heptane and 3 molar equivalents of THF because it was much too soluble in THF alone to yield crystals. The fact that **1d** prefers the cubane structure over the THF coordinated dimer structure is of great interest and DFT calculations were performed in an attempt to explain the preference.

2.1.1 Tautomers of Ketoimines

Ketoimines could theoretically exist in three different tautomers: enol **A-5**, enamine **B-5**, and ketimine **C-5** (Figure 2.2). This has been a primary question of interest in the literature since 1949 and as recently as 2007 a paper was published on the subject.[9] The evidence that ketoimines primarily exist in the enamine form – whether in gas, solution, liquid, or solid phase – has become overwhelming and it has become largely accepted that this is the case.

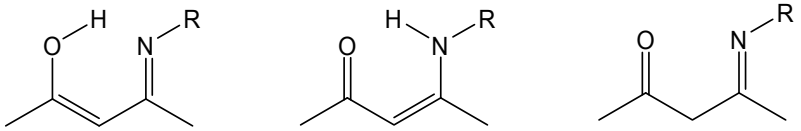

A-5 **B-5** **C-5**

Figure 2.2 – The tautomers of the ketoimines.

Initial studies of this subject in the literature looked at the ultraviolet and IR spectra of these types of compounds for clues as to the tautomeric composition. In 1949, Cromwell et al. showed that the ultraviolet absorption maximum was consistent with that of other α,β-unsaturated carbonyl compounds which excludes the ketimine tautomer from consideration.[10] Although it is difficult to discern from the IR data which of the two remaining tautomers is present because of the similarity between important signals (such as the O–H or N–H),[11] a detailed comparison, also by Cromwell et al., between the spectra of ketoimines and various known structures containing the geometries of interest provided the first evidence for the enamine tautomer being the primary form.[10] This same conclusion was reached for diketoimines by Hay and Caughly in 1965 because the spectra lacked the C=N stretch which leaves the enamine form as the only viable option.[12]

A ^{1}H NMR study of numerous ketoimines in a variety of solvents was published in 1962.[13] First of all, the lack of the appropriate CH_2 signals again excludes the ketimine tautomer as a possibility. The discerning resonance here is the broadened signal that appears in the 10 – 12

ppm region which could either be the O–H or N–H of either the enol or enamine form. Analysis of the splitting of this resonance, which could only occur if the signal was in fact due to N–H (the O–H proton would not have any protons for normal 3-bond H-H coupling), gave definitive evidence that in all the solvents used, excluding acetone, the enamine tautomer is present in solution state as well as pure solid or liquid (the IR's were done as Nujol mulls or as pure liquid samples). This greater stabilization was attributed to resonance and hydrogen bonding. Other extensive ^{1}H and ^{17}O NMR studies have also shown that the enamine tautomer is preferred even if there is additional resonance stabilization in the enol form.[14]

Recent extensive calculations have been done on all possible conformers (those with and without hydrogen bonding) of parent compound 2-methylaminopent-2-en-4-one in order to study the intramolecular hydrogen bond strength and energy.[9] In comparison of the non-hydrogen bonded conformers, the enamine was found to be more stable than the ketimine by 10.33 kJ/mol, and 52.30 kJ/mol more stable than the enol form. In the hydrogen bonded case the enamine was shown to still be more stable than the enol form by 27.83 kJ/mol. Calculations were also performed in this same study on ketoimines in water. This changed the hydrogen-bond strength for each conformer with a decrease for the enamine and an increase for the enol; however, the enamine form still maintained greater stability than the enol form. In the gas phase calculations the enol form was found to have an approximately 30 kJ/mol stronger hydrogen bond than the enamine form. The findings here show that the hydrogen-bond is the lesser reason for the stability of the enamine form. The much more important reason for the stability of the enamine form was concluded in this paper to be the complete participation of the nitrogen lone pair in the π-electron resonance in the backbone of the molecule because in the enamine form the lone pair is perpendicular to the molecular plane whereas it is not in the enol form.

Finally, a number of X-Ray crystal structures of ketoimines have been determined.[15] In all cases the hydrogen atom was found to be located on the nitrogen atom with intramolecular hydrogen bonding to the oxygen atom.

2.1.2 Literature Synthesis of β-Ketoimines

The most typical and often used literature synthesis of ketoimines has been the acid catalyzed condensation reaction of a 1,3-diketone with a primary amine, most often in benzene with removal of water by the use of a Dean Stark trap. Many acids have been successful in catalyzing the reaction using this method. Some examples are: sulfuric acid[16], aluminum (III) oxide,[17] trimethylsilyl trifluoromethane sulfonate (TMSTf) (a synthon for trifluoromethylsulfonic acid upon hydrolysis),[18] formic acid,[1g] concentrated hydrochloric acid,[19] boron trifluoride etherate,[20]and acetic acid.[21] Recently, a movement towards more environmentally friendly syntheses has resulted in many more options.

Some of these routes are done under solvent-free conditions with different catalysts such as indium tribromide,[22]silica gel,[23]and $CeCl_3 \cdot 7H_2O$[24]with stirring at room temperature. Others use more environmentally friendly solvent options such as ethanol with the catalyst $NaAuCl_4$[25]or even water with silca gel[23]or $Bi(TFA)_3$[26] as catalysts or even with no catalyst at all.[27] Other more environmentally friendly routes include the use of montmorillonite K-10 as a solid support catalyst with energy added through use of domestic microwave ovens[28] or ultrasound baths. Another option that has been pursued is the reaction done with catalysis in ionic liquid.[24,29] Supported heteropoly acids, tungstophosphoric acid on silica gel and tungstosilicic acid on aluminum (III) oxide have also been effectively used in the synthesis of ketoimines from diketone and amine.

Lastly, ketoimines have also been synthesized by reaction of acylbenzotriazoles with methylated imines[30] (Scheme 2.1):

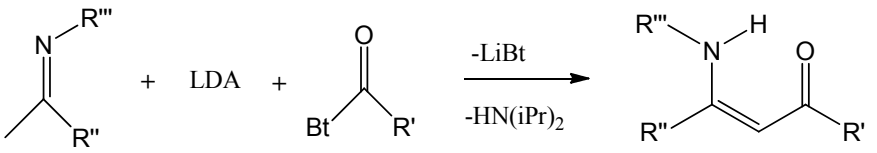

Bt = benzotriazolyl

Scheme 2.1 – Synthesis of ketoimines by reaction of acylbenzotriazoles.

2.2 Synthesis

Out of the many synthetic strategies in the literature that yield β-ketoimines, the one used for generating both the known β-ketoimines and the new β-ketoimines in this work followed the general method for the preparation of β-enamino ketones and esters presented by Zhang et al[22] using indium tribromide as a catalyst. The lithium complexes were all generated by reaction of the ketoimines with n-butyl lithium; in THF for the coordinated dimer structures and in heptane for the cubane structures (except **4d** which could be generated in either solvent with a preference for the reaction in THF) as shown in Scheme 2.2.

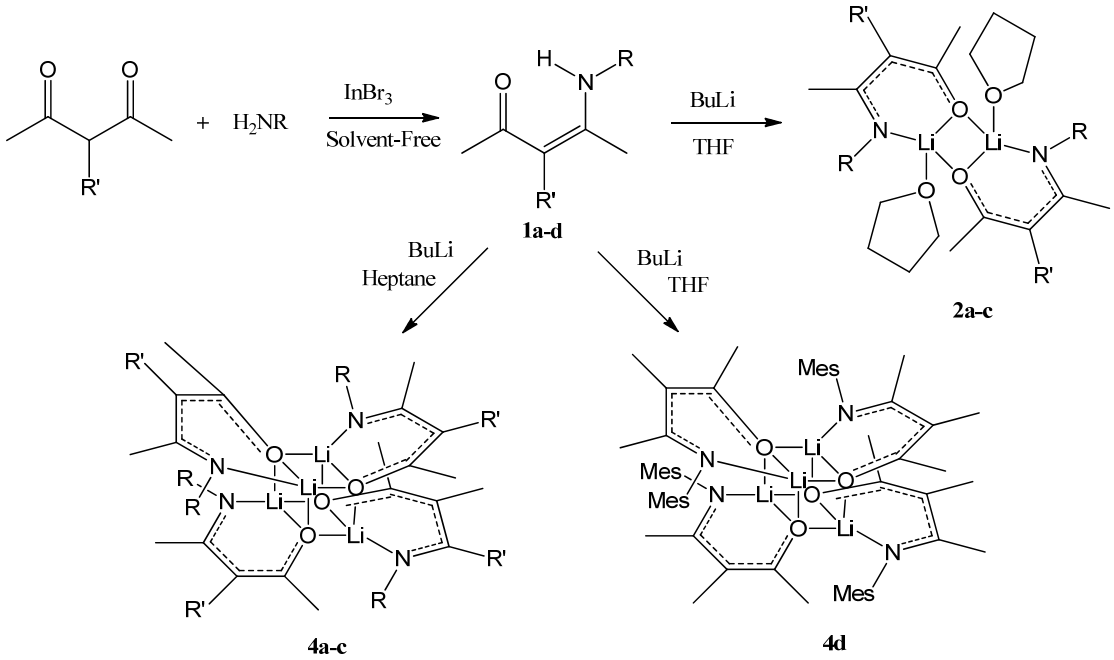

a : R = Dipp, R' = H; b : R = Mes, R' = H; c : R = Dipp, R' = Me; d : R = Mes, R' = Me

Scheme 2.2 – Synthesis of 1a-d, 2a-c, and 4a-c.

Also related and presented at the end of the chapter is a magnesium complex isolated for **1b** (Scheme 2.3). The expected product was (**1b**$^-$)$_2$Mg) but the isolated product was (**1b**$^-$)$_3$Mg$_2$Bu, which means that the intended stoichiometry of **1b**:MgBu$_2$ of 2:1 was actually 3:2. This is likely due to the concentration of the MgBu$_2$ solution being greater than the labelled 1M.

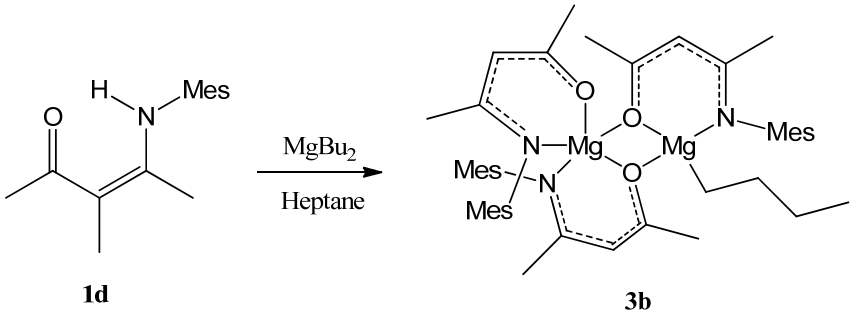

1d **3b**

Scheme 2.3 – Synthesis of 3b.

2.3 X-Ray Crystallography Results and Discussion

Ketoimines, much like the related AcAc and NacNac type compounds have more than one possible tautomeric form. The primary tautomer, at least in solution,[13] has long since been concluded to be the one where the hydrogen is located on the nitrogen of the ketoimine. This is conclusively proven by the crystal structures presented here as the NH hydrogen in all cases was unambiguously detected in the Fourier difference map with the positions and isotropic temperature factors able to be freely refine. Other crystal structures of ketoimines in the literature show a similar result.[31]

This tautomer is partially stabilized by the intramolecular hydrogen bonding between the N–H and O, with an average hydrogen bond length of 1.86(9) Å (range from 1.77 Å to 1.98 Å) for **1a-d** and an average N–H···O bond angle of 139.4(3.8)° (range from 133.6° to 141.9°). **1a** (Figure 2.3) compares well to (Z)-3-(2,6-diisopropylphenyl)amino)-1-phenylbut-2-en-1-one[32] with an identical (within experimental error) *d*(N···O) of 2.613 Å, although the packing through weak intermolecular contacts is more symmetrical than in **1a**. **1b** (Figure 2.4) also has additional weak

intermolecular hydrogen bonding between pairs of molecules that link the pairs about a crystallographic centre of inversion with longer a H-bonding length at 2.29 Å and a larger bond angle at 136.5°. The intramolecular *d*(N···O) of 2.657(2) Å and intermolecular *d*(N···O) of 2.984(1) Å can be compared to 2-(2,6-diisopropylphenylamino) cyclohex-1-enyl phenyl ketone[33] which has intramolecular *d*(N···O) of 2.598(3) Å and 2.614(3) Å and intermolecular *d*(N···O) of 3.205(3) Å and 3.206(3) Å. This comparison indicates that the steric crowding of the aryl substituent does not determine these motifs.

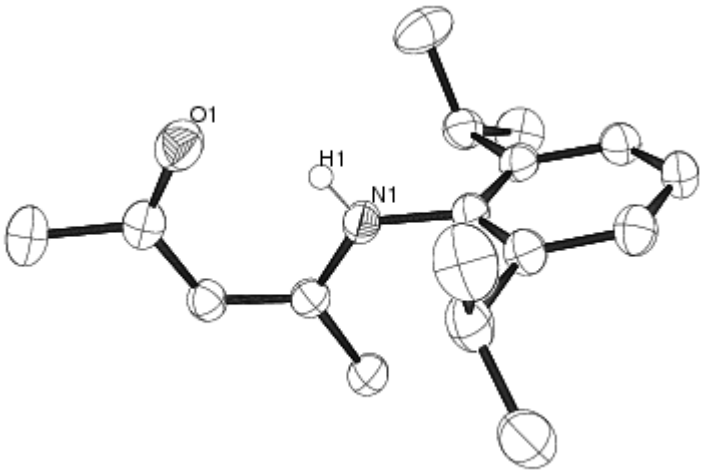

Figure 2.3 – ORTEP diagram of 1a with all but the amine hydrogen atoms omitted for clarity (50% probability ellipsoids shown).

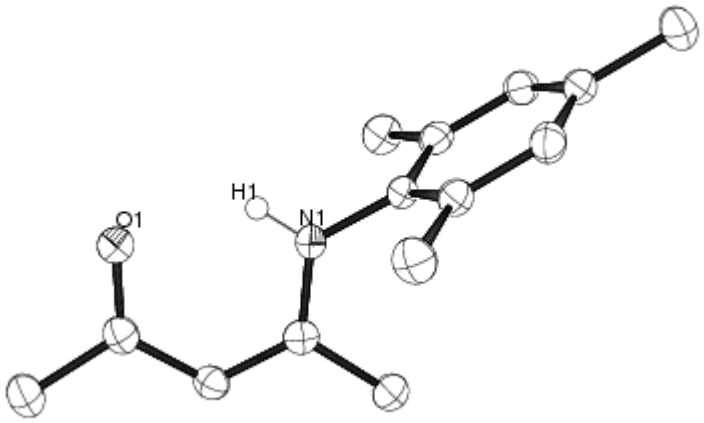

Figure 2.4 – ORTEP diagram of 1b with all but the amine hydrogen atoms omitted for clarity (50% probability ellipsoids shown).

1c (Figure 2.5) and **1d** (Figure 2.7) have 3% shorter *d*(N···O) than **1a** and **1b** with values of 2.549(2) Å and 2.582(2) Å, respectively. This pinching in of the ligand can be attributed to the additional methyl group on the backbone, which although is not a large substituent, has been known to demonstrate local steric pressure at short distances.[34] This pinching in effect is maintained in the lithium complexes **2c** and **4c,d** with **2c** having 4% shorter *d*(N···O) than in **2a** and **2b** with 2.805(1) Å and 2.809(1) Å in comparison with 2.913(2) Å and 2.914(2) Å, respectively, and **4c,d** having 3-4% shorter *d*(N···O) values than **4b** with an average value of 2.780(8) Å for **4c**, 2.800(2)Å for **4d**, and 2.878(15) Å for **4b**.

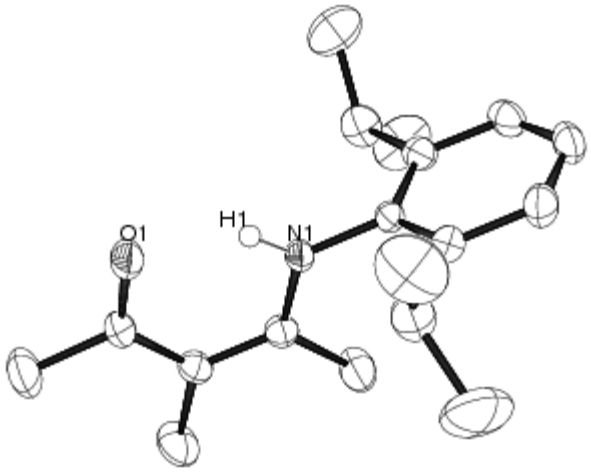

Figure 2.5 - ORTEP diagram of 1c with all but the amine hydrogen atoms omitted for clarity (50% probability ellipsoids shown).

Another bonding interaction seen, for example, in many aromatic organic molecules in the solid state known as π-π stacking, in which areas of π electron density interact with one another, is evident in the crystal structure of **1d** (Figure 2.6). The molecules are arranged such that the aromatic mesityl rings of pairs of molecules are parallel-displaced edgewise at close to the ideal distances for the π-π stacking interaction,[35] 3.546 Å measured as the distance of the centroid of one mesityl to the least squares plane made by the other and an average edgewise displacement of 1.337 Å.

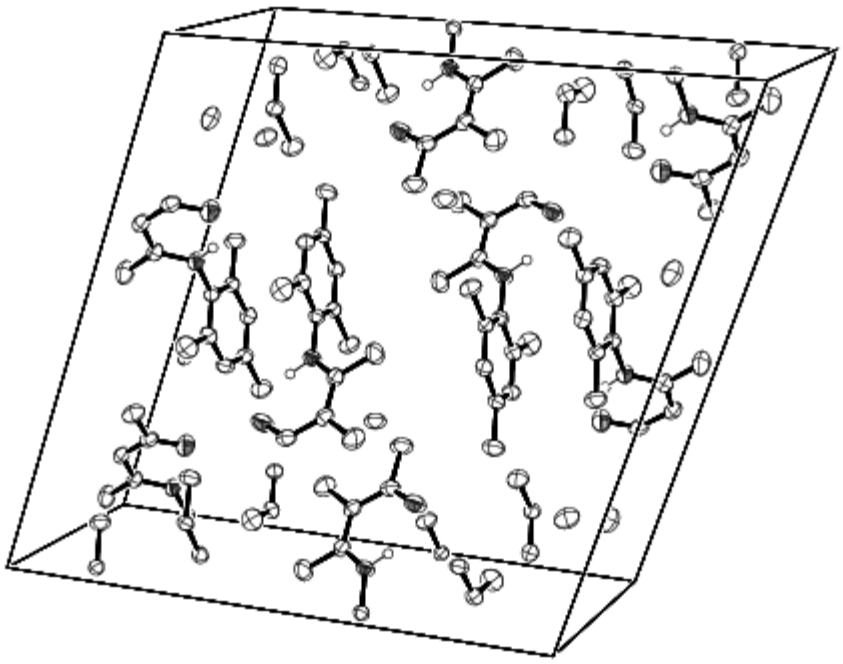

Figure 2.6 – ORTEP diagram of the unit cell contents of 1d showing the π-π stacking of the mesityl substituents. Hydrogens are omitted for clarity.

Some electron delocalization of the pseudo-six membered ring is seen even in the case of the uncoordinated ketoimine molecules (see Table 2.1 in section 2.4) with intermediate values between typical single and double bond lengths for all of the bonds within the ring, with the structure leaning towards the generally accepted enamine form, particularly with regards to the carbonyl bond. A greater level of delocalization is seen with the coordinated dimer and cubane complexes of the ketoimines, with a lengthening of the carbonyl bond and a shortening of the ketoimine CN bond as well as a reversal of the ring C–C bond lengths to give more double bond character to the C–C bond closer to the carbonyl and less to the C–C on the CN side.

The uncoordinated ketoimine molecules have bond angles in the expected range for the given structure with average bond angles of 123.3(4)° for C_3–C_2–O (refer to Figure 2.16 for atom numbering used here), 123.24(19)° (**1a,b**) and 120.33(18)° (**1c,d**) for C_2–C_3–C_4, 121.3(7)° for C_3–C_4–N, and 126(1)° for C_4–N–C_6. A moderate increase is seen for the lithium complexes except for the

understandable decrease in the last listed (125.3(3)°, 128.2(4)° (**2a,b** and **4b**) and 123.84(17)° (**2c** and **4c,d**), 123.3(4)°, and 119.9(8)° following the same order as above). These changes can be explained by the formation of a nearly planar or purely planar 6-membered delocalized ring with Li in most cases. This by the rules of mathematics should have an ideal interior bond angle sum of 720° (planarity defined here by the root-mean-square deviation of the calculated least-squares plane of the 6 atoms in question). The average interior bond angles therefore increase to give a sum of 718.2° (**2a**), 719.3° (**2b**), 714.7° (**2c**), 719.7° (**4b**), 719.5° (**4c**), and 714.1° (**4d**) which are all quite close to the ideal value. The decrease in bond angles for C_4–N–C_6 is in part to accommodate the much larger C_4–N–Li angle (average 123 (2)° for all the lithium complexes) in comparison to the C_4–N–H (average 114(2.)°). Another likely contributing factor is that the aromatic R-groups in the lithium complexes, due to steric congestion, need to bend away from the centre of the complex, thus decreasing the above mentioned angle.

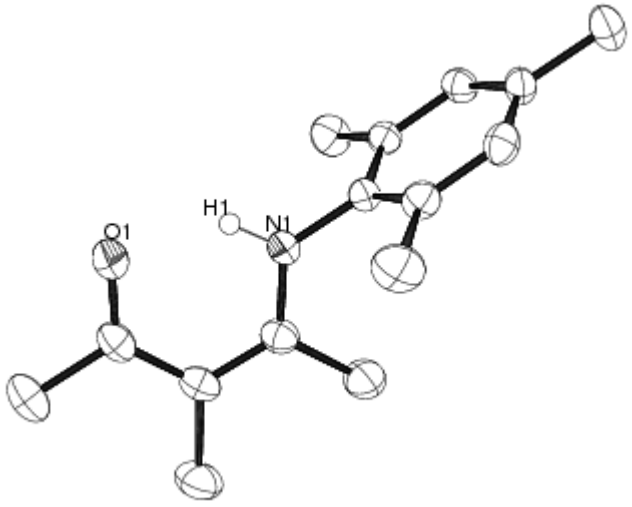

Figure 2.7 – ORTEP diagram of 1d with all but the amine hydrogen atoms omitted for clarity (50% probability ellipsoids shown).

The cubane Li_4O_4 structures **4b-d** isolated here have approximately D_2 symmetry (see Figure 2.9). This is unlike the majority of Li_4O_4 cubane structures that have been previously determined which have the less symmetric S_4 symmetry; included in that group is the sole

previously reported ketoimine complex.[7] However, other D_2 symmetric cases have been reported.[36] In the case of the bulky ketoimines used in this work, the D_2 symmetry is much more favorable to the steric bulk of the ligands than S_4 symmetry which forces much more of the steric bulk close together (see Figures 2.16 and 2.17 in section 2.4) This is in contrast to the previously reported structure which was much less bulky with only an isopropyl group attached to the nitrogen.

Each cubane structure can be viewed as a dimer of dimers (Figure 2.8). In viewing the previously reported S_4 structure as such, the two dimers come together to form the cubane orthogonal to one another. The angles between the planes made by the ligands and the 4-membered Li_2O_2 central ring of each dimer averaged 48.2° with a range of 46.1° to 50.9°. In the case of the D_2 structures, **4b-d** (Figures 2.9, 2.10, 2.14), the measurement of this angle becomes ambiguous because the dimers come together parallel to one another to form the cubane, and as such, each cubane molecule can be viewed as two different possible dimer of dimers. This makes little difference between the two possibilities for **4c,d** with ranges of 41.4° to 47.4° (average 44(3)°) and 42.5° to 48.3° (average 45(3)°) for **4c** and 37.4° to 53.8° (average 46(7)°) and 35.6° to 60.26° (average 47(1)°) for **4d**. However, for **4b**, the two different possibilities give quite different results, with ranges from 42.5° to 50.9° (average 48(4)°) and 39.8° to 47.2° (average 42(3)°). Note that the **4b,c** structures were solvates and **4d** was solvent free.

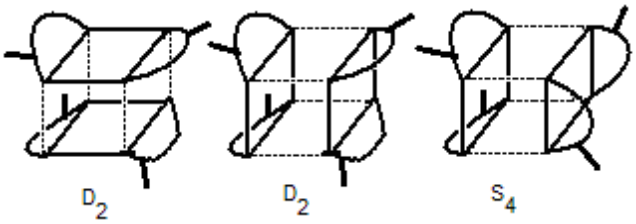

Figure 2.8 – Comparison of the D_2 and S_4 dimers of dimers for the cubane molecules.

In the coordinated dimer structures (Figures 2.11-2.13) the ketoimine ligands lie transoid to the central Li_2O_2 ring with varying angles (37.90° for **2a**, 48.28° for **2b**, and 29.62° for **2c**) to the cubane structures. The smaller values for the dipp containing species are due to the increased steric bulk. The large difference between **2a** and **2c** is most likely due to a necessary compensation for the change in the C_2–C_3–C_4 bond angle (values mentioned above) and the corresponding decrease in the O–Li–N bond angle from 95.96(13)° in **2a** to 92.28(6)° in **2c** which would bring the aromatic group closer to the centre of the complex if the angle of the ligand to the Li_2O_2 ring did not change. In fact, this structural change gives otherwise similar structures, with the separation of the isopropyl methyls from the similarly placed THF carbons at almost the same distance (closest contact for each is 3.656 Å with an average distance of 4.266 Å for **2a** and 4.143 Å for **2c**).

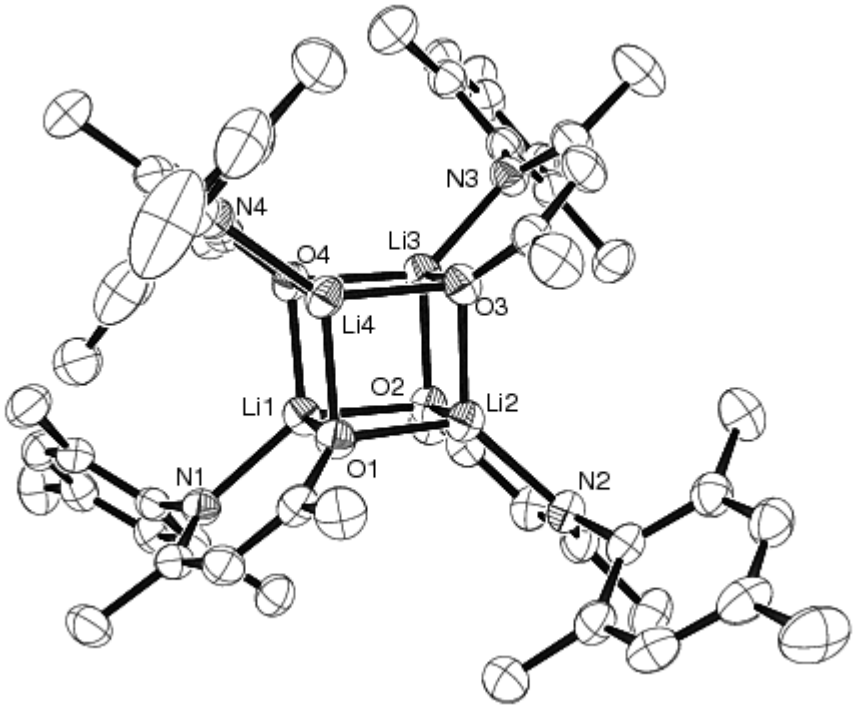

Figure 2.9 – ORTEP diagram of 4b with the hydrogen atoms omitted for clarity (50% probability ellipsoids shown).

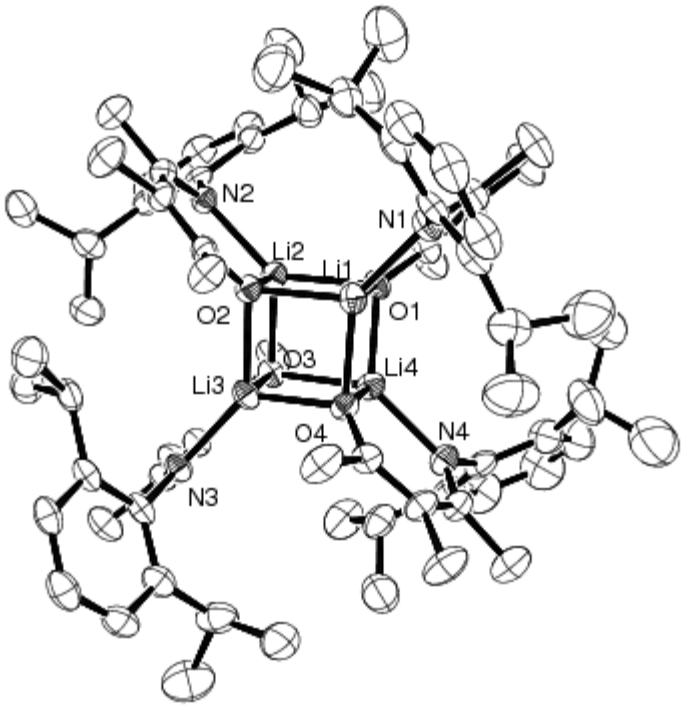

Figure 2.10 – ORTEP diagram of 4c with hydrogen atoms omitted for clarity (50% probability ellipsoids shown).

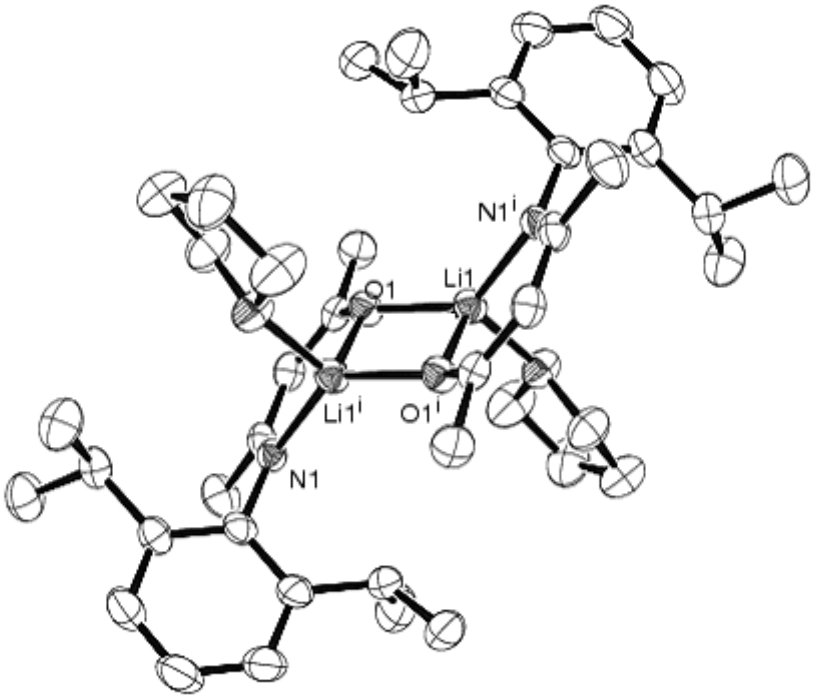

Figure 2.11 – ORTEP diagram of 2a with hydrogen atoms omitted for clarity (50% probability ellipsoids shown). Atoms denoted by superscript "i" were generated by a centre of symmetry.

The more appropriate viewpoint of the cubanes is as aggregates of four monomers, as concluded previously,[7] because the Li–O bond lengths within each cubane structure vary depending on the type of bond. In all cases, the shortest Li–O bond lengths are those between the lithium atoms bonded to the oxygen of the ligand with which they lie in plane. The most difference is seen for **4c**, an average of 1.874(3) Å with a range of 1.871(4) Å to 1.876(4) Å versus an average of 2.01(4) Å with a range of 1.970(4) Å to 2.077(4) Å. Less, but still enough of a difference is seen for **4b**, an average of 1.924(5) Å with a range of 1.917(3) Å to 1.930(3) Å versus an average of 1.976(22) Å with a range from 1.960(3) Å to 1.991(3) Å and for **4d**, an average of 1.903(15) Å with a range from 1.887(3) Å to 1.918(3) Å versus an average of 1.98(2) Å with a range from 1.941(3) Å to 2.012(3) Å.

As described above, the Li–O bond lengths in the structure of **4c** show the greatest amount of variation, containing the shortest and the longest bond lengths of the cubane ketoimine structures, as well as the shortest average bond length for the lithium bonded to the oxygen of the ligand with which it lies in plane and the longest average bond lengths for remaining Li–O bonds (0.206 Å difference between highest and lowest). In contrast, the Li–O bond lengths show the least amount of variation in the structure of **4b** (0.075 Å difference between highest and lowest). The variation of the Li–O bond lengths in the cubane structure of 4-isopropylaminopent-3-en-2-one from the literature and in the structure of **4d** are median to the two extremes and are similar to one another (0.129 Å and 0.125 Å difference between lowest and highest, respectively). These differences are likely factors of the need to accommodate different amounts of steric bulk. More specifically, the extra methyl on the backbone of the ligand in **4d** in comparison with **4b**, the S_4 geometry of the literature structure accommodating much less steric bulk with isopropyl itself being a bulky enough group to necessitate the variation in bond

lengths, and the extra bulk of the dipp isopropyl groups in **4c** in comparison with the mesityl methyls in **4d**.

The coordinated dimer structures, except for **2a**, also have a large enough difference between the types of Li–O bonds (the shorter bonds are between the lithium and oxygen of the ligand with which they lie in plane; longer bonds join monomers together) that the appropriate way to look at them are as aggregates of monomers (1.888(3) Å versus 1.948(3) Å for **2b** and 1.867(2) Å versus 1.908(2) Å for **2c**). However, the difference is much smaller for **2a**, which closely approaches a pure dimer with Li–O bond lengths of 1.899(3) Å versus 1.917(3) Å.

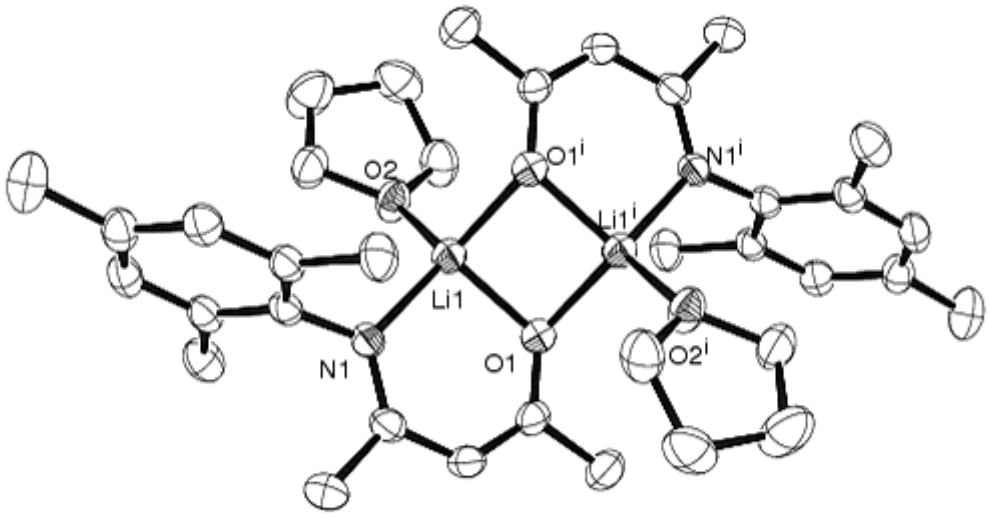

Figure 2.12 – ORTEP diagram of 2b with hydrogen atoms omitted for clarity (50% probability ellipsoids shown).

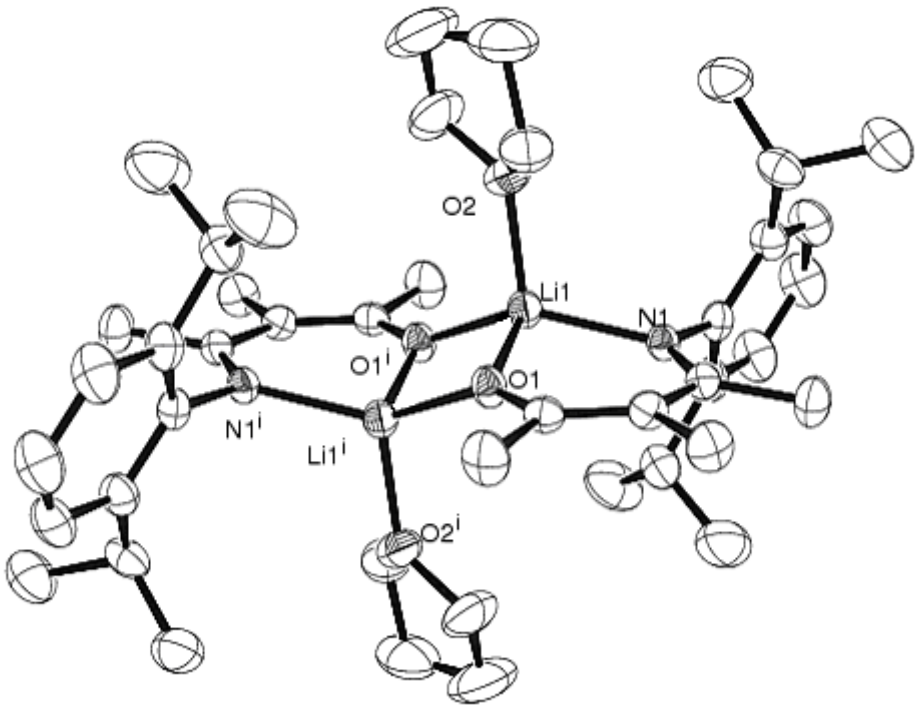

Figure 2.13 – ORTEP diagram of 2c with hydrogen atoms omitted for clarity (50% probability ellipsoids shown).

In the previously reported cubane,[7] the ketoimine was the first ligand reported to form a planar six-membered ring with the lithium atom [root-mean-square deviation of 0.056(4) Å averaged over the four cystallographically independent monomers]. **4b,c** both show this type of planarity as well with a root-mean-square deviation of 0.0225 and 0.0271, respectively. However, **4d** only has one such planar six-membered ring with a root-mean-square deviation of 0.064 Å, whereas the other 3 Li atoms are out of plane with the ligands they are associated with in a fashion similar to the coordinated dimer structures. This is likely a factor of crystal packing as the individual molecule when optimized to a minimum energy with DFT calculations discussed further in the next section has all of the ligands as six-membered planar rings with the lithium atom.

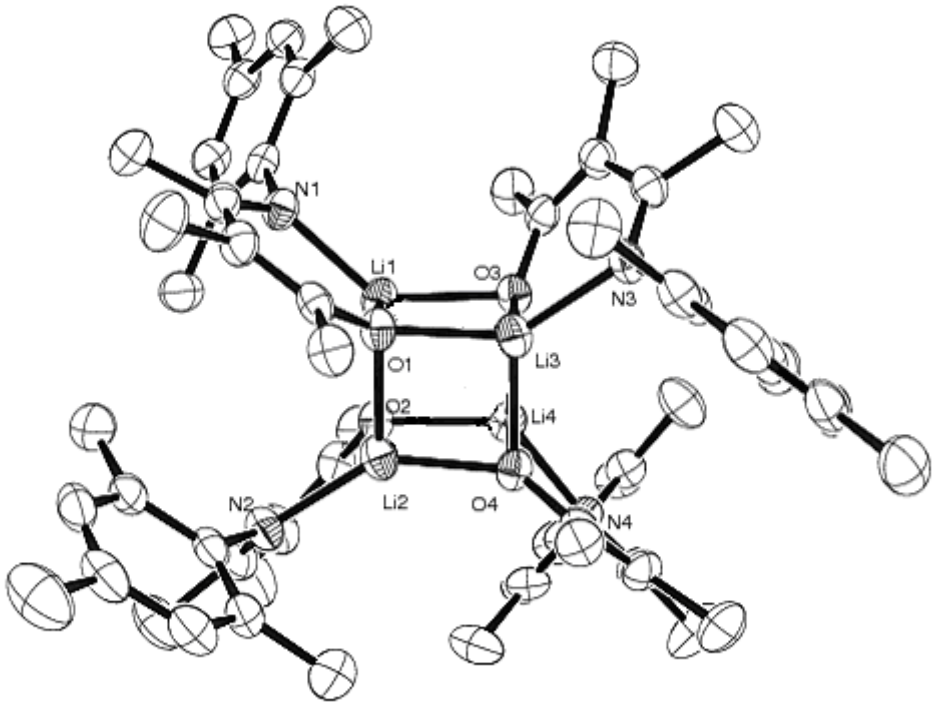

Figure 2.14 – ORTEP diagram of 4d with hydrogen atoms omitted for clarity (50% probability ellipsoids shown).

The bond angles of the Li_2O_2 rings of the coordinated dimer and cubane structures are all similar with an average Li–O–Li bond angle of 86(1)° (with a range in the averages for each structure being 85(1)° to 88(1)°) and an average O–Li–O bond angle of 94(1)° [with a range in the averages for each structure being 92(1)° to 95(2)°]. The bite angle of the ketoimines with lithium [N–Li–O] is an average of 95.7 (9)° for **2a,b** and **4b** and 92.1(7)° for **2c** and **4c,d**. These numbers are also similar to the published ketoimine lithium complexes[7] and other similar lithium complex structures.[37]

2.4 DFT Calculation Results and Discussion

The geometry of the individual molecules as found in the crystal structures were optimized to minima on the potential energy surface at the B3LYP//6-31G(d) level in part to compare the geometry to the crystal structure geometry. The cubane clusters required the use of

maxstep criteria to find the minima on the flat wide well which worked well in all cases but **4c**, which would not quite converge under tight convergence criteria, but the energy did plateau and the fit was well within the loose convergence criteria. The geometries for the theoretical **2d** molecule, and the **4a** molecule, of which no X-ray quality crystals were found, were also computed at the same level of theory. The average bond lengths and angles of the X-ray and computed structures are presented below in Tables 2.1, 2.2, and 2.3. The general atom numbering scheme used in the tables is shown in Figure 2.15. To help in the understanding of why the rare D_2 structure was observed for all of the ketoimine cubanes instead of the S_4 structure, two of the cubane molecules, one representative of each aromatic substituent, were also calculated, partially to obtain the energy of the minimum structures. Therefore, included in the latter table are the bond lengths and angles for the calculated geometry of the S_4 versions of **4c,d** for comparison. The DFT calculations of the alternate S_4 structures for **4c,d** show that although S_4 is able to accommodate the extra steric bulk, the D_2 structure is energetically favoured by 23.37 and 40.81 kJ/mol, respectively.

The majority of the calculated bond lengths and angles are in good agreement with those found in the X-ray structures. There are a few notable exceptions. For **1c,d** the C_2–C_3 bond length is over-estimated, as is the C_4–N–C_6 bond angle. In general, most of the Li–N bond lengths were calculated to be longer than found in the crystal structure. The largest degree of this difference was found for **2a** and **4c**. Also generally over-estimated were the Li–O bond lengths - those not in the plane of the ligand and to the THF. This particularily applies to **2a,c** and **4c,d**.

The calculated values for the computed geometries of molecules **2d** and **4a** are similar to the other structures, well within the expected range given by the other known structures. The geometric values for the alternate S_4 structures are also similar to those found for the D_2 geometries.

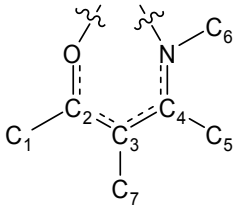

Figure 2.15 – The general numbering scheme used in the following tables.

Table 2.1 – The observed and calculated average bond lengths (Å) and angles (°) for compounds 1a-d.

	1a		1b		1c		1d	
Bond	**Actual**	**Calc**	**Actual**	**Calc**	**Actual**	**Calc**	**Actual**	**Calc**
O–C$_2$	1.2498(19)	1.251	1.2405(18)	1.250	1.2482(17)	1.252	1.2482(17)	1.252
C$_2$–C$_3$	1.421(2)	1.438	1.425(2)	1.438	1.4287(15)	1.450	1.4275(19)	1.450
C$_3$–C$_4$	1.376(2)	1.385	1.3823(19)	1.385	1.3867(18)	1.395	1.3867(18)	1.395
C$_4$–N	1.3395(18)	1.354	1.3398(18)	1.385	1.3473(16)	1.358	1.3473(16)	1.358
C$_7$–C$_3$					1.5120(19)	1.517	1.512(19)	1.517
Angle								
O–C$_2$–C$_3$	123.16(14)	123.50	123.01(13)	123.47	123.68(12)	123.98	123.69(16)	123.99
C$_2$–C$_3$–C$_4$	123.22(14)	123.04	123.27(13)	123.07	120.09(11)	120.40	120.18(14)	120.46
C$_3$–C$_4$–N	120.46(13)	120.78	121.81(13)	120.99	121.08(12)	120.99	121.96(16)	120.91
C$_4$–N–C$_6$	127.46(13)	126.85	124.90(12)	126.46	125.31(11)	128.03	125.20(14)	128.37

Table 2.2 – The observed and calculated average bond lengths (Å) and angles (°) for compounds 2a–d.

	2a		2b		2c		2d
Bond	**Actual**	**Calc**	**Actual**	**Calc**	**Actual**	**Calc**	**Calc**
O–C$_2$	1.2860(19)	1.290	1.283(2)	1.291	1.284(1)	1.289	1.292
C$_2$–C$_3$	1.372(2)	1.390	1.377(2)	1.390	1.385(4)	1.403	1.402
C$_3$–C$_4$	1.431(2)	1.437	1.432(2)	1.435	1.450(1)	1.451	1.451
C$_4$–N	1.301(2)	1.312	1.306(2)	1.312	1.307(0)	1.317	1.315
C$_7$–C$_3$					1.523(2)	1.524	1.523
Li–N	2.021(3)	2.065	2.016(3)	2.022	2.022(2)	2.041	2.007
Li–O (in plane of ligand)	1.899(3)	1.912	1.888(3)	1.902	1.868(1)	1.882	1.881
Li–O (not in plane of ligand)	1.917(3)	1.939	1.948(3)	1.960	1.903(7)	1.947	1.947
Li–O (to THF)	1.988(3)	2.040	1.991(3)	2.016	1.979(23)	2.037	2.026
Angle							
O–C$_2$–C$_3$	125.34(16)	125.76	125.57(16)	125.81	125.47(4)	125.47	125.32
C$_2$–C$_3$–C$_4$	128.68(16)	128.79	128.08(16)	128.20	123.66(11)	124.11	123.75
C$_3$–C$_4$–N	122.86(15)	123.90	123.40(16)	123.50	123.66(15)	124.15	123.82
C$_4$–N–C$_6$	120.58(14)	121.48	118.78(14)	122.10	120.76(9)	121.76	122.27
O–Li–N	95.96(13)	96.58	96.49(13)	97.03	92.28(6)	92.98	92.99
Li–O–Li	85.89(13)	85.76	86.52(13)	85.57	88.05(1.47)	86.73	85.74
O–Li–O	94.11(13)	94.24	93.48(13)	94.43	91.95(1.47)	93.27	94.26
O–Li–O$_{THF}$	107.59(1.12)	107.81	112.30(8.58)	111.02	108.15(2.80)	108.96	112.06
C$_4$–N–Li	121.68(14)	119.82	121.33(14)	121.29	122.92(8)	122.59	123.92
C$_2$–O–Li	123.68(14)	123.27	124.39(14)	123.70	126.68(19)	127.04	127.13

Table 2.3 – The observed and calculated average bond lengths (Å) and angles (°) for the compounds 4a-d and the alternate S_4 structures of 4c,d.

	4a	4b		4c			4d		
Bond	**Calc**	**Actual**	**Calc**	**Actual**	**Calc**	**$S_{4(Calc)}$**	**Actual**	**Calc**	**$S_{4(Calc)}$**
O–C_2	1.305	1.303(2)	1.306	1.310(2)	1.310	1.307	1.310(3)	1.308	1.308
C_2–C_3	1.378	1.366(2)	1.382	1.370(3)	1.392	1.395	1.374(1)	1.392	1.394
C_3–C_4	1.443	1.440(2)	1.442	1.460(7)	1.464	1.461	1.454(2)	1.458	1.457
C_4–N	1.311	1.302(3)	1.308	1.309(2)	1.314	1.318	1.305(4)	1.312	1.314
C_7–C_3				1.524(4)	1.525	1.525	1.522(4)	1.524	1.524
Li–N	2.078	1.988(4)	2.002	2.012(5)	2.056	2.036	1.968(12)	1.983	2.003
Li–O (in plane of ligand)	1.914	1.924(5)	1.931	1.874(3)	1.878	1.881	1.903(15)	1.897	1.887
Li–O (not in plane of ligand)	2.026	1.976(10)	1.997	2.009(39)	2.046	2.049	1.976(22)	2.014	2.036
Angle									
O–C_2–C_3	125.12	125.15(16)	125.34	124.8(4)	124.85	124.91	125.17(30)	125.32	125.52
C_2–C_3–C_4	129.08	127.82(37)	128.91	124.0(3)	124.06	125.32	123.88(63)	124.41	124.71
C_3–C_4–N	124.27	122.77(24)	123.62	123.5(3)	124.83	124.96	123.33(28)	123.84	124.12
C_4–N–C_6	120.71	120.29(98)	121.46	119.1(1.1)	120.80	120.58	120.17(95)	121.95	121.38
O–Li–N	95.96	94.77(71)	97.33	91.3(4)	92.28	96.08	92.68(45)	93.88	94.73
Li–O–Li	87.72	85.65(1.92)	85.84	86.1(2.8)	86.53	87.37	84.79(1.35)	85.38	84.99
O–Li–O	91.90	94.07(2.26)	93.96	93.5(3.4)	93.18	92.57	94.95(1.54)	94.36	93.98
C_4–N–Li	120.34	124.14(58)	121.68	125.7(4)	123.63	119.91	123.89(87)	124.78	122.75
C_2–O–Li	125.09	125.08(78)	123.13	130.2(4)	130.01	126.04	125.18(2.55)	127.20	125.92

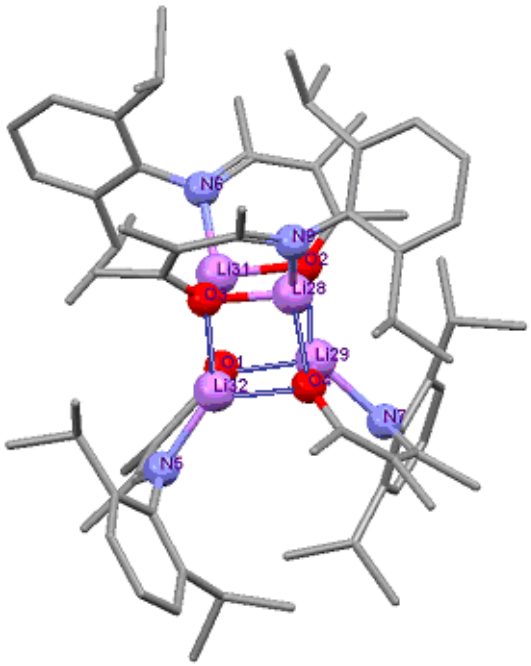

Figure 2.16 – B3LYP//6-31G(d) optimized structure of the S_4 geometry for 4c (visualized with Mercury 2.2). The Li, N and O atoms are represented by spheres and the carbon atoms by tube-junctions. H atoms are omitted.

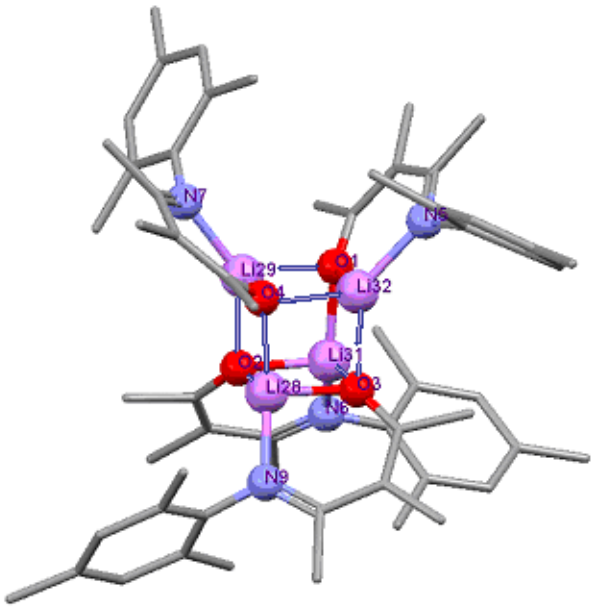

Figure 2.17 - B3LYP//6-31G(d) optimized structure of the S_4 geometry for 4d (visualized with Mercury 2.2). The Li, N and O atoms are represented by spheres and the carbon atoms by tube-junctions. H atoms are omitted.

The cubane structure, **4d** surprisingly crystallized in the presence of enough of the highly coordinating solvent THF that it could have, and was expected to, crystallize in the coordinated dimer type structure. This posed the interesting question of why the cubane formed preferentially in the case of **4d** and not the other ketoimines. DFT calculations, in addition to the standard optimization for geometric comparison to the determined crystal structure geometries, were done in order to help answer this question.

One hypothesis is that the addition of the methyl onto the backbone (because of its donor substituent properties) allows more electron density to be donated to the positively charged lithium atoms, decreasing the need for lithium to coordinate to another molecule such as THF. The extra bulkiness of the dipp on **1c** in this case would have to be a preventive factor to give the expected result. A computational study was designed to test this hypothesis by looking at the changes in energy of the following reactions at the B3LYP//6-31G(d) level of theory:

1. 2 ketoimine + 2 BuLi + 2 THF → ((ketoiminate)LiTHF)$_2$ + 2 BuH

2. 4 ketoimine + 4 BuLi → ((ketoiminate)Li)$_4$ + 4 BuH

If equation 2 is subtracted from 2 times the first it gives the equation for the conversion of the cubane to coordinated dimer upon the addition of THF which is the equation of interest to the hypothesis:

3. (ketoimineLi)$_4$ + 4 THF → 2 ((ketoiminate)LiTHF)$_2$

The resultant changes in energy (ΔE) as calculated without and with inclusion of the zero point correction (ZPC) are given in Table 2.4.

The numbers show that the enthalpy change alone is not the reason for the formation of **4d** in the presence of THF. However, there is a noticable trend with respect to the dipp (**1a** and **1c**) and mes (**1b** and **1d**) substituents in ΔE for reaction 3. The ΔE for **1a,c** is almost double that of **1b,d**. This difference is even more extreme once the zero point correction energies obtained from

the frequency calculations were included (because there was no frequency calculation done for **4c** due to not converging under tight convergence criteria only **1a,b,d** are available for comparison). The ΔE for **1b,d** changes relatively little in magnitude while for **1a**, the ΔE changed to more than four times that of the calculations that did not take the ZPC into consideration. Other energy factors, such as the crystal packing energy, which is not easily calculated,[38] may overcome the favorable formation energy of the coordinated dimer structure when THF is added to the cubane molecule in the case of **4d** only. Another factor may be the entropic energy change, which would not be favorable for the third reaction.

Table 2.4 – The reaction energies for formation of the lithium complexes in reactions 1, 2, and 3 of ketoimines 1a-d.

	ΔE (kJ/mol)*					
	Without ZPC			**Including ZPC**		
Ketoimine	**1**	**2**	**3**	**1**	**2**	**3**
1a	–889	–1675	–104	–865	–1307	–423
1b	–902	–1746	–59	–875	–1703	–47
1c	–865	–1597#	–133*	–835	–	–
1d	–878	–1686	–70	–852	–1647	–58

* The normal uncertainty in B3LYP//6-31G(d) is approximately +/- 5 kJ/mol.
# The optimization of **4c** did not fully converge to the tight criteria although the energy plateaued and the criteria were well within the loose convergence limits.

Another possible explanation is that a combination of the energy factors above and the solubility differences between the complexes played a part in the cubane result. The dipp containing species, **2a** and **2c** were highly soluble in THF, whereas the mesityl containing species **2b** and "**2d**" (the reaction resulted in the isolation of **4d** although made in THF) were on opposite ends of the spectrum – **2b** was much less soluble in THF (about double the amount of THF was

required to dissolve a similar number of moles) and "**2d**" was so soluble in THF that solid did not precipitate until nearly all of the THF was removed under high vacuum.

2.5 NMR Results and Discussion

Of primary interest in the study of the lithium complexes is the structure of the complexes in solution state. The analysis of the NMR results was therefore approached with this goal in mind. Many interesting and at times apparently contradictory results were obtained with regards to the 7 lithium complexes presented here, in particular with regards to the substituent change from dipp to mesityl. To start with: the simple mesityl to dipp change in the substituent on the ketoimine has a surprisingly large effect on the solubility of the lithium complexes. The NMR for the coordinated dimer complexes were collected in a 1:1 THF:C_6D_6 solution initially, and then for comparison purposes the NMR for all 7 complexes was attempted in C_6D_6. The mesityl based compounds, even the coordinated dimer complex **2b** are all highly soluble in benzene. However, the dipp containing Li species showed limited solubility in C_6D_6 and become much more soluble once THF was added to the solution.

The dipp complexes in 1:1 THF:C_6D_6 gave high quality NMR spectra, with only one sharp signal in the ^{7}Li NMR spectrum. This shows that in this particular solution only one species is present. The mesityl complex **2b** behaved differently than the dipp complexes **2a,c** when dissolved into the 1:1 THF:C_6D_6 solution. Two closely placed signals became apparent in the ^{7}Li NMR spectrum as shown in Figure 2.18. The ^{1}H NMR spectrum also showed a great deal of change, with broadened signals, two obvious sets at lower concentration which at higher concentration began to merge together (Figure 2.19). This shows that two species (possibly closely related) are present in solution and some sort of relatively slow exchange processes are likely occuring. Also interestingly, the mesityl species, **2b** and **4b**, had precisely the same NMR

chemical shifts for the ^{1}H and ^{7}Li in C_6D_6 except that **2b** contained THF signals and **4b** contained toluene signals (the crystals of **4b** contained toluene in the lattice).

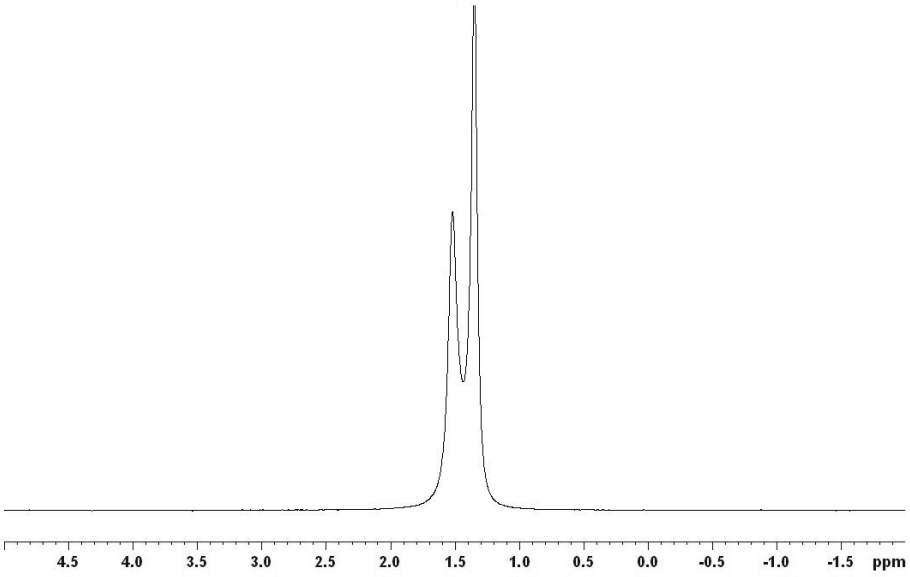

Figure 2.18 – ^{7}Li NMR of 2b in 1:1 THF:C_6D_6.

This means that the coordinated dimer structure (with coordination to THF) is not the structure in solution state for **2b** because such a solution-state is not possible for **4b** without addition of THF to the sample. Therefore, the structure of both **2b** and **4b**, is likely either the monomeric or the cubane structure, however, several other combinations are also possible with consideration of the literature.[39] Only 1 species is present though given the sharp singlet in the ^{7}Li NMR spectrum. The proton spectrum for **4b** is shown in Figure 2.20.

For **2a**, NMR in THF-*d*$_8$ was also attempted. This gave a sharp ^{7}Li signal, but the ^{1}H NMR spectrum had more signals which were broadened, also denoting slow exchange, possibly between THF-*d*$_8$ and undeuterated THF coordination. This spectrum is shown in Figure 2.21 to demonstrate the odd effects observed. The peaks in this spectrum were not assigned or conclusively analysed further.

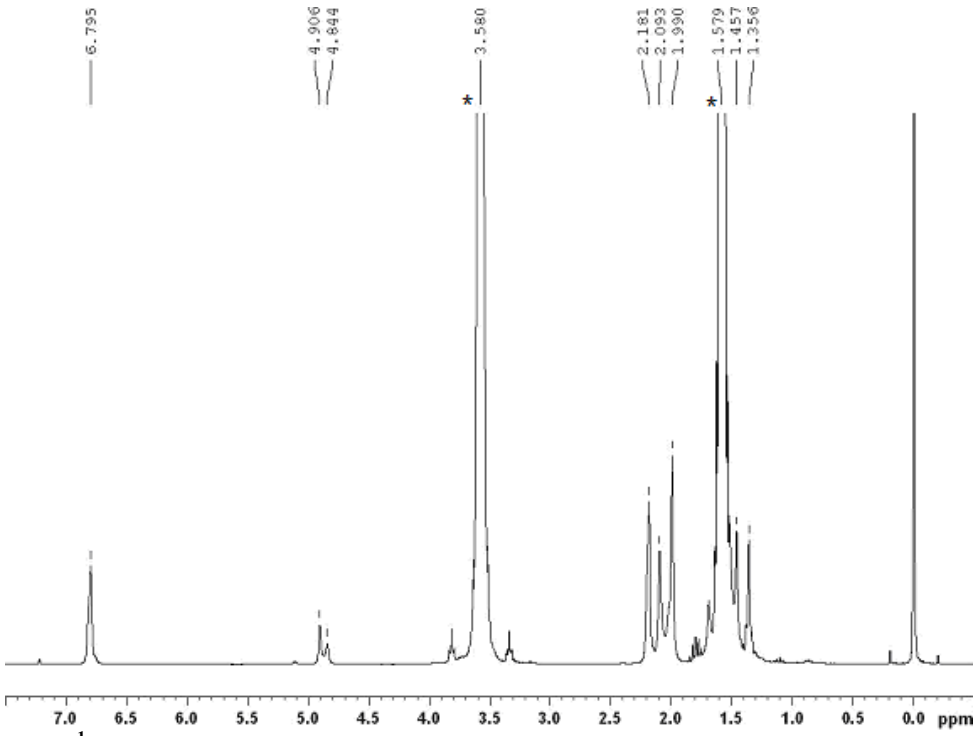

Figure 2.19 – ^{1}H NMR spectrum of 2b in 1:1 THF:C_6D_6. The THF solvent peaks are shown by the * above them.

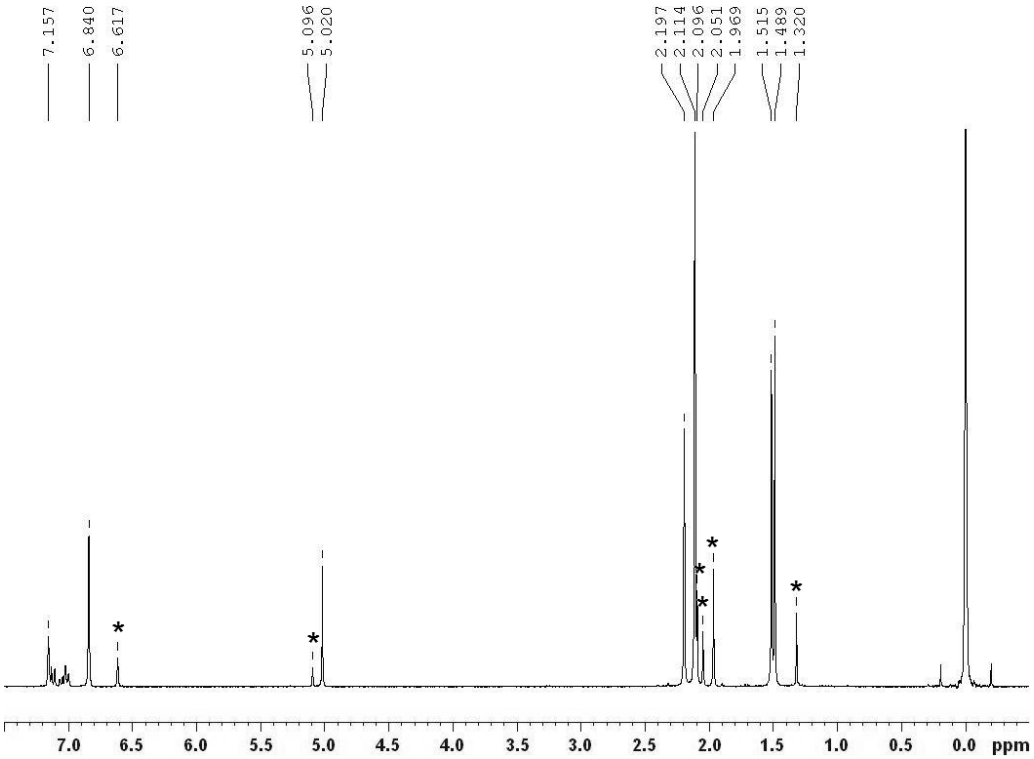

Figure 2.20 – The ^{1}H NMR spectrum of 4b in C_6D_6 at 25°C. The peaks with * above them are uncoordinated ketoimine peaks. The crystals were shown to be pure material via the elemental analysis results in conjunction with the knowledge that only 0.4:1 molar ratio of toluene:4b remained at the time this NMR and the elemental analysis were performed.

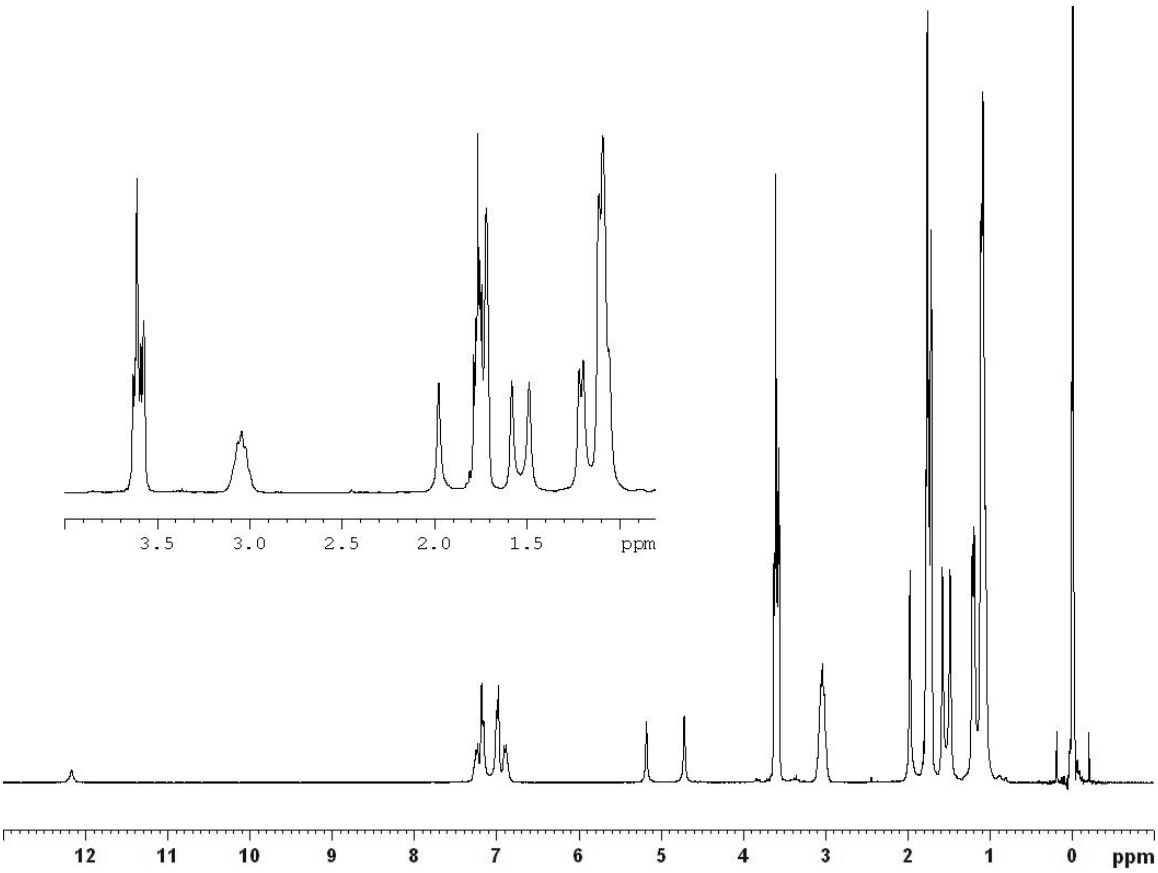

Figure 2.21 – ^{1}H NMR spectrum of 2a in THF-*d*$_8$.

The first attempt to determine the solution state structure was through analysis of the ^{7}Li NMR. However, there are a few things to keep in mind when looking at ^{7}Li NMR spectra especially for the comparison of chemical shift with respect to the structural information that can be gleaned. With ^{7}Li NMR spectroscopy, chemical shift arguments for particular structure are made much less often than other nuclei because lithium shifts are as sensitive to solvent effects, viscosity, temperature and concentration as they are to structural differences. Reliably detecting structural differences in ^{7}Li NMR spectra usually requires the use of spin-spin coupling to other nuclei and often the slowing-down of the often fast fluxional exchange processes of lithium complexes by cooling in VT-NMR.[40] Below, comparisons are made between a paper in the literature and the results for the ketoimine complexes presented here. This is done on the basis that the ligands themselves are quite similar and the NMR experiments were done in the same

solvents at the same temperature. The cited paper had analytically controlled concentration, however no appreciable effect on the lithium shift was observed here when the concentrations of the ketoimines was changed.

The Sasamori research group made three new overcrowded diketoiminates with 2,4,6-tris[bis(trimethylsilyl)methyl]phenyl (Tbt) on one of the nitrogens and an aryl group on the other (Figure 2.22). This was successful with high yield for phenyl, o-tolyl, and mesityl; trace amounts of the dipp version was made and a second Tbt could not be placed on the ligand.[41] The lithium complexes of the phenyl and mesityl containing species were then prepared and analyzed by ^{1}H, ^{13}C, and ^{7}Li NMR spectroscopy in C_6D_6 (which they were highly soluble in). The mesityl species was also characterized by X-ray crystallography. The NMR work on these lithium complexes of overcrowded β-diketoiminate ligands (versions of NacNac) may give some insight into the above observations with the ketoimine complexes, in particular with the interpretation of the lithium signal shift with regards to what type of complex is present in solution state.

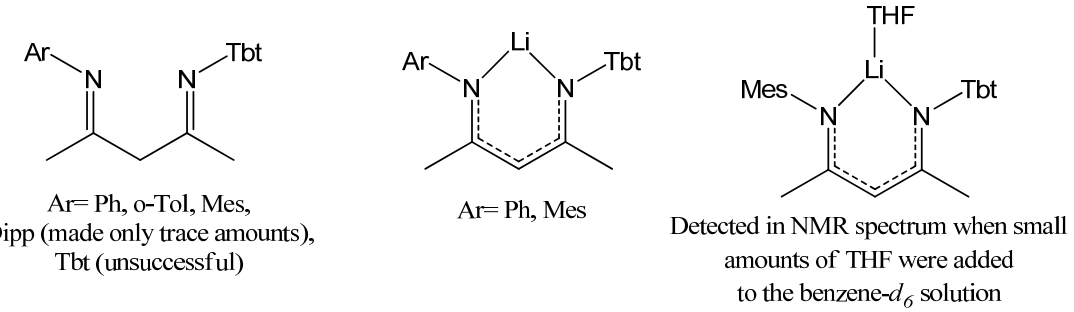

Figure 2.22 – The literature structures from the Sasamori paper discussed above used for comparison and interpretation of the ketoimine ^{7}Li NMR results.

The bulky ligands complexed with lithium in a monomeric form and did not have any coordinating solvent molecules present, shown by all of the above methods. The group then proceeded to a detailed NMR study of the mesityl complex by adding various amounts of THF to the NMR solution in order to determine the equilibrium between the free monomer and the THF coordinated monomer for the mesityl containing ligand. The ^{7}Li and ^{1}H NMR spectra were

monitered for changes. With increasing amounts of added THF to the NMR solution the ^{7}Li signal shifted upfield while the THF signals in the ^{1}H NMR spectrum shifted downfield towards the normally expected regions. The free monomer in pure C_6D_6 had a sharp ^{7}Li signal at 2.33 ppm. Ittook only a small addition for a large difference in the shift of the ^{7}Li signal to be observed. With 50:1 C_6D_6:THF ratio, the ^{7}Li signal shifted to 1.79 ppm (a sharp singlet denoting a fast exchange process between the free monomer and THF-coordinated monomer).

Table 2.5 – ^{7}Li NMR signals in ppm of the lithium ketoimine complexes in various solvents.

	NMR Solvent Used		
Sample	**C_6D_6**	**1:1 THF:C_6D_6**	**THF-d_8**
2a	–	–2.14	1.22
2b	2.76	1.52 1.35 (1.7x taller)	–
2c	2.76 (v br)	1.33	–
4b	2.76	–	–
4d	1.44	–	–

When these numbers are compared with the lithium complexes of the ketoimines in Table 2.5, a few parallels can be drawn and more can be potentially understood about these species in the solution state. The mesityl complexes **2b** and **4b** each have a sharp lithium signal at 2.76 ppm in the ^{7}Li NMR spectrum. If direct comparison of the ^{7}Li NMR shifts can be drawn this would mean that a monomer (uncoordinated to THF for **2b** and **4b**) is what is present in C_6D_6. In 1:1 THF:C_6D_6 solution, the mesityl compound **2b** has two sharp singlets at 1.52 and 1.35 ppm and **2c** comes in at 1.33 ppm denoting primarily THF-coordinated species with fast exchange (if any) of the THF. The ^{7}Li NMR signal for **2a** in 1:1 THF:C_6D_6 and for **4d** in C_6D_6 are both remarkably different from the others: –2.14 and 1.44 ppm, respectively.

One theory to explain this is that **2a** may actually exist in the 1:1 THF:C_6D_6 solution as the THF-coordinated dimer instead of the monomer (which would be expected to shift the lithium in this direction although not this far). As far as the result for **4d** goes, if the coordination number is the important part of lithium shift for these similar complexes, then this likely indicates that the coordination number of the lithium in solution is 3 – which fits with the structure being a dimer in the uncoordinating solution. In addition, for **2a**, for which the NMR spectrum was also recorded in THF-*d*$_8$, the lithium signal came in at 1.22 ppm. Taking the obvious slow exchange between more than one species taking place in the ^{1}H NMR spectrum into account as well, this is also an interesting result, given that a signal in this region for similar types of compounds denotes fast exchange between uncoordinated monomer and coordinated monomer.

The analysis of the ^{7}Li NMR spectrum was an interesting approach to answering the question of solution state, however, closer analysis of the much more reliably (recall the sensitivity of ^{7}Li NMR shift on numerous variables) diagnostic ^{1}H NMR spectra, discussed below, shows that the ^{7}Li NMR shifts cannot be used for the determination of the solution state for these complexes.

As alluded to above, the analysis of the ^{1}H NMR spectra yields a much different conclusion about the solution-state structure of these complexes. In particular, the shift of the signal of the methyl adjacent to the carbonyl on the ketoimine in the free ligand versus the lithium complexes as well as the shift of the THF signals is indicative of the solution-state structure. In the free ligand, the signal of the methyl adjacent to the carbonyl is 0.6 to 0.7 ppm downfield of the signal of the methyl adjacent to the CN. Looking at the X-ray crystal structure shows that it is likely that this is largely because of strong ring shielding of the aryl group on the CN side of the molecule with an average distance of 3.85 Å from the centroid of the ring to the methyl group. In all of the lithium complexes this methyl signal shifts upfield to close to the CN

adjacent methyl signal (0.03 to 0.06 ppm away), so close that it becomes difficult to unambiguously assign the signals even with analysis of the HSQC and HMBC. This shifting can be attributed to the ring shielding effect that would occur only in the case of ring shielding of the CO side from an adjacent ligand, which excludes the presence of a monomeric solution state for **2a-c** and **4b,d**. In **4b**, the distance of the centroid of the ring to the methyl adjacent to the carbonyl averages 4.78 with a total of 8 interactions. In **4d**, this measurement averages 3.88 Å with 4 such interactions. In **2a-c**, the distance averages 5.30 Å. Previously published characterization data[1g] of aluminum complexes of ketoimine **1a** show definitively that ring shielding of an adjacent ligand is the cause of the shift. Some examples of single ketoimine ligand containing complexes and examples of those containing two ketoimine ligands with the appropriate conformation for ring shielding to have an effect on the methyl adjacent to the carbonyl. The complexes containing only one ligand have the shifts of the methyls on the carbonyl similar to the free ligand, where as the complexes with two ketoimine ligands show the dramatic shift similar to **2a-c** and **4b,d**. The ^{1}H NMR data comparison of **1a,c** with **2a,c** as well as the aluminum complexes noted above is shown in Table 2.6 and the ^{1}H NMR data comparison of **1b,d** with **2b** and **4b,d** is shown in Table 2.7. The average distance from the centroid of the aryl ring to the methyls adjacent the carbonyl and amine are shown in Table 2.8.

The above observations, along with the similar NMR spectra of **2b** and **4b** (excluding solvent) and the fact that the THF signals in the ^{1}H NMR of **2b** is the same as that for free THF in benzene at 3.57 and 1.41 ppm,[42] leads to the conclusion that for **2b** and **4b,d** the solution state structure is the cubane. This also helps explain the cubane crystallizing out of a solution containing THF in the case of **4d**. As well, looking at the nature of the crystal structures of the cubane molecules in space filling view, explains the solubility differences between the mesityl and dipp containing species. **4a,c** are tightly-enclosed and almost spherical surfaces which are

difficult to solvate with benzene, whereas **4b,d** have much more open surface cavities where solvation can initiate.

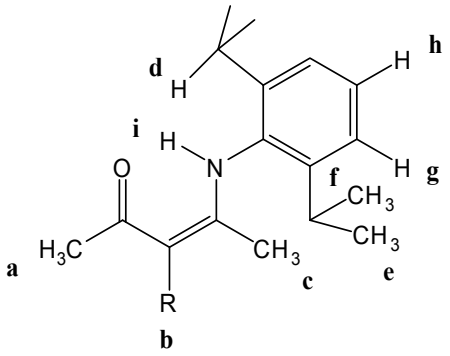

R = H, CH_3

Figure 2.23 – Proton labeling scheme for Table 2.6 below.

Table 2.6 – The ^{1}H NMR data for 1a,c; 2a,c; and literature aluminum complexes with ligand 1a.

	^{1}H Signal								
	a	**b**	**c**	**d**	**e**	**f**	**g**	**H**	**i**
1a ($CDCl_3$)	2.13	5.22	1.64	3.02	1.15	1.21	7.19	7.30	12.05
1a (C_6D_6)	2.06	5.14	1.41	3.10	1.08	1.02	7.20	7.14	12.70
1c ($CDCl_3$)	2.24	1.92	1.70	3.01	1.14	1.18	7.17	7.28	13.18
1c (C_6D_6)	2.15	1.74	1.51	3.13	1.05	1.09	7.05	7.16	13.86
2a (C_6D_6:THF)	1.66	4.82	1.61	3.16	1.19	1.14	7.11	7.02	–
2c (C_6D_6:THF)	1.74	1.85	1.68	3.11	1.16	1.10	7.10	7.00	–
($1a^-$)$AlMe_2$	2.07	5.34	1.74	2.92	1.19	1.08	7.20		–
($1a^-$)$AlEt_2$	2.10	5.34	1.75	2.93	1.10	1.22	7.20		–
($1a^-$)$_2$AlMe	1.61	5.60	1.17	2.93 3.06	1.12		7.10		–
($1a^-$)$_2$AlEt	1.62	5.00	1.17	2.94 3.19	1.06 - 1.28		7.12		–
($1a^-$)$_2$AlCl	1.68	5.22	1.21	2.82 3.30	1.04 - 1.25		7.15		–
($1a^-$)$_2$AlF	1.63	5.15	1.21	2.77 3.18	1.04 - 1.25		7.15		–

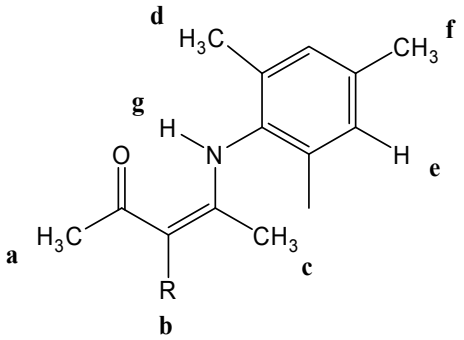

R = H, CH_3

Figure 2.24 – ^{1}H numbering scheme for Table 2.7 below.

Table 2.7 – The ^{1}H NMR data for 1b,d; 2b; and 4b,d.

	^{1}H Signal						
	a	**b**	**c**	**d**	**e**	**f**	**g**
1b ($CDCl_3$)	2.10	5.19	1.62	2.15	6.90	2.28	11.85
1b (C_6D_6)	2.08	5.10	1.33	1.97	6.63	2.06	12.33
1d ($CDCl_3$)	2.22	1.91	1.70	2.13	6.89	2.28	12.99
1d (C_6D_6)	2.14	1.73	1.45	2.00	6.82	2.10	13.49
2b (C_6D_6)	1.52	5.02	1.49	2.12	6.84	2.20	–
4b (C_6D_6)	1.52	5.02	1.49	2.12	6.84	2.20	–
4d (C_6D_6)	1.61	1.92	1.56	2.01	6.86	2.22	–

The THF signals in **2a-c** in the ^{1}H NMR spectrum in mixed solvent 1:1 C_6D_6:THF gives evidence that in coordinating solvent, there is fast exchange between coordinated and uncoordinated THF with signals at 3.59 and 1.61 ppm for **2a**, 3.58 and 1.58 ppm for **2b**, and 3.59 and 1.63 ppm for **2c**, eliminating the cubane structure as the solution state. The shift of the ^{1}H signal of the methyl on the carbonyl side indicates that ring shielding is occurring and therefore

an adjacent ligand must be present, which means that a monomeric solution state is eliminated as well. For **2a,c** with sharp ^{1}H signals and a single sharp lithium signal, this means it is likely that the coordinated dimer structure is the solution state structure for these two compounds and that the larger distance between the centroid of the aryl ring and the carbonyl adjacent methyl is still able to exude enough ring shielding to move the signal for that methyl so strongly downfield. Another possible structure would be some sort of trimeric solution state that may also allow for coordination by THF. For **2b**, which recall had broad signals in the ^{1}H NMR spectrum and two closely placed sharp signals in the ^{7}Li NMR spectrum, there is likely a slow exchange going on between the coordinated dimer and cubane structures.

Table 2.8 – Average distances of the aryl centroid to the methyl adjacent to CO and CN which results in ring shielding effects seen in the ^{1}H NMR spectrum.

	Distance of Aryl Centroid to:			**Distance of Aryl Centroid to:**	
	CH_3 adjacent CN	**CH_3 adjacent CO**		**CH_3 adjacent CN**	**CH_3 adjacent CO**
1a	3.941	–	**4b**	3.786	4.775
1b	3.827	–	**4c**	3.698	4.919
1c	3.770	–	**4d**	3.739	3.881
1d	3.853	–	**(1a)$AlMe_2$**	3.784	–
2a	3.790	5.361	**(1a)$AlEt_2$**	3.681	–
2b	3.702	5.317	**$(1a)_2AlMe$**	3.622	3.903
2c	3.773	5.224	**$(1a)_2AlEt$**	3.628	3.927
2d*	3.830	5.055	**$(1a)_2AlCl$**	3.626	3.904
4a*	3.786	4.960	**$(1a)_2AlF$**	3.635	3.912

* Measurements are from the DFT calculated structures.

2.6 Crystal Structure of the Magnesium Complex of 1b

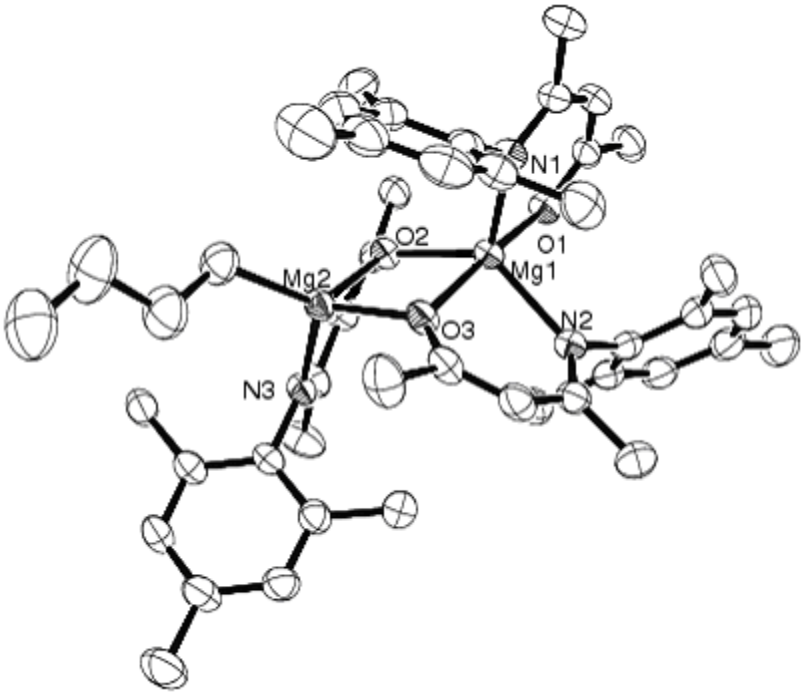

Figure 2.25 – ORTEP diagram of magnesium complex 3b with hydrogen atoms omitted for clarity (50% probability ellipsoids shown).

In addition to the lithium complexes above, the magnesium complex of **1b** was also isolated and studied by X-ray crystallography (Figure 2.25). Only four ketoimine Mg complexes have been previously reported which have an aryl or the closely related cyclohexane substituent on nitrogen.[1h,5a] This includes both four-coordinate and five-coordinate monomeric complexes – a rareity for the four-coordinated magnesium which generally exist as a dimer or trimer in the crystalline state.[43] The previous four-coordinate and five-coordinate magnesium ketoimine complexes used for comparison (Figure 2.26) studied by X-ray crystallography have been found to consist of ligands arranged in a distorted tetrahedral and trigonal bipyramidal geometry, respectively. Eight other Mg complexes of closely related structures have also been reported[44] but will not be used below for comparison purposes.

The particular magnesium complex isolated for **1b** was therefore an unexpected result, consisting of two different types of magnesium – one four-coordinate with coordination to one

ketoimine through both the oxygen and nitrogen, to another through the oxygen only, and to a butyl group and one five-coordinate with coordination to two ketoimines through both the oxygen and nitrogen and to another through the oxygen only. The two magnesium atoms are joined via two of the three ketoimine ligands providing a bridging oxygen atom to be shared between the metal centres, creating a planar Mg_2O_2 centre ring much like the lithium coordinated dimer complexes. The other ketoimine ligand is solely coordinated to the five-coordinate magnesium. As expected the four-coordinate and five-coordinate magnesium centres exhibit distorted tetrahedral and trigonal bipyramidal geometry. Selected bond lengths and angles for the crystal structure as well as for the B3LYP//6-31G(d) optimized geometry are given in Table 2.9.

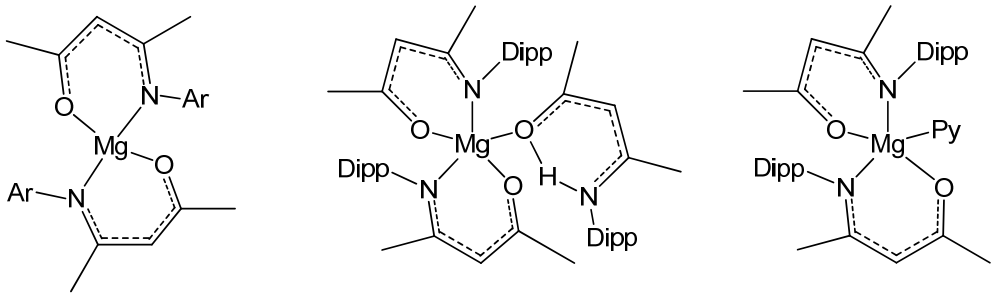

Ar= Dipp, Cyclohexane

Figure 2.26 – The four literature ketoimine Mg complexes which have been previously reported and used for structural comparison.

Different levels of electron delocalization are observed in the ketoimine backbone for the bridging ligands versus the non-bridging with an increase in all of the bond lengths seen for the bridging in comparison with the non-bridging. The analysis of the N–Mg and O–Mg bond lengths are a little more complex in this case, given the different types present. All of the N–Mg bond lengths in **3b** are elongated in comparison to the four-coordinate ketoimine magnesium complexes in the literature – 2.105(2), 2.153(2), and 2.107(2) Å in comparison with 2.059(1) and 2.076(9) Å – and similar to the five-coordinate – 2.144(10) and 2.161(3) Å in the literature structures. To summerize, in **3b**, the four-coordinate N–Mg (which is for a bridging ligand) is

similar to the five-coordinate N–Mg bond length for the non-bridging, and the bridging of the five-coordinate is much longer.

Generally speaking, the five-coordinate Mg has longer bond lengths to nitrogen than four-coordinate Mg due to increased steric congestion and greater dissipation of the electrostatic charge over five donor lone pairs versus four. In **3b**, the bridging ligands have even longer bond lengths due to more sharing of the electron density. A similar consideration can be used to make sense of the O–Mg bond lengths, 1.9514(18) Å for the non-bridging ligand, 2.0008(4) Å for the four coordinate bridging, and 2.06(4) Å for the five-coordinate bridging ligand. In the literature, four-coordinate Mg–O ketoimine bond lengths are an average of 1.908(16) Å while the five-coordinate are an average of 1.97(3) Å.

All of the bite angles here for the ketoimine ligands for both magnesium centres are slightly less than 90° (85.09(8)°, 88.84(8)°, 89.00(8)°) which is similar to the five-coordinate ketoimine literature structures which have a range of 86.25(8)-88.4(1)°, whereas the four-coordinate literature structures tend to have slightly larger bond angles with an average of 92.50(1.46)°. This increase is likely due to the distorted tetrahedral geometry trying to get as close as possible to the ideal bond angle of 109.28°. The remaining angles around the four-coordinated Mg are 80.10(7)°, 110.96(8)°, 117.15(11)°, 120.85(11)°, and 130.98(10)°, to give an average of 108.00(19.3)° – close to the expected tetrahedral. The four-coordinate dipp ketoimine complex in the literature exhibits a more distorted tetrahedral geometry with a range of angles from 91.58(6) – 143.43(7)° with an average of 111.43(5.1)°. The four-coordinate cyclohexane ketoimine in the literature is the least distorted tetrahedron with the range of angles being from 93.34(4) – 123.80(5)° with an average close to a perfect tetrahedron at 109.83(14.4)°.

Table 2.9 – Selected average bond lengths (Å) and angles (°) of magnesium complex 3b.*

Bond	Actual	Calc	Angle	Actual	Calc
O_{br}–C_2	1.320(9)	1.317	O–C_2–C_3	123.79(88)	124.32
O_{nbr}–C_2	1.278(3)	1.283	C_2–C_3–C_4	127.52(57)	128.13
C_2–C_3 (brlig)	1.354(3)	1.376	C_3–C_4–N	122.83(29)	123.88
C_2–C_3 (nbrlig)	1.380(4)	1.396	C_4–N–C_6	118.68(71)	119.56
C_3–C_4 (brlig)	1.441(11)	1.442	C_2–O–Mg	126.6(3.1)	125.78
C_3–C_4 (nbrlig)	1.410(4)	1.422	C_4–N–Mg	124.82(80)	122.73
C_4–N (brlig)	1.302(3)	1.312	O_{br}–Mg_{4-coor}–O_{br}	80.09(7)	79.43
C_4–N (nbrlig)	1.318(3)	1.329	O_{br}–Mg_{5-coor}–O_{br}	77.45(7)	76.91
O–Mg_{4-coor}	2.0008(4)	2.045	O_{br}–Mg_{5-coor}–O_{nbr}	170.21(8)	168.95
O_{br}–Mg_{5-coor}	2.058(39)	2.101		97.11(7)	95.70
O_{nbr}–Mg_{5-coor}	1.9514(18)	1.981	Mg_{4-coor}–O_{br}–Mg_{5-coor}	100.87(1.32)	101.13
N–Mg_{4-coor}	2.105(2)	2.159	O_{nbr}–Mg_{5-coor}–N_{nbrlig}	89.00(8)	89.39
N–Mg_{5-coor} (brlig)	2.153(2)	2.154	O_{nbr}–Mg_{5-coor}–N_{brlig}	92.46(8)	93.07
N–Mg_{5-coor} (nbrlig)	2.107(2)	2.214	O_{br}–Mg_{5-coor}–N_{brlig} (same ligand)	85.09(8)	85.10
Mg_{4-coor}–C_{Bu}	2.134(3)	2.138	O_{br}–Mg_{5-coor}–N_{brlig} (different ligands)	130.01(8)	126.88
			O_{br}–Mg_{5-coor}–N_{nbrlig}	100.61(8) 113.46(8)	101.17 115.45
			N–Mg_{4-coor}–O (same ligand)	88.84(8)	89.29
			N–Mg_{4-coor}–O (different ligands)	110.96(8)	112.77
			N–Mg_{5-coor}–N	115.66(9)	116.93
			N–Mg_{4-coor}–C_{Bu}	117.15(11)	117.51
			O–Mg_{4-coor}–C_{Bu}	120.85(11) 130.99(10)	121.90 126.74

* Key : Br = bridging, lig=ligand, n=non, coor=coordinate, Bu=butyl.

The five-coordinate ketoimine magnesium centre in this complex exhibits a more distorted trigonal bipyramidal geometry than the other two in the literature, in particular shown by the angle of the axial oxgyens with the magnesium centre. In the literature, these angles are closer to linear with 178.62(8)° and 174.9(1)° in comparison with this complex which was found to be 170.21(8)°. There is also a larger range of the angles from the axial atoms to the equitorial atoms, which should ideally be 90°, from 85.09(8)° – 100.62(8)° with an average of 89.57(6.2)° in comparison to the literature which have a range of 85.75(7)° - 94.98(8)° (average: 90.00(4.3)°) and 87.4(1)° – 93.91(1)° (average: 89.93(2.5)°). The angles between the equitorial atoms should ideally be 120°. Observed for **3b** was 115.67(9)°, 113.46(8)°, and 130.00(8)° (average: 119.71(9.0)°) which is similar to the literature values of 114.34(8)°, 115.15(8)°, and 130.49(8)° (average: 119.99(9.1)°) and 117.3(1)°, 117.3(1)°, and 125.4(1)° (average: 120.00(4.7)°).

The magnesium atoms in complex **3b** extend above the plane of the ketoimine by varying amounts – 0.582 Å for the five-coordinate Mg to the bridging ligand, 0.222 Å for the terminal ligand, and 0.570 Å for the four-coordinate Mg bridging ligand. The literature values vary greatly from close to planar with the five coordinate (0.052 - 0.189 Å, average: 0.099(79) Å) to less close to planar with the four-coordinate (0.241 – 0.378 Å, average: 0.340(67) Å) for the same measurement. The values for **3b** are likely due to the four-coordinate and five-coordinate magnesium atoms being attached to one another via the planar Mg_2O_2 central ring. This central ring has Mg–O–Mg bond angles averaging 100.87(1.3)° and O–Mg–O bond angles averaging 78.77(1.9)°. This is quite a bit different from the observed Li_2O_2 central rings in the lithium complexes discussed above which have angles much closer to 90°.

The calculated geometry matches, for the most part, the observed geometry of **3b**. Most significantly, the Mg_2O_2 central ring is calculated to not be planar, and five out of seven of the

bond lengths to the magnesium centres are predicted to be much longer than observed. The remainder of the geometry is well predicted.

2.7 Conclusions

The crystal structures of **1a-d** show, once again, that the solid state of ketoimines is unambiguously the enamine. The crystal structures of **2a-c** were the expected THF coordinated dimer. The cubane complex **4d** was an unexpected result from the same reaction conditions as **2a-c,** but was crystallized in heptane plus approximately 3 molar equivalents of THF with respect to **1d** because of its level of solubility in THF. In interest of comparison, **4a-c** were also made and recrystallized (reaction conditions excluded any coordinating solvent) and for **4b,c** crystal data was collected and solved. The crystals of **4a** were too small for quality X-ray data to be collected.

The NMR spectra of all of the lithium complexes were attempted, but **4a** and **4c** were not soluble enough in the uncoordinating C_6D_6 and therefore spectra for those two complexes could not be collected. **2a,c** were also poorly soluble in pure C_6D_6, but fully assignable spectra were collected using a 1:1 ratio of C_6D_6 and THF. **2b** was soluble in pure C_6D_6 and a high quality ^1H spectrum was collected. The spectra collected in 1:1 C_6D_6:THF for **2b** to compare with **2a,c** showed evidence of relatively slow exchange processes between two lithium species. Interestingly, the ^1H and ^7Li NMR spectra collected for **4b** in C_6D_6 was the same as for **2b** (excluding solvent peaks) and the THF signals in **2b** were the same as previously shown to be free THF in C_6D_6. This, along with evidence of ring shielding of adjacent ligands on the ^1H signal of the methyl on the carbonyl, led to the conclusion that **2b**, **4b**, and **4d** exist in the cubane form in solution state. **2a,c** were concluded to be in either the dimeric or trimeric state in coordinating solution because the ^1H NMR spectra for these species show evidence of exchange between coordinated and uncoordinated THF and also retain the evidence of ring shielding from adjacent ligand(s).

The magnesium complex **3b** of **1b** was also isolated as X-ray quality crystals. Complex **3b** is unlike the other reported magnesium complexes of similar ligands because it has two magnesium centres: one which is 4 coordinate with coordination to butyl along with the nitrogen and oxygen of one ketoimine ligand and the oxygen of another and the oxygens of both of those ketoimine ligands bridging to the other magnesium centre which is 5 coordinate with coordination to the oxygen of one ligand, the nitrogen and oxygen of the other bridging, and the nitrogen and oxygen of a ketoimine ligand which is not shared with the other magnesium centre. This complex was not otherwise characterized because it decomposed before any NMR spectra could be attempted and there was not available time to remake it.

References

1. For example: a. Cho, M.H.; Yoon, J.S.; Lee, I.M. *Bull. Korean Chem. Soc.* **2007**, *28,* 2471; b. Wang, L.Y.; Wu, Q. *Eur. Polym. J.* **2007,** *43,* 3970; c. Jones, D.; Roberts, A.; Cavell, K.; Keim, W.; Englert, U.; Skelton, B.W.; White, A.H. *J. Chem. Soc., Dalton Trans.* **1998,** 255; d. Kim, J.; Hwang, J.-W.; Kim, Y.; Lee, M.H.; Han, Y.; Do, Y. *J. Organomet. Chem.* **2001,** *686,* 1; e. He, X.; Yao, Y.; Luo, X.; Zhang, J.; Liu, Y.; Zhang, L.; Wu, Q. *Organometallics* **2003,** *22,* 4952; f. Chen, Y.; Wu, G.; Bazan, G.C. *Angew. Chem. Int. Ed.* **2005,** *44,* 1108; g. Yu, R.-C.; Hung, C.-H.; Huang, J.-H.; Lee, H.-Y.; Chen, J.-T. *Inorg. Chem.* **2002,** *41,* 6450; h. Lee, W.-Y.; Hsieh, H.-H.; Hsieh, C.-C.; Lee, H.M.; Lee, G.-H.; Huang, J.-H.; Wu, T.-C.; Chuang, S.-H. *J. Organomet. Chem.* **2007,** *692,* 1131; i. He, X.; Chen, Y.; Liu, Y.; Yu, S.; Hong, S.; Wu, Q. *J. Polym. Sci.* **2007,** *45,* 4733; j. Yu, S.; He, X.; Chen, Y.; Liu, Y.; Hong, S.; Wu, Q. *J. Appl. Polym. Sci.* **2007,** *113,* 500.

2. For example: a. Lee, D.-H.; Cho, M.-H.; Kwon, I.-H.; Jun, I.-C.; Lee, I.-M.; Jin, M.-J. *Catal. Commun.* **2008,** *9,* 1517; b. Sachse, A.; Mösch-Zanetti, N.C.; Lyashenko, G.; Wielandt, J.W.; Most, K.; Magull, J.; Dall'Antonia, F.; Pal, A.; Herbst-Irmer, R. *Inorg. Chem.* **2007,** *46,* 7129; c. Xue, F.; Cai, C.; Sun, H.; Shen, Q.; Rui, J. *Tetrahedron Lett.* **2008,** *49,* 4386.

3. For example: a. Lim, S.W.; Lee, J.C.; Shon, D.S.; Lee, W.I.; Lee, I.M. *Chem. Mater.* **2002**, *14,* 1548; b. Lim, S.W.; Choi, B.; Min, Y.S.; Lee, S.S. *J. Organomet. Chem.* **2004**, *689,* 224; c. Neculai, D.; Neculai, A.M.; Roesky, H.W.; Magull, J.; Bunkòczi, G. *J. Fluorine Chem.* **2002,** *118,* 131; d. Turgambaeva, A.E.; Krisyuk, V.V.; Stabnikov, P.A.; Igumenov, I.K. *J. Organomet. Chem.* **2007,** *692,* 5001; see also references 1h and 5.

4. For example: a. Kuo, P.C.; Chen, I.C.; Chang, J.C.; Lee, M.T.; Hu, C.H.; Hung, C.H.; Lee, H.M.; Huang, J.H. *Eur. J. Inorg. Chem.* **2004**, 4898; b. Vajpayee, V.; Singh, Y. *Main Group Metal Chem.* **2006,** *29,* 267; c. Shukla, P.; Gordon, J.C.; Cowley, A.H.; Jones, J.N. *J. Organomet. Chem.* **2005**, *690,* 1366; d. Kuo, P.C.; Chen, I.C.; Lee, H.M.; Hung, C.H.; Huang, J.H. *Inorg. Chim. Acta* **2005,** *358,* 3761; see also reference 1g.

5. a. Ouattara, T.S.; Butcher, R.J.; Matthews, J.S. *J. Coordination Chem.* **2005**, *58,*461; b. Matthews, J.S.; Just, O.; Obi-Johnson, B.; Rees Jr., W.S. *Chem. Vap. Deposition* **2000,** *16,* 129.

6. For example: Hsu, S.-H; Chang, J.-C.; Lai, C.-L.; Hu, C.-H.; Lee, H.M.; Lee, G.-H.; Peng, S.-M.; Huang, J.-H. *Inorg. Chem.* **2004,** *43,* 6786; see also references 1c,d,g,f.

7. Brehon, M.; Cope, E.K.; Mair, F.S.; Nolan, P.; O'Brien, J.E.; Pritchard, R.G.; Wilcock, D.J. *J. Chem. Soc., Dalton Trans*. **1997**, 3421.

8. Allen, F.H.; *Acta Cryst*. B58, **2002**, 380-388.

9. a. Raissi, H.; Moshfeghi, E.; Jalbout, A.F.; Hosseini, M.S.; Fazli, M. *Int. J. Quantum Chem.* **2007,** *107,* 1835; b. Raissi, H.; Bakavol, M.; Jimenez-Fabian, I.; Tajabadi, J.; Mdoshfeghi, E.; Jalbout, A.F. *J. Mol. Struc. : THEOCHEM.* **2007,** *536,* 47.

10. Cromwell, N.H.; Miller, F.A.; Johnson, A.R.; Frank, R.L.; Wallace, D.J. *J. Am. Chem. Soc.* **1949,** *71,* 3337.

11. Holtzclaw, H.F.; Collman, J.P.; Alice, R.M. *J. Am. Chem. Soc.* **1958,** *80,* 1100.

12. Hay, R.W.; Caughly, B.P. *Chem. Commun.* **1965,** 58.

13. Dudek, G.O.; Holm, R.H. *J. Am. Chem. Soc.* **1962,** *84,* 2691.

14. a. Zhuo, J.C. *Magn. Reson. Chem.* **1997,** 21; b. Kashima, C.; Aoyama, H.; Yamamoto, Y.; Nishio, T. *J. Chem. Soc., Perkin Trans. II.* **1975,** 665; c. Brown, N.M.D.; Nonhebel, D.C. *Tetrahedron.* **1968,** *24,* 5688.

15. a. Ribeiro Da Silva, M.A.V.; Ribeiro Da Silva, M.D.M.C.; Paiva, J.P.A; Nogveira, I.M.C.S.; Damas, A.M.; Barkley, J.V.; Harding, M.M.; Akello, M.J.; Pilcher, G. *J. Chem. Soc., Perkin Trans. II* **1993,** 1765; b. Kabak, M.; Elmali, A.; Elerman, Y. *J. Mol. Struc.* **1998,** *470,* 295; c. Chi, Y.; Ranjan, S.; Chung, P.W.; Liu, C.-S.; Peng, S.M.; Lee, G.H. *J. Chem. Soc., Dalton Trans.* **2000,** 343; d. Brbot-Saranovic, A.; Pavlović, G.; Vrdoljak, V.; Cindrić, M. *Croat. Chem. Acta.* **2001,** *74,* 441; e. Cunha, S.; da Silva, V.C.; Napolitano, H.B.; Lariucci, C.; Vencato, I. *J. Braz. Chem. Soc.* **2003,** *14,* 107; f. Rodriguez, J.M.; Hamilton, A.D. *Tetrahedron Lett.* **2006,** *47,* 7443.

16. Martin, D.F.; Janusonis, G.A.; Martin, B.B. *J. Am. Chem. Soc.* **1961,** *83,* 73.

17. Ferraz, H.M.C.; de Oliveira, E.O.; Paynet-Arrua, M.E.; Brandt, C.A. *J. Org. Chem.* **1995,** *60,* 7357.

18. Cartaya-Marin, C.P.; Henderson, D.G.; Soeder, R.W. *Synthetic Commun.* **1997,** *27,* 4275.

19. Osowole, A.A.; Woods, J.A.O.; Odunola, O.A. *Synth. React. Inorg. Met.-Org. Chem.* **2003,** *33,* 167.

20. Azzaro, M.; Geribaldi, S.; Videau, B. *Synthesis-Stuttgart* **1981,** 880.

21. Baraldi, P.G.; Simoni, D.; Manfredini, S. *Synthesis-Stuttgart* **1983,** 902.

22. Zhang, Z.H.; Yin, L.; Wang, Y.M. *Adv. Synth. Catal.* **2006,** *348,* 184.

23. Gao, Y.; Zhang, Q.; Xu, J. *Synthetic Commun.* **2004,** *27,* 909.

24. Khodaei, M.M.; Khosropour, A.R.; Kookhazadeh, M. *Synthesis-Stuttgart* **2004,** 1980.

25. Arcadi, A.; Bianchi, G.; Di Guiseppe, S.; Marinelli, F. *Green Chem.* **2003,** *5,* 64.

26. Khosropour, A.R.; Khodaei, M.M.; Kookhazadeh, M. *Tetrahedron Lett.* **2004,** *45,* 1725.

27. Stefani, H.A.; Costa, I.M.; De O'Silva, D. *Synthesis-Stuttgart* **2000,** 1526.

28. a. Rechsteiner, B.; Texier-Boullet, F.; Hamelin, J. *Tetrahedron Lett.* **1993,** *34,* 5071; b. Braibante, H.T.S.; Braibante, M.E.F.; Rosso, G.B.; Oriques, D.A. *J. Braz. Chem. Soc.* **2003,** *14,* 994; c. Valduga, C.J.; Squizani, A.; Braibante, H.S.; Braibante, M.E.F. *Synthesis-Stuttgart* **1998,** 1019.

29. Khodaei, M.M.; Khosropour, A.R.; Kookhazadeh, M. *Can. J. Chem.* **2005,** *85,* 209.

30. Katritzky, A.R.; Fang, Y.; Donkor, A.; Xu, J. *Synthesis-Stuttgart* **2000,** 2029.

31. Kabek, M.; Elmali, A.; Elerman, Y. *J. Mol. Struc*. **1998**, *470,* 295; see also references 14a,d,e,f.

32. NAWKUS, Allen, F.H.; *Acta Cryst*. B58, **2002**, 380-388.

33. Gui, G.-Q.; Bao, F.; Lü, X.-Q.; Wu, Q.; Ng, S.W. *Acta Crystallogr., Sect. E: Cryst. Struc. Commun.* **2005**, o1070.

34. Boeré, R.T; Zhang, Y. *J. Organomet. Chem.* **2005**, *690,* 2651.

35. a. Hunter, C.A.; Sanders, J.K.M. *J. Am. Chem. Soc.* **1990,** *122,* 5525. b. Arnstein, S.A.; Sherrill, C.D. *Phys. Chem. Chem. Phys.* **2008**, 2646.

36. a. Klump, G.W.; Vos, M.; De Kanter, F.J.J.; Slob, C.; Krabbendam, H.; Spek, A.L. *J. Am. Chem. Soc.* **1985**, *117,* 8292. b. Lee, K.S.; Williard, P.G.; Suggs, J.W. *J. Organomet. Chem.* **1986**, *671,* 311.

37. a. Fernandez, I.; Price, R.D.; Bolton, P.D.; Mahon, M.F.; Davidson, M.G.; Lopez-Ortiz, F. *J. Organomet. Chem.* **2004,** *689,* 1890; b. Cetinkaya, B.; Gumrukcu, I.; Lappert, M.F.; Atwood, J.L.; Shakir, R. *J. Am. Chem. Soc.* **1980,** *112,* 2086; c. Scholz, J.; Gorls, H.; Schumann, H.; Weimann, R. *Organometallics* **2001,** *20,* 4394; d. Hvoslef, J.; Hope, H.; Murray, B.D.; Power, P.P. *Chem. Commun.* **1983,** *23,* 1438; e. Schmidpeter, A.; Burget, G.; von Schnering, H.G.; Weber, D. *Angew. Chem., Int. Ed.* **1984,** *24,* 816; f. Huffman, J.C.; Geerts, R.L.; Caulton, K.G. *J. Crystallogr. Spectrosc. Res.* **1984,** *14,* 541; g. Bruce, S.; Hibbs, D.E.; Jones, C.; Steed, J.W.; Thomas, R.C.; Williams, T.C. *New J. Chem.* **2003,** *27,* 466; g. Arnett, E.M.; Nichols, M.A.; McPhail, A.T. *J. Am. Chem. Soc.* **1990,** *112,* 7059; h. Davidson, M.G.; Davies, R.P.; Raithby, P.R.; Snaith, R. *Chem. Commun.* **1996,** 1695; h. Henderson, K.W.; Kennedy, A.R.; MacDougall, D.J.; Strachan, D. *Acta Crystallogr., Sect. C: Cryst. Struc. Commun.* **2003,** m49; i. Mair, F.S.; Scully, D.; Edwards, A.J.; Raithby, P.R.; Snaith, R. *Polyhedron* **1995,** *14,* 2397; i. Apeloig, Y.; Zharov, I.; Bravo-Zhivotovskii, D.; Ovchinnikov, Y.; Struchkov, Y. *J. Organomet. Chem.* **1995,** *680,* 73.

38. Ringer, A.L.; Sherrill, C.D. *Chem. Eur. J.* **2008**, *14,* 2542–2547.

39. For example: a. Armstrong, D.R.; Henderson, K.W.; Kennedy, A.R.; Kerr, W.J.; Mair, F.S.; Moir, J.H.; Moran, P.H.; Snaith, R. *J. Chem. Soc., Dalton Trans.* **1999,** 4063; b. Andrews, P.C.; Calleja, S.M.; Maguire, M. *J. Chem. Soc., Dalton Trans.* **2002,** 3640**.**

40. Günther, H. "Lithium NMR". *Encyclopedia of Magnetic Resonance.* **2007,** John Wiley and Sons, Ltd (Accessed on Wiley Interscience).

41. Hamaki, H.; Takeda, N.; Yamasaki, T.; Sasamori, T.; Tokitoh, N. *J. Organomet. Chem.* **2007,** *692,* 44.

42. Gottlieb, H.E.; Kotlyar, V.; Nudelman, A. *J. Org. Chem.* **1997**, *62,* 7512.

43. a. Ellison, J.J.; Power, P.P. *J. Organomet. Chem.* **1996,** 263; b. Bartlett, R.A.; Olmstead, M.M.; Power, P.P. *Inorg. Chem.* **1994,** *33,* 4800; c. Westerhausen, M.; Schwarz, W.Z. *Z. Z. Anorg. Allg. Chem.* **1992,** *618,* 39; d. Engelhardt, L.M.; Jolly, B.S.; Junk, P.C.; Raston, C.S.; Skelton, B.W.; White, A.H. *Aust. J. Chem*. **1986,** *39,* 1337; e. Zechmann, C.A.; Boyle, T.J.; Rodriguez, M.A.; Kemp, R.A. *Polyhedron*, **2000,** *19,* 2557.

44. a. Matthews, J.S.; Ouattara, T.S.; Butcher, R.J. *Acta Crystallogr. Sect. E: Struct. Rep. Online,* **2005,** m2598; b. Corazza, F.; Floriani, C.; Chiesi-Villa, A.; Guastini, C.; Ciurli, S. *J. Chem. Soc., Dalton Trans.* **1988**, 2341; c. Matthews, J.S.; Just, O.; Obi-Johnson, B.; Rees Junior, W.S. *Chem. Vap. Deposition* **2000,** *6,* 129; d. Sedai, B.; Heeg, M.J.; Winter, C.H. *J. Organomet. Chem.* **2008,** *693,* 3495.

Chapter 3

Alkynyl Imines and Diimines

3.1 Literature Background on Alkynyl Imines

Alkynyl imines (**A-6**) have been investigated extensively particularly in the last 15 – 20 years due to their synthetic utility as precursors for a variety of potentially biologically active molecules and molecules with potential utility in materials science. The following discussion will be limited to alkynyl imines where R ≠ H, although much of the synthetic uses can be expanded to similar types of reactions for all alkynyl imines.

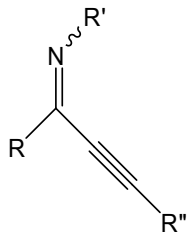

A-6

Figure 3.1 – The general form of alkynyl imines.

3.1.1 Literature Synthesis of Alkynyl Imines

A variety of synthetic methods have been used to make alkynyl imines of the type of interest here. Most of them are summarized in Scheme 3.1:

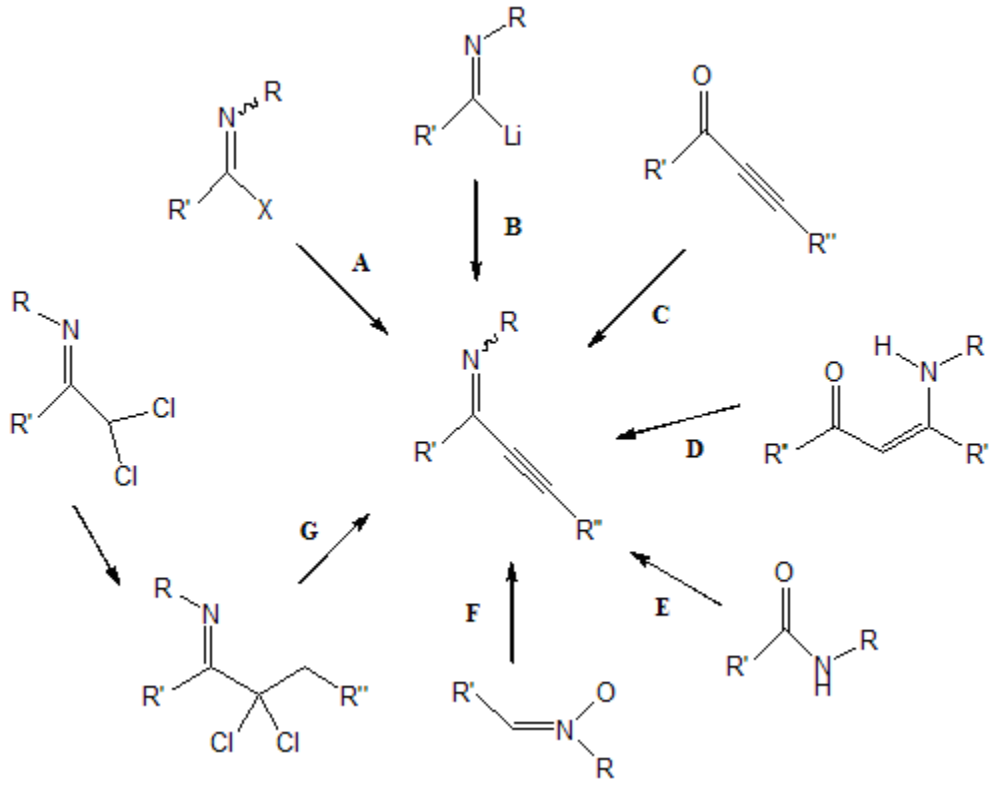

Scheme 3.1 – Summary of the synthetic methods used in the literature for obtaining alkynyl imines. Reaction conditions as follows: A. (1) R″–C≡C–H, Et_3N, Pd(II) acetate, Ph_3P, X=Cl;[1] (2) R″–C≡C–H, Et_3N, $Cl_2(Ph_3P)_2Pd$, CuI, X= Cl, I;[2] (3) R″–C≡C–H, Pd(0) catalyst, Cu(I) species, X = Cl, I;[3] (4) Li[R″–C≡C–Cu–I, X = Cl;[4] (5) R″–C≡C–MgBr, X = Cl;[5] (6) R″–C≡C–H, Step 1: EtMgBr, Step 2: CuBr·Me_2S, Step 3: the imidoyl chloride;[6] B. Ph–C≡C–Br;[7] C. (1) R–NH_2, molecular sieves;[2a, 8] (2) silica gel in CCl_4;[5b] (3) RN=CHR′, reduced pressure;[8] D. 3 Steps: 1. LiTMP, 2. TMSCl, 3. NH_4Cl;[9] E. (1) 3 Steps: 1. $CHCl_2$, C_5H_4ClN, 2. $(CF_3SO_2)_2O$, 3. TMSC≡CCu;[10] (2) Tf_2O, Ph_3PO, CH_2Cl_2, R″–C≡C–TMS;[11] F. R″–C≡C–H, CuI–dppe, K_2CO_3, DMF;[12] G. NaH, DMSO.[13]

The synthesis of alkynyl imines was first reported by Austin et al.[1] in 1981 as the group's research into acetylene-terminated aromatic and heteroaromatic oligomers prompted the development of an efficient synthesis of ethynylated compounds. As a part of this development they made one alkynyl imine via route A, which is a palladium-catalyzed coupling reaction between imino halides and mono-substituted acetylene which is a reaction that was further developed by other groups and has been used commonly in the literature.[2, 3] Also starting from the imidoyl chloride, Wurthwein in 1987,[4] through the development of the synthesis for the novel type of compound, 2-azabut-1-en-3-nes (Figure 3.2), reported the synthesis of one alkynyl imine

by use of a lithium copper iodide alkyl acetylene reagent. In addition, other groups have reported using Grignard or copper reagents to add the alkynyl group to various imidoyl chlorides.

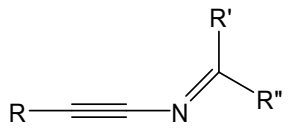

Figure 3.2 – The general form of 2-azabut-1-en-3-nes.

The second alkynyl imine in the literature was generated by the B reaction as a portion of a synthetic study which used imines as a synthetic precursor to the corresponding ketones via hydrolysis of the imine. The starting point here was instead the lithiated imine to which a brominated acetylene was added.[7]

Two types of reactions starting from the alkynyl ketone: (1) condensation[2a, 5b, 8] and (2) exchange[8] are shown as reaction type C. The condensation type of reaction is used commonly to make imines or add an imino group to make other types of compounds such as ketoimines as done in the previous chapter. The first attempt at the condensation reaction was one of the initial attempts of the synthesis of alkynyl imines and it was only minutely successful which led the same group to the exchange reaction which worked better in their case. Other groups have since been more successful with the condensation reaction with changes to the reaction conditions.

Reaction type D in Figure 3.2 with the ketoimine, was designed with the intention of the synthesis of ketones, and alkynyl imines were simply the unexpected product of the reaction which could be converted into the intended ketone. A few minor tweaks to the reaction conditions gave the group their desired product.[9]

The E reaction type uses an amide as a starting point, which can be converted to the respective alkynyl imine via either a copper acetylene reagent or bis(trimethylsilyl)acetylene under metal free reaction conditions. This type of reaction saves the step of converting the amide

into an imidoyl chloride before conversion into the respective alkynyl imine, since amides are the usual precursor to imidoyl chlorides.[10, 11]

Reaction type F, reported by Okura in 1993[12] makes use of a mono-substituted acetylene and copper catalyst under basic conditions to convert a nitroxide into an alkynyl imine. Finally, reaction type G is an elimination reaction that can be used to form the desired alkynyl imine.[13]

Lastly, in addition to the reactions summarized above, one more synthesis of alkynyl imines was discovered in 2005[14] as a result of an odd outcome of a reaction where the desired products were the respective amines (Scheme 3.2).

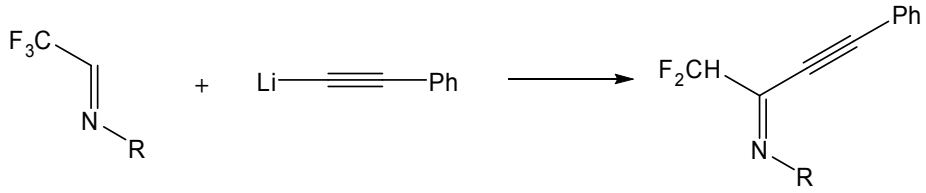

Scheme 3.2 – Unexpected product reported by Magueur in 2005.[14] Reaction conditions: Toluene, -78°C to room temperature. R = Bn, PMP.

3.1.2 Uses of Alkynyl Imines

Alkynyl imines are widely useful synthetic precursors to potentially biologically active molecules and in materials science (Figure 3.3). In particular, these compounds can undergo cyclization reactions (ring-closing reactions) to five and six-membered heterocycles such as pyrrolines **A-7**,[2a] pyrroles **B-7**,[3, 5b, 6, 15] quinolines[6, 16] **C-7** and other pyridine derivatives **D-7**.[10, 16a] In addition to this, alkynyl imines can yield propyne iminium salts **E-7** which are important building blocks in the organic synthesis of aminoallenes, 1- & 2-dienamines, and propargylamines.[5a, 17] Most recently, alkynyl imines have been important precursors to optically pure β,γ-alkenyl α-amino esters **F-7**.[18]

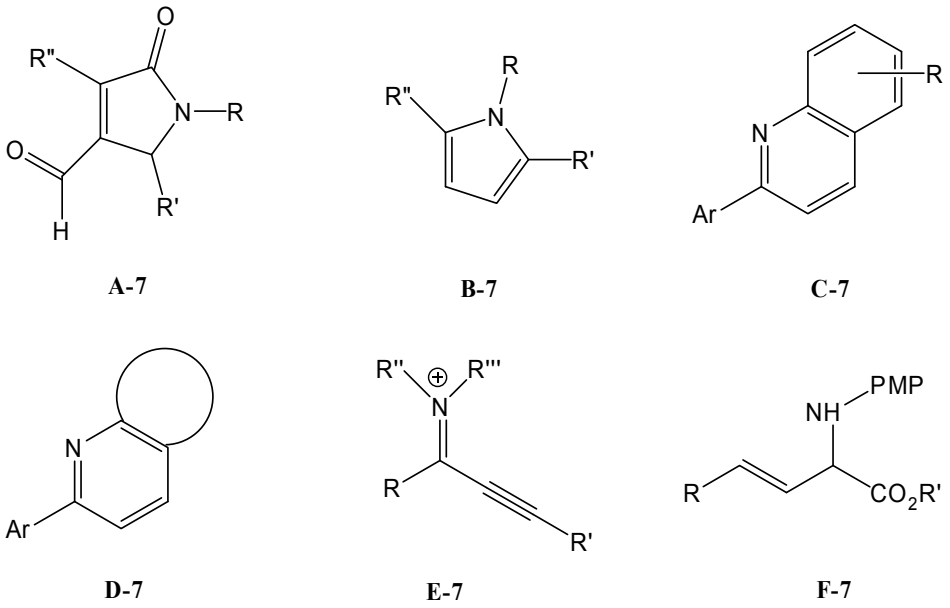

Figure 3.3 – The important molecules that alkynyl imines can be used to make.

3.2 Synthesis

The first attempts to synthesize the desired alkynyl imines involved reaction of imidoyl chloride and sodium or lithium acetylide (Scheme 3.3).

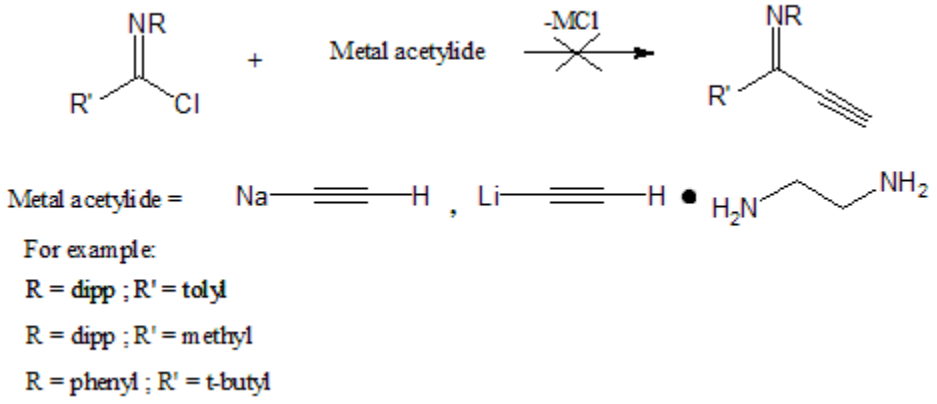

Scheme 3.3 - Metal acetylide synthesis tried first for synthesis of desired alkynyl imines.

These reactions resulted in alkynyl diimines (Figure 3.4) instead of alkynyl imines, which, to the best of our knowledge, are a novel type of compound. The mechanism for this reaction is proposed in Scheme 3.4 using the sodium acetylide reaction as a representative example.

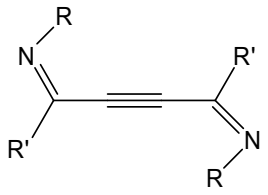

5a : R = Ph, R' = t-Bu
5b : R = Dipp, R' = p-Tol

Figure 3.4 – Novel alkynyl diimines isolated in the first attempted synthesis of alkynyl imines.

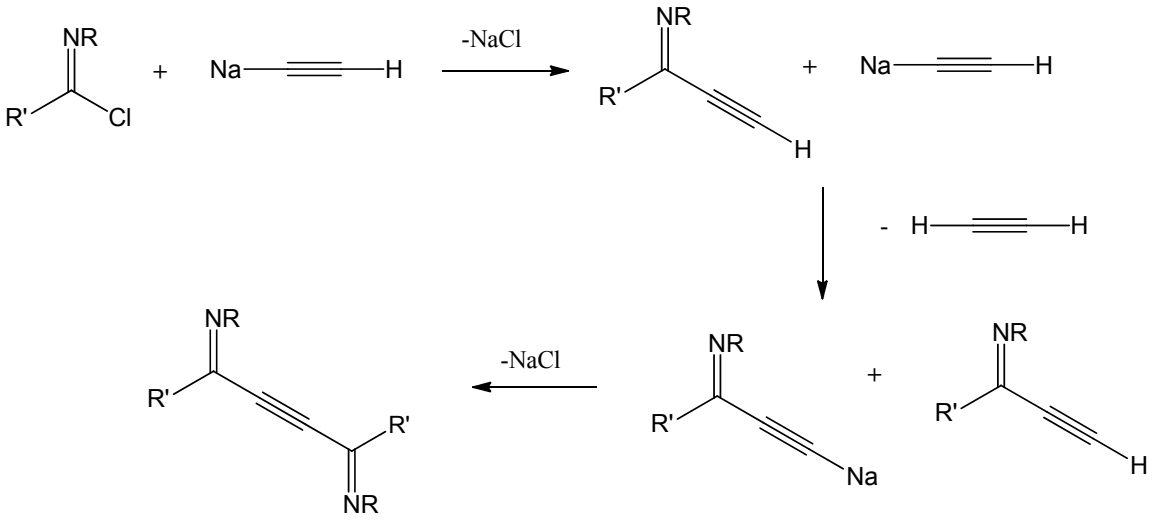

5a: R = Ph, R' = t-Bu
5b: R = Dipp, R' = Tol

Scheme 3.4 – Proposed reaction mechanism which lead to the alkynyl diimine result.

Following this, an alternate route was derived which involved reaction between the imidoyl chloride and bis(trimethylsilyl)acetylene with aluminum chloride catalyst (Scheme 3.5). This reaction proceeds from a different mechanism and therefore was successful in isolating the desired compound after desilylation via the literature method.[19] The less bulky N-dipp-methyl imidoyl chloride gave mixtures from which the desired product was not able to be isolated.

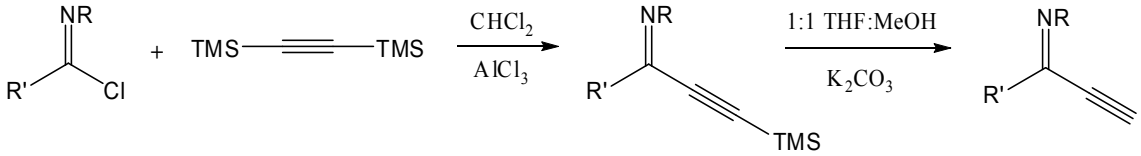

Scheme 3.5 - Reaction scheme for the exact analogue based on literature for acid chlorides.

Therefore, the alkynyl imines to be presented here are shown in Figure 3.5. **6a** and **7a** have been previously reported[10] and the literature values are compared here to the new molecules **5a,b** and **6b, 7b**.

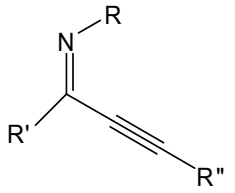

6a: R = Ph, R' = t-Bu, R" = $SiMe_3$
6b: R = Dipp, R' = p-Tol, R" = $SiMe_3$
7a: R = Ph, R' = t-Bu, R" = H
7b: R = Dipp, R' = p-Tol, R" = H

Figure 3.5 – The literature alkynyl imines (6a and 7a) and the new alkynyl imines (6b and 7b) prepared during the research presented here.

3.3 X-Ray Crystallography Results and Discussion

Although many alkynyl imines have been reported, many of them are oils at room temperature, and the few that are crystalline have not had X-ray crystal structures reported on them. In fact, only a few structures containing the R–N=C–C(R)≡C(R) moiety have been reported (Figure 3.6) and are available for comparison to the alkynyl imine and diimines reported here. Key bond lengths and angles are listed in Table 3.1.

Table 3.1 – Important bond lengths (Å) and angles (°) for the alkynyl imine and diimines compared to the B3LYP//6-31G(d) optimized structures, and the average literature values for similar structures.

Bond/Bond Angle	5a	Calc 5a	5b	Calc 5b	6b	Calc 6b	Lit Avg[20]
C≡C	1.1958(18)	1.218	1.193(5)	1.216	1.202(3), 1.203(3)	1.221	1.198(12)
C=N	1.2774(12)	1.285	1.286(3)	1.289	1.283(2), 1.280(2)	1.290	1.282(8)
N=**C–C**≡C	1.4505(12)	1.444	1.456(3)	1.446	1.453(3), 1.448(3)	1.444	1.444(11)
C–C$_R$	1.5270(12)	1.538	1.475(3)	1.487	1.477(3), 1.479(2)	1.488	1.479(23)
C$_{AR}$–N	1.4252(12)	1.407	1.425(3)	1.416	1.420(3), 1.427(2)	1.417	1.434(25)
C–Si					1.850(2), 1.842(2)	1.849	1.863(44)
C$_{AR}$–N=C	119.53(8)	123.26	120.0(2)	122.71	119.60(16), 120.58(16)	122.27	120.0(1.7)
N=C–C$_R$	121.19(8)	119.55	120.8(2)	119.68	119.72(16), 120.03(18)	119.46	118.12(1.48)
N=C–C≡C	122.46(8)	123.52	121.4(2)	122.65	120.79(17), 120.82(18)	122.50	123.86(3.00)
C≡**C–C–C$_R$**	116.28(8)	116.89	117.9(2)	117.68	119.48(16), 119.15(17)	118.02	117.63(1.17)
C–C≡C	177.85(13)	176.37	177.6(2)	179.25	172.1(2), 173.6(2)	177.63	175.76(1.83)
C≡C–Si					169.59(18), 171.34(19)	176.38	174.45(3.51)

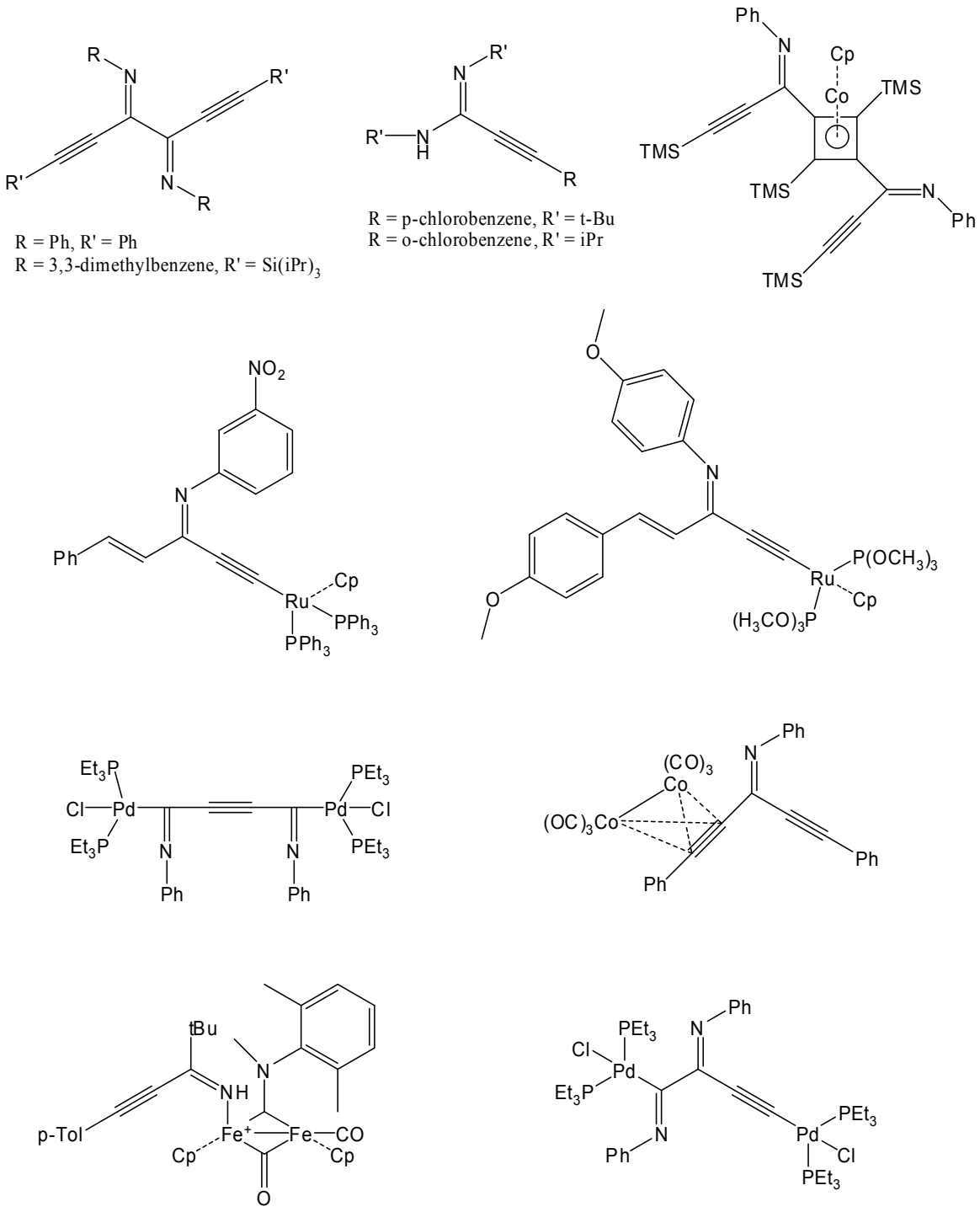

Figure 3.6 – Literature structures containing the R–N=C–C(R)≡C(R) moiety used for comparison to the crystal structures of 5a,b and 6b, 7b.

The alkynyl imine **6b** (Figure 3.7) crystallized with two geometrically similar but independent molecules per equivalent position. Both of these molecules show an unusually large amount of distortion from linearity in the alkynyl portion of the molecule with a C–C≡C bond angle of 172.8(3)° and a C≡C–Si bond angle of 170.46(26)°. The averages in the literature for similar structures are considerably closer to linear with 175.8(1.8)° and 175(4)°, respectively, although some individual structures do show the same type of deviation for those bond lengths. The DFT calculated structure the angles are 177.63° and 176.38°, respectively. The alkynyl diimines are closer to linearity with C–C≡C bond angles of 177.85(13)° and 177.6(2)° for **5a** and **5b**, respectively.

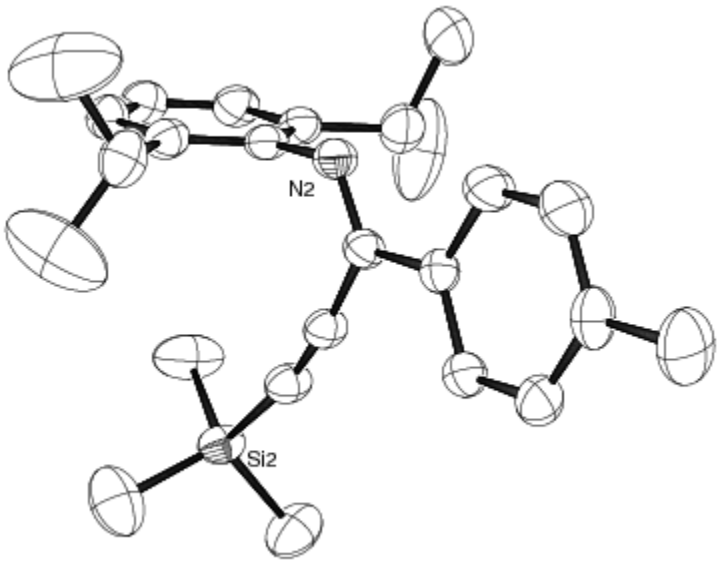

Figure 3.7 – The ORTEP diagram of alkynyl imine 6b. Hydrogen atoms have been omitted for clarity (50% probability ellipsoids shown).

The alkynyl diimines **5a,b** (Figures 3.8 and 3.9) crystallize with a crystallographic centre of symmetry. The geometric parameters as outlined above show a great deal of similarity to each other as well as to the alkynyl imine to a lesser degree. All of these values match reasonably well with the literature values of similar structures and with the DFT calculated structures.

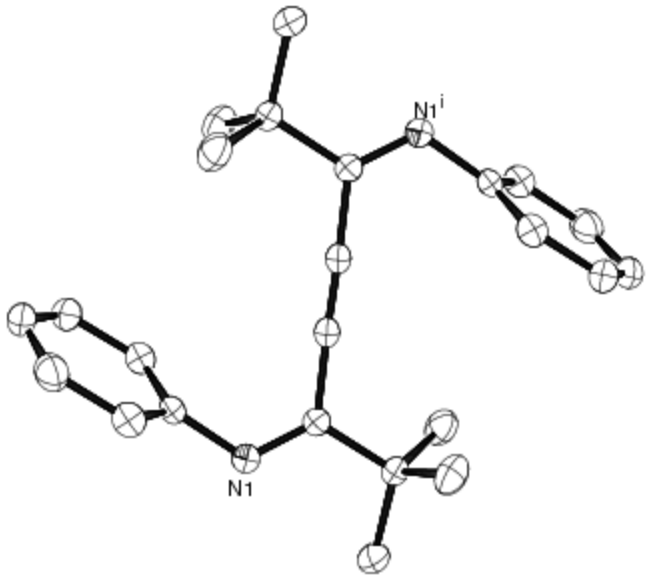

Figure 3.8 – ORTEP diagram for alkynyl diimine 5a. Hydrogen atoms omitted for clarity (50% probability ellipsoids shown). N_1^i was generated by a centre of symmetry.

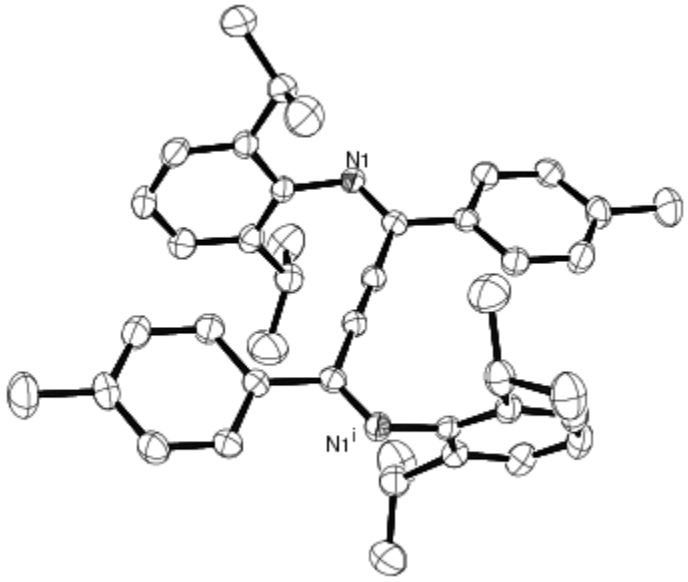

Figure 3.9 – ORTEP diagram for alkynyl diimine 5b. Hydrogen atoms omitted for clarity (50% probability ellipsoids shown). N_1^i was generated by a centre of symmetry.

For all three structures, the arrangement of the substituents are similar with the plane of the aryl group on the nitrogen close to perpendicular to the plane of the molecule, with 70.63°, 76.87°, and 87.70° (average) for **5a**, **5b**, and **6b**, respectively. For **6b** and **5b** the plane of the second aryl

substituent, the p-tol, is close to parallel to the plane of the molecule, with angles of 6.99° and 7.90°, respectively.

3.4 NMR results and discussion

Comparison of the ^{1}H NMR spectrum of the alkynyl diimine **5a**, with the literature NMR spectrum of alkynyl imines **6a** and **7a,**[10] and of the NMR spectra of **5b** with **6b** and **7b** reveals interesting parallels. The NMR data is given in Tables 3.2 and 3.3.

Table 3.2 – ^{1}H NMR spectral comparison of 5a and literature analogs 6a and 7a in $CDCl_3$.

^{1}H Signal	5a	6a[10]	7a[10]
Meta-Ph	7.31 - 7.25 (m, 2H)	7.32 - 7.28 (m, 2H)	7.32 - 7.28 (m, 2H)
Para-Ph	7.08 (t, 1H)	7.11 - 7.06 (m, 1H)	7.12 (t, 1H)
Ortho-Ph	6.72 (d, 2H)	6.92 - 6.88 (m, 2H)	6.92 - 6.88 (m, 2H)
Alkyne H			3.14 (s, 1H)
t-Bu	0.991 (s, 12H)	1.31 (s, 12H)	1.33 (s, 9 H)
TMS Me		0.5 (s, 9H)	

In general, for both sets of compounds, the silylated and desilylated alkynyl imines have similar signals in the ^{1}H NMR spectra. Most of the ^{1}H NMR signals for the alkynyl diimines are noticeably shifted upfield from those of their alkynyl imine analogues, in particular the ortho-Ph and t-Bu for **5a** and the ortho-tol for **5b**. The origin of the shielding effects on these signals in the diimines is most likely to be found in mutual anisotropic ring-shielding effects between the substituents facing each other across the double bonds in **5a,b**. This is particularly noticeable in the anti conformations adopted by both in the crystals (possibly indicative of some preference for this conformation in which ring shielding effects are maximized). More likely the observed

shielding is attributable to an average effect from free rotation about the single bonds. Any correlation of bond rotation that keeps the larger ends of the molecules out of each other's way would be expected to enhance ring shielding. Examination of space filling models suggests that correlation due to interlocking of substituents across the triple bond is strongly indicated.

Table 3.3 – ^{1}H NMR spectral comparison of 5b and 6b and 7b in $CDCl_3$.

^{1}H Signal	5b	6b	7b
Aromatic	m-tol & dipp: 7.31 - 7.24 (m, 5H) o-tol: 7.07 (d, 2H)	o-tol: 8.11 (d, 2H), m-tol: 7.30 (d, 2H), dipp: 7.14 - 7.07 (m, 3H)	o-tol: 8.13 (d, 2H), m-tol: 7.30 (d, 2H), dipp: 7.18 - 7.07 (m, 3H)
Alkyne H			3.22 (s, 1H)
iPr CH	2.71 (sept, 2H)	2.79 (sept, 2H)	2.80 (sept, 2H)
Tol Me	2.40 (s, 1H)	2.44 (s, 1H)	2.44 (s, 1H)
iPr Me	1.11 (d, 6H), 1.03 (d, 6H)	1.15 (d, 6H), 1.13 (d, 6H)	1.17 (d, 6H), 1.13 (d, 6H)
TMS Me		–0.02 (s, 9H)	

3.5 Electrochemistry results and discussion

Alkynyl diimines **5a** and **5b** have an extended π system which could have interesting electrochemical properties. The presence of electrochemical activity was therefore studied by square wave voltammetry and cyclic voltammetry. **5a** has two 1 electron irreversible oxidation processes and one 2 electron irreversible reduction process as shown in Figure 3.10. The peak current for the oxidation processes were found at +1.76 and +1.96 V with a small offset return wave at a peak current of –0.20 V. The peak current for the reduction process is at –1.92 V with no return wave observed.

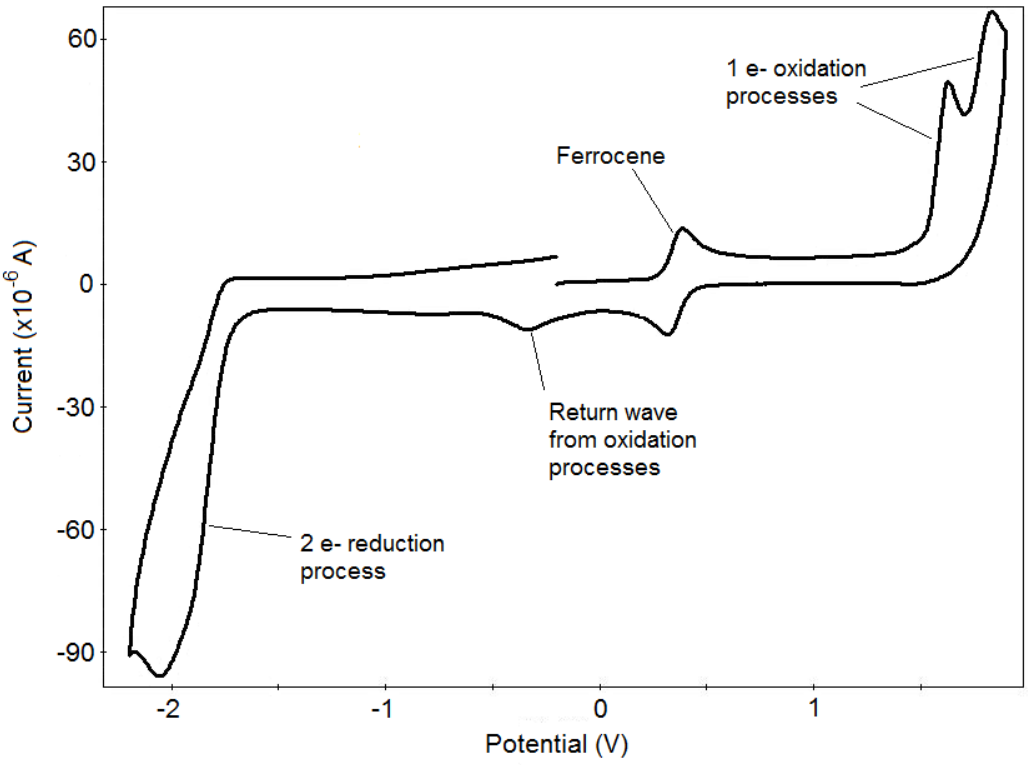

Figure 3.10 – CV of 5a in CH_2Cl_2 on a GC electrode at 0.7 M [^{n}Bu$_4$N][PF_6], ν = 0.2 V s^{-1} referenced to ferrocene at 0 V.

The alkynyl diimine **5b** showed similar activity for the oxidation processes with two 1 electron irreversible processes with two small offset return waves. The reduction side was different than **5a** with an apparent 1 electron process that shows a non-offset return wave. The peak currents as labeled in the full CV in Figure 3.11 were found to be as follows: E_{pc1} = 1.65 V, E_{pc2} = 1.88 V, E_{pa1} = 1.36 V, E_{pa2} = –0.04 V, E_{pa3} = –1.58 V, and E_{pc3} = –1.43 V. The $E_{1/2}$ for the reduction process was found to be –1.50 V. This process became less reversible with increasing rate as shown by the I_{pc}/I_{pa} ratio which decreased from 0.54 at 100 mv/s to 0.44 at 500 mv/s. The CV of the various rates of the reduction process is shown in Figure 3.12 and the ΔEp versus scan rate is shown in Table 3.4. Additionally, a dark red colour was generated at the auxiliary electrode during the reduction process which may indicate that a radical is produced in the process.

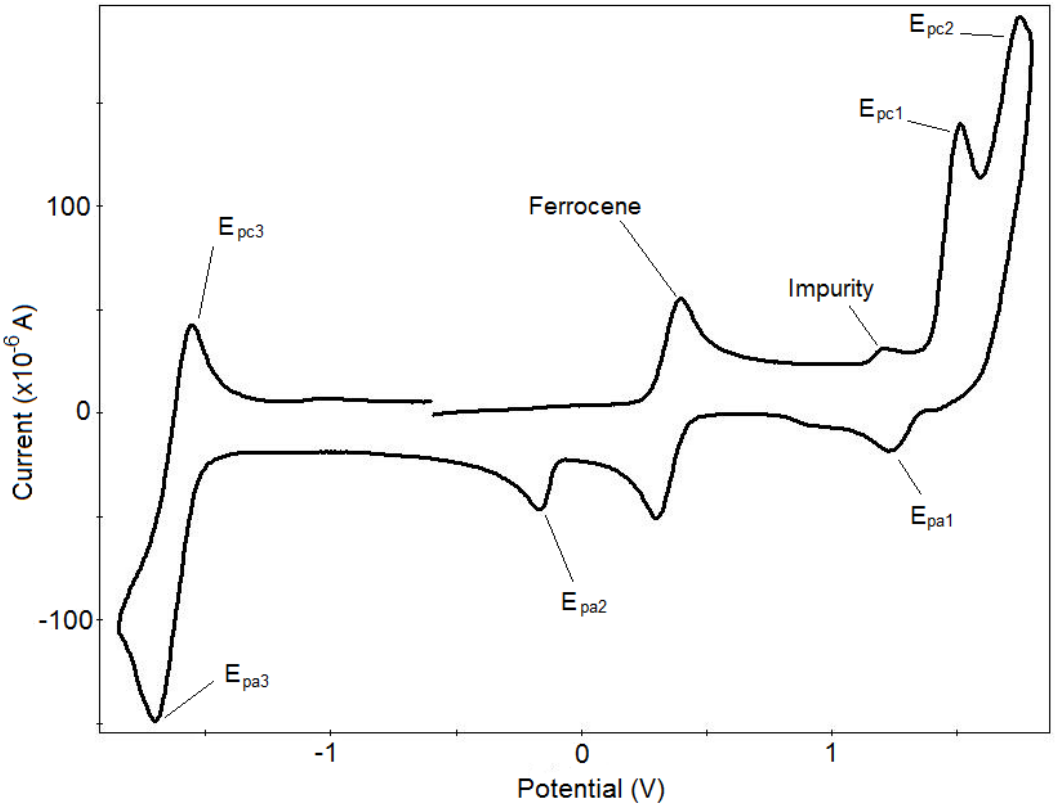

Figure 3.11 – CV of 4.65 mM 5b in CH_2Cl_2 on a GC electrode at 24.5 °C, 0.7 M [^{n}Bu$_4$N][PF_6], ν = 0.2 V s^{-1} referenced to ferrocene.

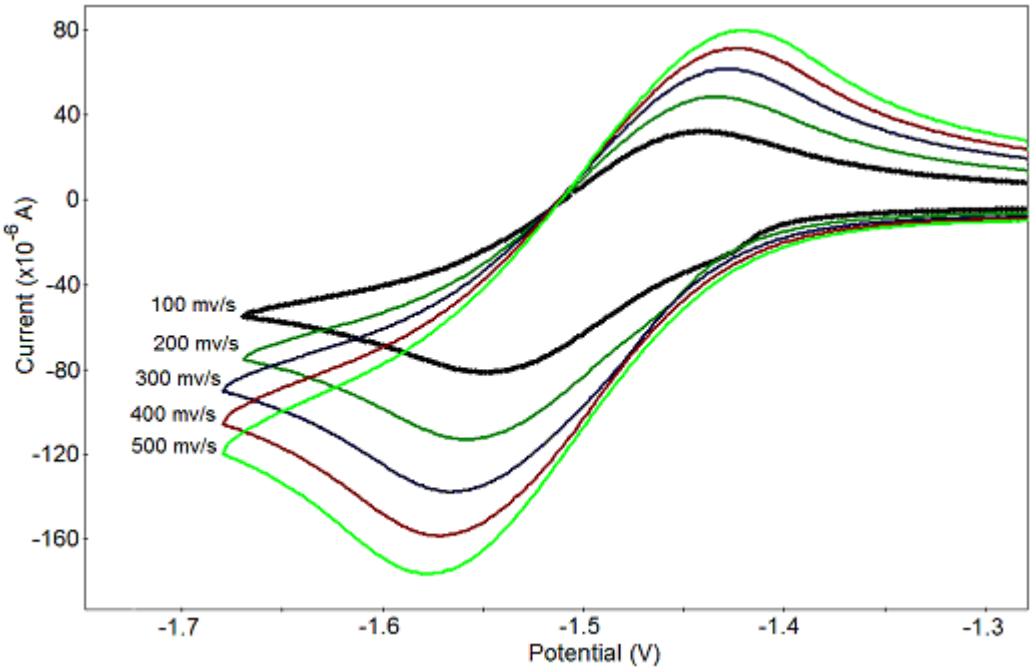

Figure 3.12 – CV of 4.65 mM 5b in CH_2Cl_2 on a GC electrode at 24.5 °C, 0.7 M [^{n}Bu$_4$N][PF_6], at various rates referenced to ferrocene.

Table 3.4 – ΔE_P versus the scan rate for the 5b reduction process referenced to ferrocene with conditions as given above in Figure 3.16.

Scan Rate (mv/s)	E_{pc3} (V)	E_{pa3} (V)	$E_{1/2}$ (V)
100	–1.44	–1.55	–1.50
200	–1.44	–1.56	–1.50
300	–1.43	–1.56	–1.50
400	–1.43	–1.57	–1.50
500	–1.42	–1.58	–1.50

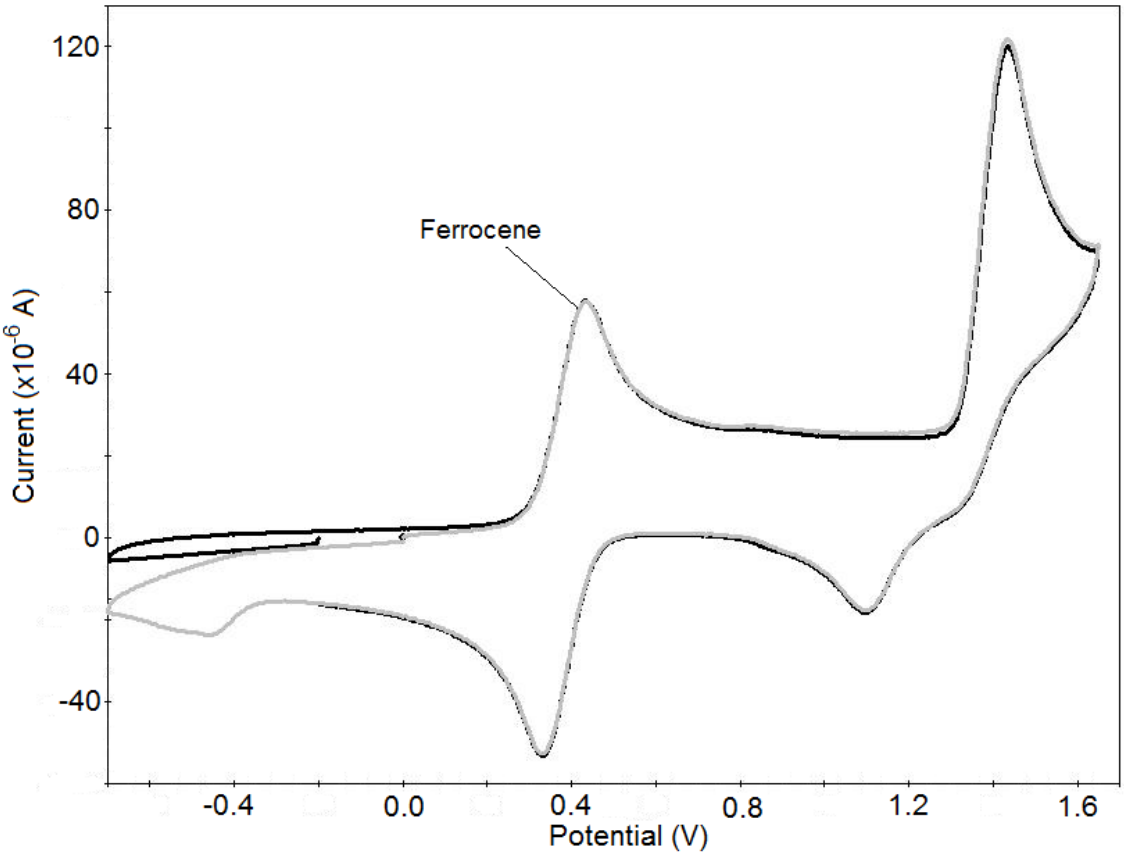

Figure 3.13 – CV of 4.30 mM 6b in CH_2Cl_2 on a GC electrode at 24.5 °C, 0.7 M [^{n}Bu$_4$N][PF_6], ν = 0.2 V s^{-1} referenced to ferrocene. No reduction processes were observed, however the light grey line shows an additional return wave in the negative region after passing through the oxidation process first.

Alkynyl imine **6b** was studied for the same electrochemical processes as the alkynyl diimines for comparison purposes and the CV is shown in Figure 3.13. A 1 electron irreversible oxidation with peak current at 1.53 V and two small offset return waves at 1.20 and –0.36 V. This oxidation is similar to those observed in the diimines. The imine did not show any reduction processes in the available electrochemical window (which was the same size as for the other compounds).

Comparison of the HOMO's and LUMO's of each of the molecules is helpful in explaining both the similarity and differences seen in the oxidation and reduction processes. The HOMO's (shown in Appendix A) are all dominated by the aryl substituent on the imino (phenyl for **5a**, Dipp for **5b**, **6b**, **7b**). This seems to stabilize the triple bond, making the molecules difficult to oxidize. The oxidation is noticeably more difficult for **5a,b** than for **6b**. The trend from most difficult to least difficult oxidation, **5a** > **5b** > **7b** > **6b**, can be assigned by the calculated energy of the HOMO for each (-5.94 eV for **5a**, -5.79 eV for **5b**, -5.64 eV for **7b**, and -5.59 eV for **6b**). This trend matches the trend observed experimentally. The HOMO's also explain why two oxidation processes are observed for **5a,b** and only one is observed for **6b**. Molecules **5a,b** have two aryl imino substituents dominated in the HOMO whereas **6b** only has one.

The LUMO is the orbital of interest for the reduction process (also shown in Appendix A). The LUMO of **5b**, shows significant conjugation between tolyl ring, the alkyne, and most importantly, the imine double bond. The other LUMO's do show conjugation between the alkyne and the tolyl ring, but not the imine bond. Therefore, the conjugation of the tolyl ring with the imine and alkyne is likely responsible for the easy and partially reversible reduction for **5b**.

3.6 UV/VIS results and discussion

All of the alkynyl imines and diimines are brightly coloured chromophores and therefore should have interesting electronic absorption spectra. In order to help explain the results of the collected spectra, the molecular orbitals and the UV/VIS spectra were also calculated by TD-DFT in Gaussian 03 of the calculated DFT structures. The results of this are shown in Table 3.5 and Figures 3.18-3.21.

The UV/VIS spectra of **6b** and **7b** were well-predicted by TD-DFT calculations as can be seen in Table 3.5 and Figures 3.14 and 3.15. The UV/VIS spectra of **5a** and **5b** (particularly **5b**) were poorly described by the same type of calculation (Figures 3.16 and 3.17), likely due to the increase in size of the system.[21] Analysis of the molecular orbitals (MO's) of the well-described alkynyl imines, and the less poorly described **5a**, revealed a distinct trend in the type of occupied MO's that electrons were being excited from. All of the occupied MO's that allowed the excitation of an electron were bonding MO's for the alkyne bond and in all but two cases (out of 8), also bonding for the C=N bond. In contrast, the occupied MO's that were calculated for poorly described **5b** to allow the excitation of an electron were either weakly bonding, non-bonding, or even anti-bonding for the above bonds. Further analysis of the MO's of **5b**, both the energies and the type with regards to the alkyne and imine bonds, led to successful assignment of the experimentally observed absorptions, which are incidentally similar to those observed for the structurally related **6b** and **7b**. The occupied MO's discussed above are shown in Appendix A.

Table 3.5 – Experimental (Exp) and calculated (Calc) values for the UV/VIS spectra of the alkynyl imines and diimines.

Sample	Conc† (M)	Wavelength of Peaks (nm)		Electronic Transition	Value of e ($Lcm^{-1}mol^{-1}$)	
		Exp	Calc		Exp	Calc
5a	$1.011x10^{-4}$	340.9	316.3	HOMO-5 → LUMO HOMO-2 → LUMO	3460	1000
			394.9	HOMO-1 → LUMO HOMO → LUMO		800
			401.3	HOMO-1 → LUMO HOMO → LUMO		5250
5b	$1.211x10^{-5}$	278.0	279.5*	HOMO-6 → LUMO*	28100	
		299.1	306.7*	HOMO-4 → LUMO*	24100	
			381.7	HOMO-3 → LUMO		25
			472.4	HOMO-1 → LUMO		10
			480.1	HOMO → LUMO		400
6b	$1.378x10^{-5}$	276.0	290.8	HOMO-5 → LUMO HOMO-2 → LUMO	20200	14900
			427.1	HOMO → LUMO		500
7b	$1.828x10^{-5}$	276.0	286.0	HOMO-3 → LUMO HOMO-4 → LUMO	20700	19800
			423.5	HOMO → LUMO		500

* The absorption values and transitions were hand calculated by analysis of the molecular orbitals; they were not found by the TD-DFT calculation in Gaussian.
† In CH_2Cl_2.

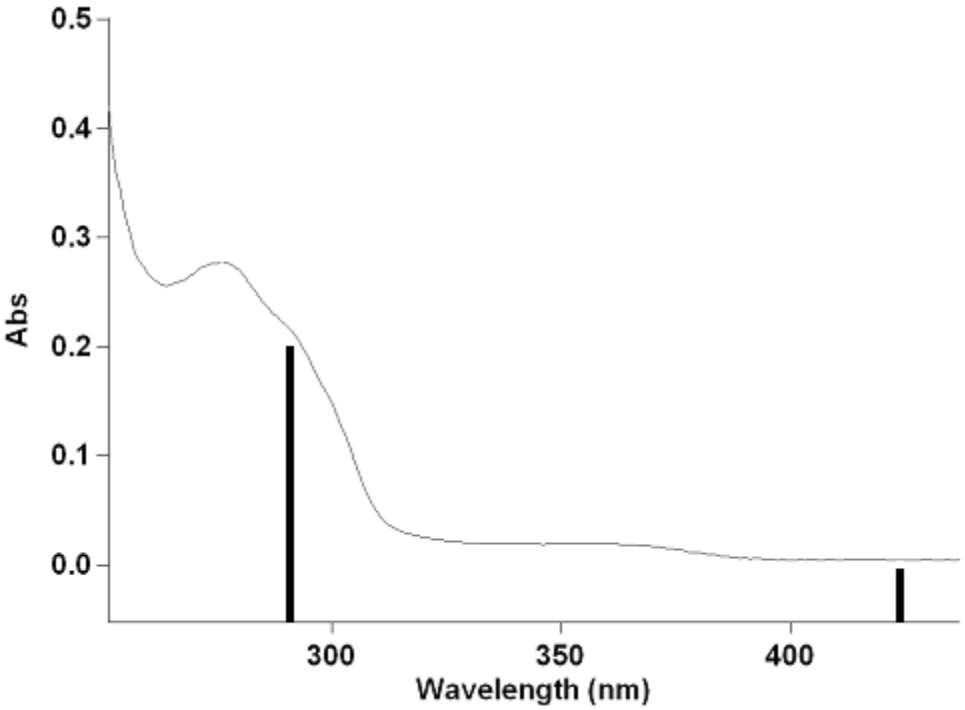

Figure 3.14 – UV/VIS spectrum of 6b (line) and calculated absorptions (bars) in CH_2Cl_2.

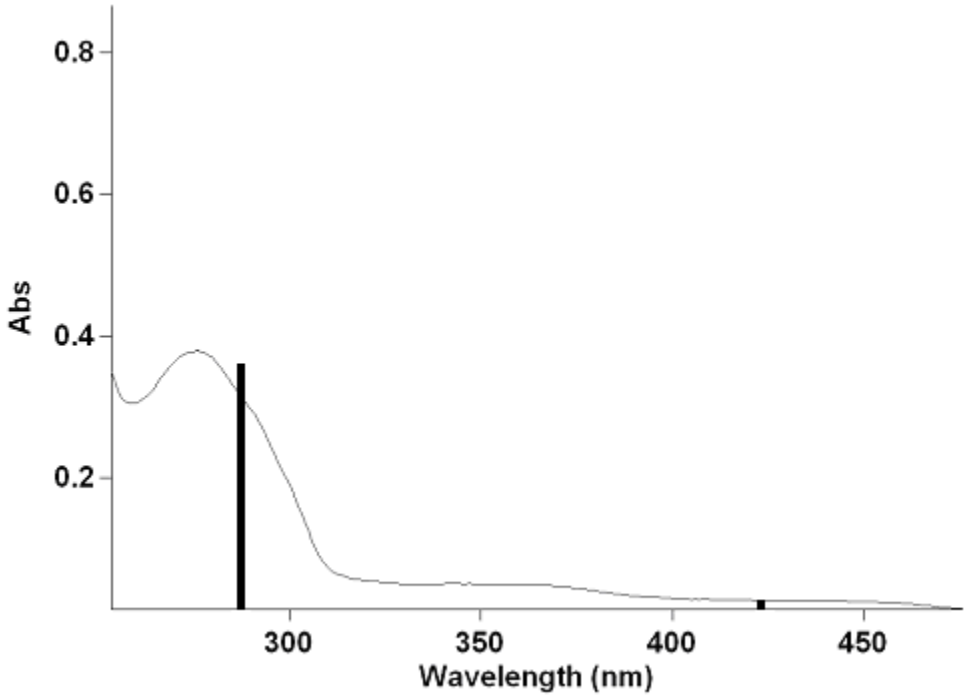

Figure 3.15 – UV/VIS spectrum of 7b (line) and calculated absorptions (bars) in CH_2Cl_2.

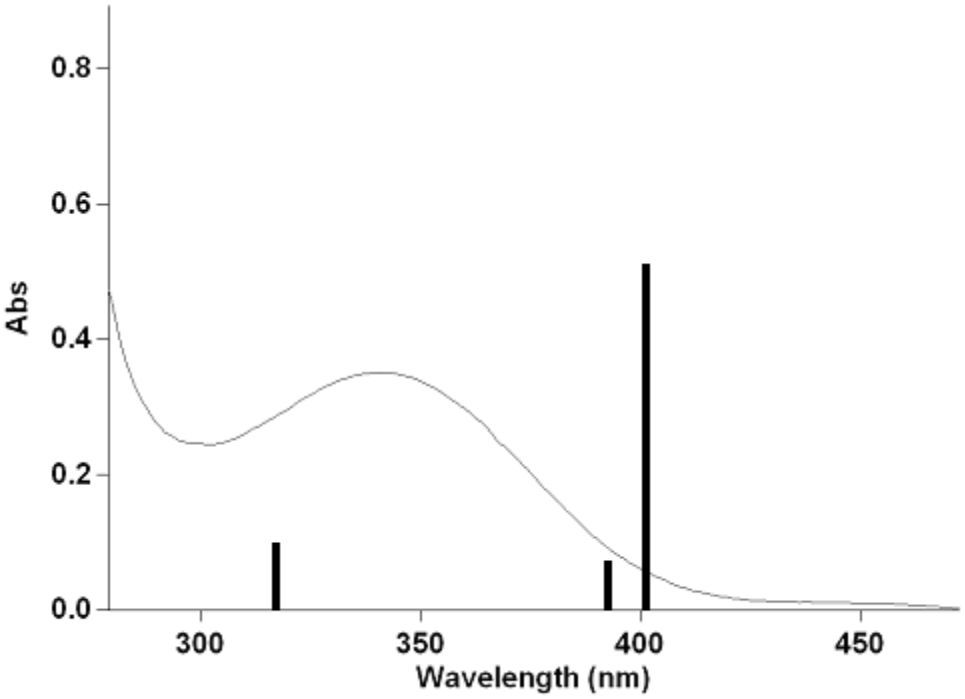

Figure 3.16 – UV/VIS spectrum for 5a (line) and calculated absorptions (bars) in CH_2Cl_2.

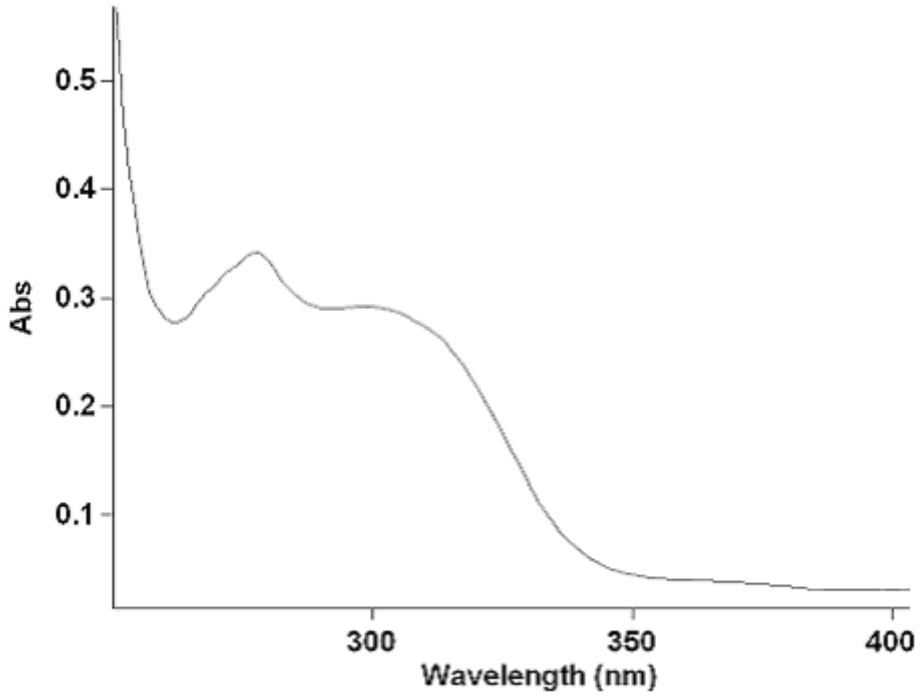

Figure 3.17 – UV/VIS spectrum for 5b in CH_2Cl_2. The calculated absorptions had too small of intensity to indicate on the above spectrum. The values are given in Table 3.5.

3.7 Conclusions

The iminophosphenate route to PacNac, which required the synthesis of particular imino alkynes which have not been previously published, led to the synthesis of the new class of molecules: diimino alkynes **5a,b** via the first attempted route to the desired imino alkynes **6b** and **7b** which were later successfully prepared by another route. The X-ray crystal structures for **5a,b** and **6b** were also successfully solved for and then compared to the few other reported literature structures containing the R–N=C–C(R)≡C(R) moiety. The structural parameters (bond lengths and angles) of **5a,b** and **6b** were similar to the already reported literature structures.

The electrochemical properties of the extended π systems of **5a,b** and **6b** were also probed via cyclic voltammetry. The molecules had similar oxidation processes, with the diimines each having what looks to be two 1 electron processes, while the imine has only one 1 electron process for the oxidation. Significant differences were seen in the CV's for all three molecules on the reduction side. Compound **6b** showed no facile reduction, **5b** showed a facile reduction with partial reversibility, while **5a** had a measurable reduction but was much more difficult to reduce than **5b**. This was explained by the similarities between the HOMO's (for the oxidation processes) and the differences between the LUMO's (for the reduction processes).

The UV/Vis spectra for **5a,b**, **6b**, and **7b** were all collected as well, because as brightly coloured chromophores they were expected to have interesting electronic absorption spectra. Then, because none of the alkynyl imines in the literature have had UV/Vis data reported, for comparison purposes, the TD-DFT calculation of the UV/Vis spectrum for each molecule was performed. The alkynyl imines **6b** and **7b** were well predicted by the TD-DFT method. The alkynyl diimine, **5a**, was less well predicted, while **5b** was predicted poorly. The experimental spectrum of **5b** was assigned by studying the calculated orbital energy differences for a variety of possible transitions. The orbitals for the transitions found to best match the experimental

absorptions for **5b** look similar to the orbitals predicted to be involved in the transitions for well-predicted **6b** and **7b**.

References

1. Austin, W.B.; Bilow, N.; Kelleghan, W.J.; Lau, K.S.Y. *J. Org. Chem.* **1981,** *46,* 2280.

2. a. Van den Hoven, B.G.; Alper, H. *J. Am. Chem. Soc.* **2001,** *123,* 10214; b. Wu, Y.-M.; Zhang, M.; Li, Y.-Q. *J. Fluorine Chem.* **2006,** *127,* 218; c. Lin, S.-Y.; Sheng, H.-Y.; Huang, Y.-Z. *Synthesis* **1991,** 235.

3. Rubin, M.; Sromek, A.W.; Gevorgyan, V. *Synlett* **2003,** 2265.

4. Würthwein, E.-U.; Weigmann, R. *Angew. Chem., Int. Ed. Engl.* **1987,** *23,* 923.

5. a. Schlegel, J.; Maas, G. *Synthesis* **1999,** 100; b. Kel'in, A.V.; Sromek, A.W.; Gevorgyan, V. *J. Am. Chem. Soc.* **2001,** *123,* 2074.

6. Sromek, A.W.; Rheingold, A.L; Wink, D.J.; Gevorgyan, V. *Synlett* **2006,** 2325.

7. Marks, M.J.; Walborsky, H.M. *J. Org. Chem.* **1982,** *47,* 52.

8. Margaretha, P.; Schröder, C.; Wolff, S.; Agosta, W.C. *J. Org. Chem.* **1983,** *48,* 1925.

9. Bartoli, G.; Cimarelli, C.; Palmieri, G. *Tetrahedron Lett.* **1991,** *32,* 7091.

10. Movassaghi, M.; Hill, M.D. *J. Am. Chem. Soc.* **2006,** *128,* 4592.

11. Dong, Q.-L.; Liu, G.-S.; Zhou, H.-B.; Chen, L. Yao, Z.-J. *Tetrahedron Lett.* **2008,** *49,* 1636.

12. Okuro, K.; Enna, M.; Miura, M.; Nomura, M. *J. Chem. Soc., Chem. Commun.* **1993,** 1107.

13. Mangelinckx, S.; Rooryck, S.; Jacobs, J.; De Kempe, N. *Tetrahedron Lett.* **2007,** *48,* 6535.

14. Magueur, G.; Crousse, B.; Bonnet-Delpon, D. *Tetrahedron Lett.* **2005,** *46,* 2219.

15. a. Schwier, T.; Sromek, A.W.; Yap, D.M.L.; Chernyak, D.; Gevorgyan, V. *J. Am. Chem. Soc.* **2007,** *129,* 9868; b. Dudnik, A.S.; Sromek, A.W.; Rubina, M.; Kim, J.T.; Kel'in, A.V.; Gevorgyan, V. *J. Am. Chem. Soc.* **2008,** *130,* 1440.

16. a. Hill, M.D.; Movassaghi, M. *Synthesis.* **2007,** 1115; b. Sangu, K.; Fuchibe, K.; Akiyama, T. *Org. Lett.* **2004,** *6,* 353.

17. a. Espenlaub, S.; Gerster, H.; Maas, G. *Arkivoc.* **2007,** 114; b. Gerster, H.; Espenlaub, S.; Maas, G. *Synthesis* **2006,** 2251.

18. Kang, Q.; Zhao, Z.-A.; You, S.-L. *Org. Lett.* **2008,** *10,* 2031.

19. Morisaki, Y.; Luu, T.; Tykwinski, R.R. *Org. Lett.* **2006,** *8,* 689.

20. a. Faust, R.; Gobelt, B.; Weber, C.; Krieger, C.; Gross, M.; Gisselbrecht, J.-P.; Boudon, C. *Eur. J. Org. Chem.* **1999,** 205; b. Ito, Y.; Inouye, M.; Murakami, M.; Shiro, M. *J. Organomet. Chem.* **1989,** *674,* C57; c. Bruce, M.I.; Ke, M.; Kelly, B.D.; Low, P.J.; Smith, M.E.; Skelton, B.W.; White, A.H. *J. Organomet. Chem.* **1999,** *684,* 184; d. Zhang, W.-X.; Nishiura, M.; Hou, Z. *J. Am. Chem. Soc.* **2005,** *127,* 16788; e. Onitsuka, K.; Joh, T.; Takahashi, S. *J. Organomet. Chem.* **1994,** *679,* 247; f. Bruce, M.I.; Hinterding, P.; Ke, M.; Low, P.J.; Skelton, B.W.; White, A.H. *Chem. Commun.* **1997,** 715; g. Ito, Y.; Inouye, M.; Murakami, M.; Shiro, M. *J. Organomet. Chem.* **1990,** 399; h. Albano, V.G.; Bordoni, S.; Busetto, L.; Marchetti, F.; Monari, M.; Zanotti, V. *J. Organomet. Chem.* **2003,** *688,* 37; i. Ammon, H.L.; El-Sayad, K.; Fouli, F.A. *Acta Crystallogr., Sect. C : Cryst. Struct. Commun.* **1991,** 194; j. Onitsuka, K.; Ogawa, H.; Joh, T.; Takahashi, S.; Yamamoto, Y.; Yamazaki, H. *J. Chem. Soc., Dalton Trans.* **1991,** 1531.

21. Jaquemin, D.; Wathelet, V.; Perpète,E.A.; Adamo, C. *J. Chem. Theory Comput.* **2009**, *5,* 2420.

Chapter 4

Future Work

4.1 Introduction

For this project, the primary focus for the future lies in the successful preparation of the PacNac molecule. In the progress of this work, a few of numerous possibilities to this end were eliminated, leaving yet many more to be attempted until success is finally reached. For the phosphaalkene route this involves much more of a change in focus, whereas for the iminophosphenato route it primarily involves adjusting the reaction conditions and possibly the substituents on the reactants in order to get the desired reaction. For the alkynyl imines and diimines many interesting possibilities exist beyond the PacNac research – particularly in the area of transition metal complexes – an area that has not been studied for the already known class of alkynyl imines, let alone the novel diimines.

4.2 Phosphaalkene Route

As stated in Chapter 1, ketoimines rarely have the same reactivity as other ketones. This means that it is possible but unlikely that the routes developed for the synthesis of phosphaalkenes from various phosphine reagents and ketones as outlined in Chapter 1 would result in formation of the PacNac molecule in reactions with the ketoimine molecule. Therefore, it would be worthwhile moving forward to other more likely possibilities from other starting points.

The first of these is based on the 1,2-elimination type reaction shown in Chapter 1 as synthetic method type **A**. This method made its first appearance in 1978 in the synthesis of a mesityl and other aryl substituted phosphaalkenes (Scheme 4.1).[1]

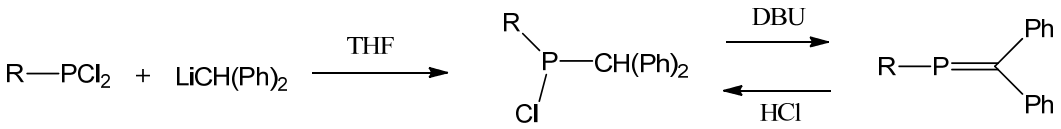

R = Mes, o-MePh, 2,6 - diMePh, Ph

Scheme 4.1 – The first reported 1,2-elimination reaction for the synthesis of phosphaalkenes.

It has since been used in the synthesis of a variety of other phosphaalkenes,[2] including the less stable alkyl substituted variety.[3] The dichlorophosphines are well known compounds which makes this an attractive route so long as a suitable lithium precursor with the remainder of the structure required to get the PacNac molecule can be made and used for the purpose (Figure 4.1).

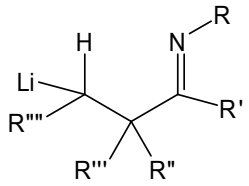

Figure 4.1 – Required structure of lithium compound to react with dichlorophosphine in the first step of the 1,2-elimination reaction to PacNac.

Suitable halogenated species to make this lithium precursor do exist in the literature and are available via well-developed syntheses. For instance, 4-chloropentan-2-one[4] or 4-chloro-3-methyl-1-phenylpentan-2-one,[5] which are both made via acylation of an olefin via a Lewis-acid catalyst. These could then be reacted with the appropriate aniline (either mesityl or dipp) in the presence of catalyst to get the amine version of the above molecules. From here, reaction with BuLi would presumably give the desired lithium reagent to react with the dichlorophosphine in hopes of making the final PacNac molecule.

The only other common method of phosphaalkene synthesis that doesn't involve a ketone precursor is double-bond migration, type E shown in Chapter 1. As this is a single molecule reaction to form the phosphaalkene double bond from the respective phosphine, this reaction is of little use here because had that type of compound (similar to the iminophosphenate compound) would already form the PacNac ligand upon addition to metals.

Another possibility involves either forming an alternate backbone which involves forming the nitrogen side and phosphaalkene side separately and then joining them together. In this case a second closer nitrogen will be present in the final molecule in hopes that it will lend stabilization to the phosphaalkene bond.

The potential nitrogen and phosphorus precursors are pictured in the proposed reaction scheme to form a PacNac-type molecule that contains nitrogen in the backbone portion of the molecule (Scheme 4.2).

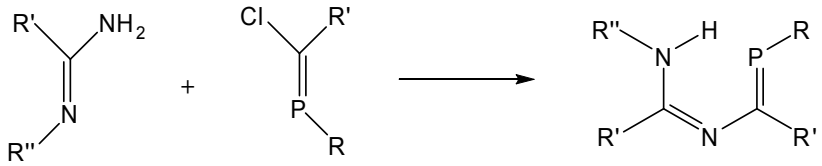

Scheme 4.2 – Proposed reaction for an alternate PacNac molecule which may have greater stabilization of the phosphaalkene portion.

In the literature, the above nitrogen precursor exists as the tautomer where each of the nitrogen has a hydrogen on it and the double bond is therefore on the nitrogen without the R substituent (Figure 4.2).[6]

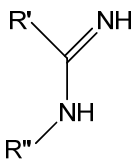

Figure 4.2 – The tautomer of the nitrogen precursor in Scheme 4.2 that has been reported in the literature.

The phosphorus precursor has been reported for the supermesityl version.[7] This phosphine could be first tried while attempting to make the equivalent dipp version, which may or may not be possible (given past lab experience with following supermesityl work to make the dipp versions) and likely would require some adjustment in the reaction conditions.

The final proposal came through reading background information on ketoimines during the preparation of this thesis. Preliminary reactions were done to test the possibility. The gold(III) catalyst, $NaAuCl_4$, was shown to be effective in the catalysis of the condensation reaction of amines as well as other nucleophiles, such as $HP(Ph)_2$, with 1,3-diketones.[8] The condensation reaction of supermestiylphosphine with **1b** as well as with acetylacetone were attempted, but no reaction of the phosphine was shown in the respective NMR spectra. The reaction in the literature was successful with $HP(Ph)_2$, a disubstituted phosphine, with 1,3-cyclohexanone. In fact, all the additions attempted with nucleophiles other than amines were with cyclic 1,3-diketones. Therefore, it would be worthwhile to attempt this reaction with a couple of alternative starting points.

One alternative would be to start with a 1,3-diketone that has one of the ketones on a cyclic portion and the other on a chain, such as 2-acetylcyclohexanone which is available to purchase from Sigma-Aldrich. Both R_2PH and RPH_2 could be reacted with this to see if the reaction would proceed with the cyclic ketone better than with the acyclic. As well, R_2PH could be reacted with acetylacetone to see if it the form of the phosphine that makes the difference in the reactivity. The original reactions were done with supermesitylphosphine, which in retrospect was not the best choice (chosen because it was available in the lab and dipp and mesityl were not) because supermesitylaniline is not reactive toward the condensation reaction with ketones, which means that it is likely that supermesityl as a substituent may have prevented the reaction

from going forward. Therefore, dipp and mesityl phosphine should likely be reacted with acetylacetone and one of **1a-d** to test if this is in fact the case.

4.3 Iminophosphenato Route

The iminophosphenato route was based on the literature synthesis of the first ketophosphenate as outlined in Chapter 1. The 1,2-addition reaction of a silyl phosphine to an alkyne had been previously reported according to the above paper; however, it was incorrectly cited and the correct citation has not been located. In the literature found on addition reactions of the silyl phosphine to unsaturated bonds (in particular for ketones and aldehydes that also contain an alkene bond,[9] but also for compounds containing imine bonds[10]) the silyl group actually adds onto the oxygen or nitrogen and the phosphine at either the 2 or 4 position. However, the 1,2-addition of the P–H bond of phosphine has been reported on much more and is a well-developed method of synthesis.

The reaction of the alkynyl imines that were made with dippPTMS(H) were attempted using both the same and slightly more harsh conditions (refluxing in toluene versus heating to 40°C). Either no reaction occurred with the phosphine, or the ^{31}P NMR spectra showed that it was unlikely to be the desired product when reaction did occur (the desired product would be expected to have a ^{31}P NMR signal in the same area as the ketophosphenate). The difference in reactivity could be attributed to a few differences between the reactants used in this case and in the successful reported reaction. For one thing, the electronics of the alkynyl imine would certainly be different than the 3-butyn-2-one, with the nitrogen atom having less electronegativity than the oxygen. However, with the aryl groups likely to attract electron density away from the alkyne, this was not expected to be a significant problem. As well, with two aryl substituents on the alkynyl imine, including the bulky dipp group, much increased steric congestion could possibly hinder the desired reaction. As well, the substituent on the silylphosphine in the case of

the reported reaction had silyl groups off of the benzene ring instead of alkyl groups which could also have an electronic effect on the reactivity.

Some simple changes might be all that is necessary to overcome the reduced reactivity in the case of the alkynyl imine and silylphosphine 1,2-addition reaction. For instance, the high pressure conditions of a heated Parr device or a "hydraulic high pressure reactor" might be all that is needed to get the existing reactants to react in the desired fashion (the added energy may overcome an unfavorable activation energy). Other obvious areas to try are less bulky alkynyl imines or silylphosphines if steric congestion is the primary hindrance to reaction. Beyond that, hydrophosphination (addition of P–H across an unsaturated bond) would be the next logical area to look at for the addition reaction.

As mentioned earlier, the hydrophosphination reaction has an extensive literature from which to design a possible reaction which would give the iminophosphenate. Except in cases of unsaturated bonds which are sufficiently activated by electron withdrawing groups in close proximity,[11] hydrophosphination reactions require radical initiation[12] or the use of a catalyst – acid, base, or transition metal based.[15,17-21,23] The catalysts activate the P–H bond toward addition across a double or triple bond. The acid catalyst plays on the relative basicity of phosphines. In many cases, however, near molar equivalents of acid are required instead of catalytic amounts, although examples of the use of catalytic amounts do exist.[11] The strong base catalyst is used to remove the proton from the phosphine, in the same way that is used in the Michael reaction in organic chemistry.[13] Some of the transition metal catalysts are shown to work similarly with the anionic phosphine complexing with the transition metal in the progress of the reaction.[14]

One of the base catalyzed reactions between primary phosphine was attempted (considerable amounts of the literature focuses on the addition of secondary phosphines) and **7b**. The formation of different phosphorus containing species was observed in the ^{31}P NMR

spectrum; however, the signals again were not in the (or even close to) the expected region. After quenching with ammonium chloride, the ^{31}P NMR spectrum did not change, but the ^{1}H was an exact match for **7b** except for the lack of the alkyne ^{1}H NMR signal (recall from the previous chapter the dimer **5b** has a discernibly different ^{1}H spectrum from **7b**), and no signals of the dipp group on phosphorus were present either.

The reaction conditions followed those in a literature reaction of primary phosphines and cyanoacetylenes.[15] In this paper, the reaction was demonstrated to proceed through the intensely red radical anion of phenylcyanoacetylene, generated by the phosphide-anion which was generated by the base. No such change in colour was observed for the reaction attempted here with dipp-phosphine and imine **7b**. Cyanoacetylenes would have a more activated triple bond toward the addition than the imines **6b** or **7b** that I tried the addition to; the cyano group is known as an excellent substrate for activating an unsaturated bond towards Michael addition in organic chemistry.[16]

Although many papers have been published on hydrophosphination reactions, enough that a few review articles have been published on various aspects of the subject,[17] many of the reported reactions only work with a select few alkynes or types of phosphine, most of the reported reactions make use of Ph_2PH as the secondary phosphorus choice. This means that many possible choices of reaction conditions are available for attempting the synthesis of our desired iminophosphenato ligand. The first reaction conditions to try are those with readily available, relatively inexpensive reagents with generally more gentle conditions.

The first of these are the commonly used super-base systems of KOH-DMSO or potassium t-butoxide (tBuOK)–DMSO. The KOH-DMSO has been used in particular with terminal aryl alkynes and a couple of primary phosphines.[18] As with most hydrophosphination

reactions done with primary phosphines, this reaction adds over two alkynes for the final result as shown in Figure 4.3.

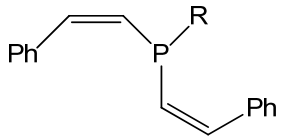

Figure 4.3 – Final result of a primary phosphine hydrophosphination reaction with alkynes catalyzed by a super basic system.

The bulkiness of **7b** should prevent the second addition from occurring. This is a important consideration for all of the hydrophosphination reactions presented here. The tBuOK-DMSO system has been used in the hydrophosphination of alkenes by secondary phosphines including a variety of terminal alkenes, for example, heterocycle **A8** (Figure 4.4).[19] Although this would still likely have greater electron withdrawing than **7b**, it is possibly closer to the same properties as **7b** than is cyanoacetylene. Other bases such as Ph–Li, which has been used successfully with terminal alkynes,[17c] and $LiNH_2$ in $NH_{3(l)}$ [17d] are also possible systems to use to base catalyze the hydrophosphination reaction. Directly reacting the lithiated phosphine with terminal alkynes have also been successful in the desired addition.[17c]

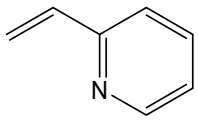

A8

Figure 4.4 – One heterocycle that has undergone successful hydrophosphination of the terminal alkene using the super base system of tBuOK-DMSO.

Next, a variety of Pd and Ni catalysts have been shown to be successful in hydrophosphination for a variety of systems, but without any general rule for which catalyst will work with any given pair of alkyne and secondary phosphine. These catalysts include Pd and Ni complexes such as ($Pd(PPh_3)_4$), $Pd(dba)_2$ [dba = dibenzylideneacetone], $Pd(OAc)_2$, $Ni[P(OEt)_3]_4$, $Ni(acac)_2$, and $NiBr_2$.[17a] One paper concluded that the nickel complexes are the more effective

catalysts for this type of reaction.[17b] Of the above, ($Pd(PPh_3)_4$), $Pd(dba)_2$, $NiBr_2$, and $Ni(acac)_2$ are available commercially for a reasonable price.

A recently published paper which used fluoride to mediate the hydrophosphination reaction worked with a variety of alkyne substrates.[20] TBAF (tetra-n-butylammonium fluoride) in DMF or DMSO worked well in short periods of time (15-20 min) at room temperature, to add the secondary silyl phosphine, Ph_2PSiR_3, to alkenes and alkynes. The fluoride removes the silyl group from the phosphine, therefore the end result is the addition of P–H over the unsaturated bond. The limiting factor here is that the alkene/alkyne used must have either an aryl group or other electron withdrawing group in order for the reaction to proceed. This did, however, work with both terminal alkynes and internal alkynes. The fluoride reagent is available from Sigma-Aldrich and is relatively inexpensive (for example 100 mL of 1M THF solution is approximately $67).

The gold catalyst mentioned in section 4.2 was shown to also activate triple bonds towards nucleophilic addition of oxygen and nitrogen groups to alkynes. This catalyst could also then be tried for such activation to allow the nucleophilic addition of the P–H group as well, recalling that it does catalyze the condensation reaction of oxygen, nitrogen, sulfur and phosphorus nucleophiles with 1,3-dicarbonyl substrates. Therefore, it would be worth an attempt to see if the reaction conditions can be expanded in this way.

A cobalt (II) catalyst, along with BuLi ,was also used generally with a variety of alkynes for hydrophosphination reactions.[21] This catalyst system gives mostly the desired linear addition and it works with terminal alkynes. The cobalt (II) acetylacetonate catalyst is quite inexpensive ($75 for 50 g) and the reaction conditions involve simply refluxing the reagents in dioxane.

A more expensive catalyst also commercially available, $[Rh(cod)Cl]_2$, that was complexed with the first ketophosphenate,[22] has been shown to work with the addition of

phosphorus from silylphosphines with a similar result to the fluoride mediated reaction mentioned above.[23] The rhodium catalyst along with the additive silver triflate was used to add P–H over a number of alkynes including terminal alkynes with reasonably high yields (53-89%). The reaction is performed in refluxing benzene and the colour change from red to yellow indicates the completion of the reaction.

Less desirable reactions to try would be the commonly used radical initiator AIBN,[12,17d] which is a more toxic chemical, or non-commercially available catalysts which would have to be made in the lab before use. One of these catalysts of interest would be **A9** (Figure 4.5),[24] which has been used for *silylphosphination* reactions, the addition of a P–Si bond over unsaturated bonds. This would not likely work with **7b** because it does not tend to work well with terminal alkynes; however, **6b** could be tried with this rare earth catalyst if the synthesis of the catalyst is in fact viable.

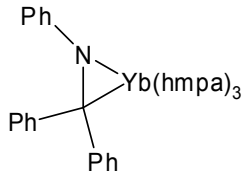

A9

Figure 4.5 – A catalyst of interest which has been used successfully for silylphosphination reactions.

4.4 Transition Metal Complexes of Alkynyl Imines and Diimines

$Mo(CO)_6$ when reacted with six-membered aromatic ring containing species, tends to form η-6 $Mo(CO)_3$ complexes. Molybdenum, along with chromium and tungsten, also complex with alkyne complexes to the triple bond of the alkyne.[25,26] Alkynyl imines and diimines have not been used as ligands to these metals, although complexation of an alkynyl imine to the above metals has been used in the transformation of the alkynyl imine to other species.[26] The alkynyl imines and diimines presented in this work could complex by either the aromatic substituents or

the triple bond or both. This is therefore a simple, though interesting direction of research into the novel alkynyl diimines and the novel alkynyl imines in comparison with one another and the many complexes that have been made of this general type. This also links into the work previously done on bulky N,N′-disubstituted amidines by the Boeré Research Group.

References

1. Klebach, T.C.; Lourens, R.; Bickelhaupt, F. *J. Am. Chem. Soc.* **1978,** *100,* 4886.

2. a. Cornet, S.M.; Dillon, K.B.; Goeta, A.E.; Howard, J.A.K.; Roden, M.D.; Thompson, A.L. *J. Organomet. Chem.* **2005,** *690,* 3630; b. Decken, A.; Carmalt, C.J.; Clyburne, J.A.C.; Cowley, A.H. *Inorg. Chem.* **1997,** *36,* 3741.

3. Gaumont, A.C.; Pellerin, B.; Cabioch, J.-L.; Morise, X.; Lesvier, M.; Savignac, P.; Guenot, P.; Denis, J.-M. *Inorg. Chem.* **1996,** *35,* 6667.

4. Odom, H.C.; Pinder, A.R. *Org. Syn.* **1988,** *6,* 883.

5. Pentrenko, L.P.; Smol`yaninova, Y.L. *Zh. Obshch. Khim.* **1963,** *33,* 2041.

6. Srimannarayana, G.; Srivastava, R. M.; Clapp, Leallyn B. *J. Heterocyclic Chem.* **1970**, *7,* 151.

7. Yoshifuji, M.; Niitsu, T.; Inamoto, N. *Chem. Lett.* **1988,** 1733.

8. Arcadi, A.; Bianchi, G.; Di Guiseppe, S.; Marinelli, F. *Green Chem.* **2003,** *5,* 64.

9. Couret, C.; Escudie, J.; Satge, J. *J. Organomet. Chem.* **1975,** *660,* 11.

10. Abel, E.W.; Sabherwal, I.H. *Inorg. Phys. Theor.* **1968,** 1105.

11. Dombek, B.D. *J. Org. Chem.* **1978,** *43,* 3408.

12. a. Mitchell, T.N.; Heesche, K. *J. Organomet. Chem.*, **1991,** *676,* 163; b. Therrien, B.; König, A.; Ward, T.R. *Organometallics* **1999,** *18,* 1565.

13. King, R.B.; Kapoor, P.N. *J. Am. Chem. Soc.* **1971,** *93,* 4158.

14. Takaki, K.; Takeda, M.; Koshoji, G.; Shishido, T.; Takehira, K. *Tetrahedron Lett.* **2001,** *42,* 6357.

15. Gusarova, N.K.; Shaikhudinova, S.I.; Arbuzova, S.N.; Vakul'skaya, T.I.; Sukhov, B.G.; Sinegovskaya, L.M.; Nikitin, M.V.; Mal'kina, A.G.; Chernysheva, N.A.; Trofimov, B.A. *Tetrahedron* **2003,** *59,* 4789.

16. Sorrell, T.N. *Organic Chemistry*. Sausalito, California : University Science Books, **1999**, 1118.

17. a. Tanaka, M. *New Aspects in Phosphorus Chem. IV.* **2004,** 25; b. Alonso, F.; Beletskaya, I.P; Yus, M. *Chem. Rev.* **2004,** *104,* 3079; c. Delacroix, O.; Gaumont, A.C. *Current Org. Chem.* **2005,** *9,* 1851; d. Arbuzova, S.N.; Gusarova, N.K.; Trofimov, B.A. *Arkivoc* **2006,** 12; e. Enders, D.; Saint-Dizier, A.; Lannou, M.-I.; Lenzen, A. *Eur. J. Org. Chem.* **2006,** 29.

18. Malysheva, S.F.; Sukhov, B.G.; Larina, L.I.; Belogorova, N.A.; Gusarova, N.K.; Trofimov, B.A. *Russian J. Gen Chem.* **2001,** *71,* 1907.

19. Bunlaksananusorn, T.; Knochel, P. *Tetrahedron Lett.* **2002,** *43,* 5817.

20. Hayashi, M.; Matsuura, Y.; Watanabe, Y. *Tetrahedron Lett.* **2004,** *45,* 9167.

21. Ohmiya, H.; Yorimitsu, H.; Oshima, K. *Angew. Chem. Int. Ed.* **2005,** *44,* 2368.

22. Sasamori, T.; Matsumoto, T.; Takeda, N.; Tokitoh, N. *Organometallics* **2007,** *26,* 3621.

23. Hayashi, M.; Matsuura, Y.; Watanabe, Y. *J. Org. Chem.* **2006,** *71,* 9248.

24. Takaki, K.; Komeyama, K.; Kobayashi, D.; Kawabata, T.; Takehira, K. *J. Alloys Compd.* **2006,** 432.

25. For example: a. Adams, H.; Blenkiron, P.; Gill, L.G.; Hervé, R.; Huesmann, A.-G.; Morris, M.J. *J. Organomet. Chem.* **2008,** *694,* 709; b. Ohnishi, T.; Tsuboi, H.; Seino, H.; Mizobe, Y. *J. Organomet. Chem.* **2008,** *694,* 269.

26. Sangu, K.; Fuchibe, K.; Akiyama, T. *Org. Lett.* **2004,** *6,* 353.

27. a. Boeré, R.T.; Klassen, V.; Wolmershäuser, G. *J. Chem. Soc., Dalton Trans.* **1998,** 4147; b. Boeré, R.T.; Klassen, V.; Wolmershäuser, G. *Can. J. Chem.* **2000,** *78,* 583.

Chapter 5

Experimental Details

5.1 General

All experimental procedures were performed under a nitrogen atmosphere using modified Schlenk techniques, unless otherwise noted. 2,6-Diisopropylaniline (Aldrich), 2,4,6-trimethylaniline (Aldrich), 2,4-pentanedione (Sigma-Aldrich), 3-methyl-2,4-pentanedione (Aldrich), indium tribromide (Aldrich), 1.6 M n-butyl lithium in hexanes (Aldrich), lithium acetylide ethylenediamine complex (Aldrich), sodium acetylide (Aldrich), bis(trimethylsilyl)acetylene (Aldrich), aluminum chloride (Merck), and benzene-d_6 (CDN isotopes 0.8 mL ampules) were used as received. Imidoyl chlorides, N-phenyl-t-butylimidoyl chloride and N-dipp-p-tolylimidoyl chloride, were previously prepared via the respective literature routes.[1] Solvents were reagent grade, or better, and were used as received (methanol, hexanes, pentane, chloroform), distilled from sodium/benzophenone (tetrahydrofuran), or obtained from an MBraun Solvent Purification System (heptane, toluene, benzene, methylene chloride). Infrared spectra were recorded on a Bruker Alpha-P spectrometer as neat samples. ^{1}H, ^{13}C, ^{31}P, and ^{7}Li NMR spectra were recorded on a Bruker Avance300 spectrometer operating at 300.1300, 75.4677, 121.4949, and 116.6419 MHz, respectively. HSQC and HMBC experiments were used to assist with assigning the ^{13}C NMR signals for most samples. ^{1}H NMR are referenced to tetramethylsilane (TMS), ^{13}C NMR are referenced to $CDCl_3$ or C_6D_6, ^{31}P NMR are referenced to an external H_3PO_4 sample, and ^{7}Li NMR are referenced to an external 9.7 m LiCl in D_2O sample. X-ray crystal data were collected on a Bruker Smart Apex II, with solution and refinement using the Shelxtl 6.14 package of software. Estimated standard deviations for averaged bond lengths and angles are reported as the standard deviation of the values used to calculate the averages. The

finalized *.cif files are located on the CD-ROM included with this thesis. Mass spectra were obtained using a Varian 4000 GC/MS/MS. Elemental analyses were obtained using an Elementar Vario Micro Cube. Optimization and frequency calculations for all of the molecules were done using the Hybrid Density Functional Method B3LYP with the 6-31G(d) basis set using Gaussian 03 and Gaussview 4.1.2 for Windows. Most of the lithium complexes required the use of the max step command to converge for the optimization because of large flat wells. For some of the lithium complexes, small imaginary frequencies were obtained for methyl rotation (in most cases) and in a couple of cases for small wagging movement of a THF ligand. For the alkynyl imines and diimines, TD-DFT (at the same level of theory) calculations were used to calculate the UV/Vis spectra and molecular orbital calculations were also performed. Cyclic voltammograms (CVs) were obtained at 24°C in CH_2Cl_2 (purified by distillation from CaH_2) solutions containing 0.7 M electrochemical grade [^{n}Bu$_4$N][PF_6] (Fluka) as the supporting electrolyte. These solutions were purged with dry nitrogen for 10 min directly before use, and were kept under a blanket of nitrogen during all experiments. The CVs were performed with a Princeton Applied Research PARSTAT 2273 potentiostat. The voltammetry cell design has been described previously.[2] The CVs were obtained over scan rates of 0.05–20 V s^{-1}. The potentials for the analyte signals are reported *vs.* the operative formal potential, $E^{0/}_{Fc+/0}$, for the Fc^+/Fc redox couple (Fc = ferrocene), which was used as an internal standard. The Ferrocene was sublimed prior to use. The working electrode was polished with an Al_2O_3 (Buehler, 0.05 μm) slurry on a clean polishing cloth, rinsed with distilled water, and dried with tissue paper prior to use.

5.2 Synthesis of Ketoimines 1a-d

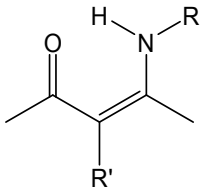

a : R = Dipp, R' = H
b : R = Mes, R' = H
c : R = Dipp, R' = Me
d : R = Mes, R' = Me

1a-d

General procedure using **1c** as an example: In a round bottom flask combined 5.00 g (43.5 mmol) of 3-methyl-2,4-pentandione, 8.85 g (43.5 mmol) dippaniline, and 0.154 g (0.435 mmol) of $InBr_3$ were combined and allowed to stir overnight. The cloudy solution was then diluted with 60 mL of distilled water, extracted 3 times with 25 mL of ethyl acetate, the organic layers combined and then dried with magnesium sulfate. The solvent was removed under reduced pressure to give a colourless solid in an orange liquid. The solid was filtered off and recrystallized in hexanes giving 2.063 g (17.3% yield, mp: 122-129 °C) of very pale yellow plates.

Anal. Calc. for $C_{18}H_{27}NO$: C, 78.72; H, 9.71; N, 5.40. Found: C, 78.45; H, 9.55; N, 5.11.

^{1}H NMR ($CDCl_3$, 25°C): δ 13.18 (br s, 1 H; NH), 7.28 (triplet, *J* 7.44, 1 H; para CH on Dipp ring), 7.17 (d, *J* 7.44, 2H; meta CH on Dipp ring), 3.01 (sept, *J* 6.87, 2 H, ; CH of isopropyl group), 2.24 (s, 3 H; Me on C=O), 1.92 (s, 3 H; central Me), 1.70 (s, 3 H; Me on CNDipp side), 1.18 (d, *J* 6.87, 6 H; isopropyl Me), 1.14 (d, *J* 6.87, 6H; isopropyl Me).

^{13}C NMR ($CDCl_3$, 25°C): δ 196.02 (C=O), 161.83 (C–N), 146.46 (C_{ortho}), 134.59 (C_{ipso}), 127.96 (C_{para}), 123.62 (C_{meta}), 98.79 (DippNHC(CH_3)**C**(CH_3)C(O)CH_3), 28.69 (Me on CO side), 28.62 (CH of isopropyl group), 24.65 (Me on isopropyl group), 22.91 (Me on isopropyl group), 16.72 (Me on CNDipp side), 14.98 (DippNHC(CH_3)C(**C**H_3)C(O)CH_3).

MS: m/z 273 (M^+, 18%), 202 (DippNCCH_3^+, 100%), 187 (DippNC^+, 24%), 160 (Dipp –H^+, 20%).

IR(neat) cm^{-1}: 2960 (s), 2924 (m), 2867 (m), 1598 (vs), 1555 (vs), 1464 (s), 1422 (s), 1384 (s), 1352 (vs), 1262 (vs), 1235 (s), 1169 (s), 1099 (m), 1053 (m), 966 (vs), 814 (vs), 776 (vs), 709 (s), 590 (m), 445 (m), 414 (m).

For the purpose of potential comparison to **2c** and **4c**, NMR experiments were also done in C_6D_6: ^{1}H NMR (C_6D_6, 25°C): δ 13.86 (br s, 1 H; NH), 7.16 (triplet, *J* 7.65, 1 H; para CH on Dipp ring), 7.05 (d, *J* 7.50, 2H; meta CH on Dipp ring), 3.13 (sept, *J* 6.82, 2 H; CH of isopropyl group), 2.15 (s, 3 H; Me on C=O), 1.74 (s, 3 H; central Me), 1.51 (s, 3 H; Me on CNDipp side), 1.09 (d, *J* 6.90, 6 H; isopropyl Me), 1.05 (d, *J* 6.90, 6H; isopropyl Me).

^{13}C NMR (C_6D_6, 25°C): δ 196.26 (C=O), 160.87 (C–N), 147.00 (C_{ortho}), 135.55 (C_{ipso}), 128.47 (C_{para}), 124.14 (C_{meta}), 99.24 (DippNHC(CH_3)**C**(CH_3)C(O)CH_3), 29.22 (CH of isopropyl group), 28.79 (Me on CO side), 24.86 (Me on isopropyl group), 23.10 (Me on isopropyl group), 16.55 (Me on CNDipp side), 15.16 (DippNHC(CH_3)C(**C**H_3)C(O)CH_3).

For **1a**: Following the general procedure above: from 10.52 g (105.1 mmol) of 2,4-pentanedione, 18.00 g (101.5 mmol) of dippaniline, 0.38 g (1.1 mmol) of $InBr_3$; diluted with 250 mL of distilled water, and extracted with 4 x 100 mL of ethyl acetate; removal of the solvent gave a bright yellow oil which was run through a column starting with 1:1 $CHCl_3$:CH_2Cl_2 until the first band of yellow came through (which was unreacted dippaniline) and then 12% ethyl acetate in petroleum ether to give 6.634 g (52.2% yield) of light yellow solid. The characterization data was consistent with that in the literature.[3] For the purpose of potential comparison to **2a** and **4a**, NMR data was also done in C_6D_6: ^{1}H NMR (C_6D_6, 25°C): δ 12.70 (br s, 1 H; NH), 7.14 (triplet, *J* 7.80, 1 H; para CH on Dipp ring), 7.02 (d, *J* 7.50, 2H; meta CH on Dipp ring), 5.14 (s, 1H; CH on backbone), 3.10 (sept, *J* 6.90, 2 H; CH of isopropyl group), 2.06 (s, 3 H; Me on C=O), 1.41 (s, 3 H; Me on CNDipp side), 1.08 (d, *J* 6.90, 6 H; isopropyl Me), 1.02 (d, *J* 6.90, 6H; isopropyl Me).

^{13}C NMR (C_6D_6, 25°C): δ 195.42 (C=O), 162.16 (C–N), 146.35 (C_{ortho}), 133.99 (C_{ipso}), 128.26 (C_{para}), 123.54 (C_{meta}), 95.69 (DippNHC(CH_3)**C**HC(O)CH_3), 28.77 (Me on CO side), 28.56 (CH of isopropyl group), 24.29 (Me on isopropyl group), 22.36 (Me on isopropyl group), 18.61 (Me on CNDipp side).

For **1b**: Following the general procedure above: from 9.11 g (91.0 mmol) of 2,4-pentanedione, 12.31 g (91.1 mmol) of mesityl-aniline, and 0.33 g (0.94 mmol) of $InBr_3$; diluted with 125 mL of distilled water and extracted with 4 x 50 mL of ethyl acetate; removal of solvent gave 17.90 g (90.5 % yield) of an orange crystalline solid of which the characterization data was consistent with the literature.[3] For the purpose of potential comparison to **2b** and **4b**, NMR data was also collected in C_6D_6: ^{1}H NMR (C_6D_6, 25°C): δ 12.33 (br s, 1H; NH), 6.63 (s, 2H; CH on Mes ring), 5.10 (s, 1H; CH on backbone), 2.08 (s, 3H; CH_3 on C=O), 2.07 (s, 3H; para-CH_3), 1.97 (s, 6H; ortho-CH_3), 1.33 (s, 3H; CH_3 on CNH(Mes)).

^{13}C NMR (C_6D_6, 25°C): δ 195.85 (C=O), 162.44 (CNH(Mes)), 137.08 (C_{para}), 136.30 (C_{ortho}), 134.93 (C_{ipso}), 129.46 (C_{meta}), 96.35 (MesNHC(CH_3)**C**HC(O)CH_3), 29.45 (CH_3 on C=O), 21.25 (CH_3 on CNH(Mes)), 18.91 (para CH_3), 18.44 (ortho CH_3).

For **1d**: Following the general procedure above: from 5.00 g (43.5 mmol) of 3-methyl-2,4-pentanedione, 5.88 g (43.5 mmol) of mesityl-aniline, and 0.154 g (0.4344 mmol) of $InBr_3$; removal of the solvent gave an orange liquid which after sitting for 2 days, had solid crystallizing out. The solid was filtered off and recrystallized from hexanes to give 3.619 g (36.0% yield, mp: 64 – 68 °C) of faintly orange plates.

Anal. Calc. for $C_{15}H_{21}NO$: C, 77.37; H, 8.81; N, 6.44. Found: C, 77.71; H, 8.80; N, 6.08.

^{1}H NMR ($CDCl_3$, 25°C): δ 12.99 (br s, 1H; NH), 6.89 (s, 2H; CH on Mes ring), 2.28 (s, 3H; para-CH_3), 2.22 (s, 3H; CH_3 on C=O), 2.13 (s, 6H; ortho-CH_3), 1.91 (s, 3H; MesNHC(CH_3)C(**C**H_3)C(O)CH_3), 1.70 (s, 3H; CH_3 on CNH(Mes)).

^{13}C NMR ($CDCl_3$, 25°C): δ 195.91 (C=O), 161.60 (CNH(Mes)), 136.57 (C_{para}), 135.80 (C_{ortho}), 134.91 (C_{ipso}), 128.92 (C_{meta}), 98.85 (MesNHC(CH_3)**C**(CH_3)C(O)CH_3), 28.60 (CH_3 on C=O), 21.02 (para CH_3), 18.40 (ortho CH_3), 16.03 (CH_3 on NH(Mes)), 14.92 (MesNHC(CH_3)C(**C**H_3)C(O)CH_3).

MS: m/z 232 (MH+, 100%), 231 (M+, 30%), 160 ($MesNCCH_3^+$, 10%).

IR(neat) cm^{-1}: 2947 (w), 2914 (w), 2859 (w), 1595 (s), 1538 (vs), 1487 (s), 1435 (m), 1417 (m), 1387 (m), 1367 (m), 1350 (m), 1263 (vs), 1198 (s), 1147 (w), 967 (vs), 884 (m), 857 (s), 814 (m), 760 (m), 696 (m), 588 (m), 532 (w), 482 (m).

For the purpose of potential comparison to **4d**, the NMR data was also collected in C_6D_6: ^{1}H NMR (C_6D_6, 25°C): δ 13.49 (br s, 1H; NH), 6.69 (s, 2H; CH on Mes ring), 2.11 (s, 3H; para-CH_3), 2.15 (s, 3H; CH_3 on C=O), 2.01 (s, 6H; ortho-CH_3), 1.73 (s, 3H; MesNHC(CH_3)C(**C**H_3)C(O)CH_3), 1.46 (s, 3H; CH_3 on CNH(Mes)).

^{13}C NMR (C_6D_6, 25°C): δ 196.02 (C=O), 160.55 (CNH(Mes)), 136.59 (C_{para}), 136.23 (C_{ortho}), 135.84 (C_{ipso}), 129.49 (C_{meta}), 99.30 (MesNHC(CH_3)**C**(CH_3)C(O)CH_3), 28.81 (CH_3 on C=O), 21.29 (para CH_3), 18.64 (ortho CH_3), 15.20 (CH_3 on CNH(Mes)), 15.89 (MesNHC(CH_3)C(**C**H_3)C(O)CH_3).

5.3 Synthesis of Lithium Complexes of Ketoimines in THF 2a-c, 4d

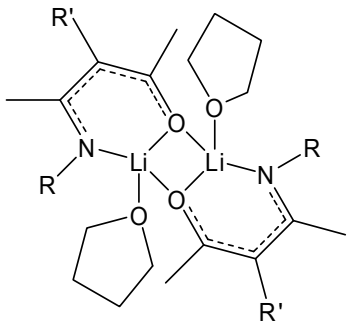

2a-c

a : R = Dipp, R' = H
b : R = Mes, R' = H
c : R = Dipp, R' = Me
d : R = Mes, R' = Me

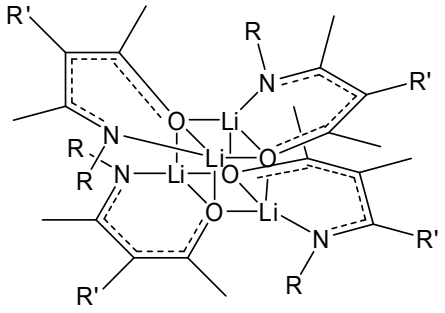

4d

General procedure using **2a** as an example: In a Schlenk tube 8 mL of dry THF and 1.006 g (3.878 mmol) of **1a** were combined while cooling in an ice/salt bath. To this, 2.5 mL (4.000 mmol) of 1.6 M BuLi in hexanes was added via syringe. The solution was stirred with cooling for a half hour and then allowed to warm up to room temperature and stir overnight. The THF was removed under vacuum until solid started to come out of solution and then the flask was heated to redissolve the solid, and placed in the freezer which resulted in 0.322 g (24.6% yield, mp: 229-230°C, decomposed 270°C) of colourless plates suitable for an X-ray crystallographic study. Anal. Calc. for $C_{42}H_{64}N_2O_4Li_2$: C, 74.75; H, 9.56; N, 4.15. Found: C, 73.94; H, 8.92; N, 4.85. ^{1}H NMR (1:1 THF:C_6D_6, 25°C, 1:30 ligand:THF): δ 7.11 (d, *J* 7.25, 2H, meta CH on Dipp ring), 7.02 (t, *J* 7.25, 1H, para CH on Dipp ring), 4.82 (s, 1 H; CH on backbone), 3.59 (m, 122 H; THF), 3.16 (septet, *J* 6.82, 2 H; isopropyl CH), 1.66 (s, 3 H; Me on C=O), 1.61 (m, 122 H; THF),1.55 (s, 3 H; Me on CNDipp side), 1.19 (d, *J* 6.82, 6 H; isopropyl CH_3), 1.14 ppm (d, *J* 6.82, 6 H; isopropyl CH_3). ^{13}C NMR (1:1 THF:C_6D_6, 25°C, 1:30 ligand:THF): δ 178.48 (C–O), 168.22 (CN), 148.84 (C_{ipso}), 140.32 (C_{ortho}), 123.72 (C_{para}), 123.52 (C_{meta}), 96.51 (CH on backbone), 28.60 (Me on CO side), 28.17 (CH on

isopropyl groups), 24.64 (Me on isopropyl group), 24.56 (Me on isopropyl group), 23.09 (Me on CN side).

^{7}Li NMR (1:1 THF:C_6D_6, 25°C): δ –2.14 ppm (line width at ½ height = 3.96 Hz) .

For **2b**: Following the general procedure above: In 9 mL of THF, from 1.005 g (4.624 mmol) of 1b and 3.0 mL (4.800 mmol) of 1.6 M BuLi in hexanes; 0.440 g (31.2% yield, mp: 272-274°C (dec)) of colourless blocks.

^{1}H NMR (C_6D_6, 25°C): δ 6.84 (s, 2H, aromatic tol), 5.02 (s, CH on backbone), 3.57 (m, 5H, THF), 2.20 (s, 3H, para Me on tol), 2.11 (s, 6H, ortho Me on tol), 1.52(s, 3H, Me on backbone), 1.49 (s, 3H, Me on backbone), 1.41 (m, 5H, THF).

^{13}C NMR (1:1 THF:C_6D_6, 25°C, 1:20 ligand:THF): δ 176.13 (C–O), 169.03 (C=N), 147.32 (C_{ipso}), 132.32 (C_{para}), 129.42 (C_{ortho}), 129.12 (C_{meta}), 99.06 (CH on bb), 28.11 (CH_3–CO), 21.82 (para-CH_3), 21.12 (CH_3–CN), 18.32 (ortho-CH_3).

^{7}Li NMR (C_6D_6, 25°C): δ 2.76 ppm (line width at ½ height = 5.60 Hz).

For **2c**: Following the general procedure above: In 10 mL of THF, from 0.930 g (3.401 mmol) and 2.2 mL (3.520 mmol) of 1.6 M BuLi in hexanes; 0.3332 g (13.9% yield, mp: 139-145°C, dec. at 196°C) of colourless blocks.

^{1}H NMR (1:1 THF:C_6D_6, 25°C, 1:26 ligand:THF): δ 7.10 (d, *J* 7.49, 2H, meta CH on Dipp ring), 7.00 (t, *J* 7.49, 1H, para CH on Dipp ring), 3.59 (m, 106 H; THF), 3.11 (sept, *J* 6.86, 2 H; isopropyl CH), 1.85 (s, 3 H; central Me), 1.74 (s, 3 H; Me on C=O), 1.68 (s, 3 H; Me on CNDipp side), 1.63 (m, 106 H; THF), 1.16 (d, *J* 6.86, 6 H; isopropyl CH_3), 1.10 ppm (d, *J* 6.86, 6 H; isopropyl CH_3).

^{13}C NMR (1:1 THF:C_6D_6, 25C, 1:26 ligand:THF): δ 175.21 (C=O), 169.21 (CN), 149.42(C_{ipso}), 140.10 (C_{ortho}), 123.59 (C_{meta}), 123.43 (C_{para}), 98.02 (DippNC(CH_3)**C**(CH_3)C(O)CH_3), 68.13 (THF), 28.21 (CH

on isopropyl groups), 27.97 (Me on CO side), 26.24 (THF), 24.56 (Me on isopropyl group), 24.33 (Me on isopropyl group), 21.73 (Me on CN side), 17.85 (DippNC(CH_3)C(**C**H_3)C(O)CH_3).

^{7}Li NMR (1:1 THF:C_6D_6, 25°C): δ 1.33 ppm (line width at ½ height = 6.38 Hz).

For **4d**: Following the general procedure above: In 10 mL of THF, from 0.706 g (3.052 mmol) of **1d** and 2.0 mL (3.200 mmol) of 1.6 M BuLi in hexanes; all of the THF was removed by vacuum, 4 mL of heptane was added to the solid along with 0.7 mL of dry THF and then the flask was heated to dissolve the solid and placed in the freezer resulting in yellow crystals (mp: 244-250°C, dec.) suitable for an X-ray crystallographic study.

Anal. Calc. for $C_{60}H_{80}N_4O_4Li_4$: C, 75.93; H, 8.49; N, 5.90. Found: C, 75.42; H, 8.39; N, 6.21.

^{1}H NMR (C_6D_6, 25°C): δ = 6.86 (s, 2H, aromatic Mes), 2.21 (s, 3H, para Me on Mes), 2.01 (s, 6H, ortho Me on Mes), 1.92 (s, 3H, Me on backbone), 1.61 (s, 3H, Me on backbone), 1.56 (s, 3H, Me on backbone).

^{13}C NMR (C_6D_6, 25°C): δ 172.69 (C=O), 170.08 (C–N), 147.83 (C_{ipso}), 132.03 (C_{para}), 129.24 (C_{ortho}), 129.07(C_{meta}), 100.64 (MeC(O)**C**(Me)C(Me)NMes), 27.36 (CH_3–CO), 21.35 (para–CH_3), 20.83 (CH_3–CN), 18.25 (ortho-CH_3), 17.85 (CH_3 on backbone).

^{7}Li NMR (C_6D_6, 25°C): δ 1.44 ppm (line width at ½ height = 8.07 Hz).

5.4 Synthesis of Lithium Cubane Complexes in Heptane 4a-c

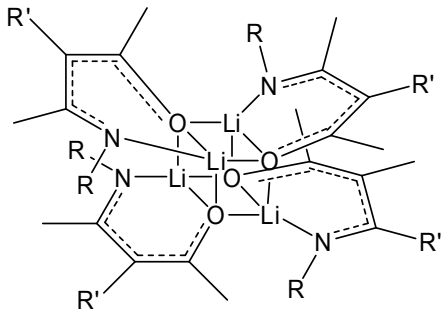

a : R = Dipp, R' = H
b : R = Mes, R' = H
c : R = Dipp, R' = Me

4a-c

General procedure using **4b** as an example: In a Schlenk tube 10 mL of heptane and 0.997 g (4.59 mmol) of **1b** were combined while cooling in an ice bath. To this, 3.0 mL (4.8 mmol) of 1.6 M BuLi in hexanes added via syringe and then heated to 70°C to dissolve. The solvent was removed under reduced pressure and then the solid was dissolved in a minimum amount of boiling toluene and placed in the freezer which resulted in colourless block-like crystals (mp: 245-250°C, dec.) that turned out to be the cubane lithium complex co-crystallized with toluene (1:1) as determined by X-ray crystallography. The NMR data showed that the crystals lost some of the toluene over time to reduce the ratio to 0.4:1. The elemental analysis was performed during the same week as the NMR was performed, therefore the elemental analysis data given is for the 0.4:1 ratio crystal.

Anal. Calc. for $C_{58.8}H_{74.8}N_4O_4Li_4$: C, 75.95; H, 8.15; N, 6.03. Found: C, 76.10; H, 8.04; N, 6.01.

^{1}H NMR (C_6D_6, 25°C): δ 7.16-7.00 (m, 2H, free toluene in crystals), 6.84 (s, 2H, aromatic tol), 5.02 (s, CH on backbone), 2.20 (s, 3H, para Me on tol), 2.11 (s, 6H, ortho Me on tol), 1.52(s, 3H, Me on backbone), 1.49 (s, 3H, Me on backbone).

^{13}C NMR (C_6D_6, 25°C): δ 176.27 (C–O), 169.14 (C–N), 147.41 (C_{ipso}), 138.22 (toluene), 132.35 (C_{para}), 129.66 (toluene), 129.28 (C_{ortho}), 129.11 (C_{meta}), 128.56 (toluene), 126.03 (toluene), 99.20 (**C**H on bb), 28.30 (CH_3–CO), 22.00 (para-CH_3), 21.76 (CH_3 toluene), 21.32 (CH_3–CN), 18.52 (ortho-CH_3).

^{7}Li NMR (C_6D_6, 25°C): δ 2.76 ppm (line width at ½ height = 5.77 Hz).

For **4a**: Following the general procedure above: From 1.01 g (3.89 mmol) of **1a** and 2.5 mL (4.0 mmol) of 1.6 M BuLi in hexanes. The immediately formed white solid would not dissolve in the heptane, even when more than double the heptane was added. The heptane was removed via vacuum and the white solid was dissolved in toluene. Small colourless needles started to come out of solution immediately when taken out of the heat despite increased amounts of toluene. This sample was not characterized further. It is included here because it was mentioned X-ray quality crystals of this sample were not obtained. The complex was not soluble in any non-coordinating NMR solvents that were accessible in the lab.

For **4c**: Following the general procedure above: From 0.508 g (1.858 mmol) of **1c** and 1.2 mL (1.92 mmol) of 1.6 M BuLi in hexanes, heated to 80°C to dissolve. The reaction was then allowed to cool to room temperature which resulted in the formation of white needle-like crystals (mp: 124.8-131.8°C, dec.) suitable for single crystal X-ray diffraction. Due to very low solubility of this lithium complex in non-coordinating solvents, in comparison with the free ketoimine ligand, the ^{1}H and ^{13}C NMR spectra of the lithium complex showed very minor peaks in the spectra attempted, and therefore was not assigned.

5.5 Synthesis of the Magnesium complex of 3b

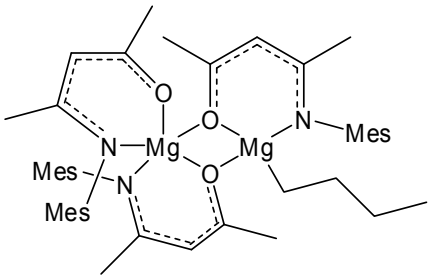

3b

In a Schlenk tube 12.5 mL of dry heptane and 0.317 g (1.459 mmol) of **1b** were combined while cooling in an ice/salt bath. To this, 0.8 mL (0.8 mmol) of 1.0 M dibutylmagnesium in heptane was added via syringe. After completion of the addition, the reaction was allowed to warm to room temperature and stirred for a further hour. The heptane was removed by vacuum until solid started coming out of solution and then the remaining heptane was heated up until the solid redissolved. This was placed in the freezer where X-ray quality crystals grew of **3b**. Characterization other than the X-ray crystal structure was not obtained because the crystals decomposed in the Schlenk tube in the freezer before any other data could be collected on them.

5.6 Synthesis of Alkynyl Diimines 5a,b

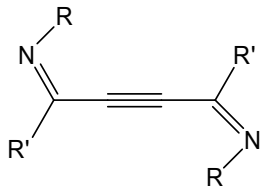

5a : R = Ph, R' = t-Bu
5b : R = Dipp, R' = p-Tol

General procedure using **5a** as an example: In a 100 mL 3-necked flask 2.6 g (9.7 mmol) of 18 wt/wt % sodium acetylide slurry in xylenes and 10 mL of THF were combined. 1.003 g (5.125 mmol) of N-phenyl-tert-butyl imidoyl chloride in 20 mL of THF was added dropwise and then the reaction mixture was heated to reflux. After refluxing for 2 days the mixture was diluted with 50 mL of pentane, filtered, and then the solvent was removed under reduced pressure using a rotovap. The crude product was then purified by column chromatography using chloroform as the eluent, and recrystallized from hexanes resulting in 0.270 g (15.3% yield, mp: 136-140°C) of neon yellow block X-ray quality crystals from which the X-ray data was collected.

Anal. Calc. for $C_{24}H_{28}N$: C, 83.68; H, 8.19; N, 8.13. Found: C, 83.33; H, 7.95; N, 8.13.

^{1}H NMR ($CDCl_3$, 25°C): δ 7.31 – 7.25 (t, *J* 7.50, 2 H; meta-phenyl), 7.08 (t, *J* 7.50, 1H; para-phenyl), 6.72 (d, 2H; ortho-phenyl), 0.991 (s, 9H; tert-butyl).

^{13}C NMR ($CDCl_3$, 25°C): δ 162.06 (C=N), 152.12 (ipso-Ph), 128.88 (ortho or meta-Ph), 124.46 (para-Ph), 119.70 (ortho or meta-Ph), 88.70 (C≡C), 40.13 (**C**(CH3)3), 27.42 (C(**C**H3)3) ppm.

MS m/z: 344 (M+, 40.69%), 287 (M–tBu, 62.52%), 227 ([C≡CC(tBu)NPh + MeCH(Me)]$^+$, 32.05%), 184 (tbuC=NPh(C≡C)+, 100%), 160 (tbuC=NPh+, 37.72%), 118 (PhNC$^+$CH$_3$, 27.41%), 104 (PhN=CH$^+$, 58.72%), 77 (Ph+, 66.55%), 57 (tbu+, 10.31%).

IR(neat) cm^{-1}: 2987 (w), 2966 (m), 2929 (w), 2865 (w), 1600 (s), 1481 (m), 1457 (m), 1391 (m), 1363 (m), 1237 (w), 1202 (m), 1157 (s), 1067 (w), 1026 (w), 915 (m), 879 (m), 829 (m), 790 (m), 741 (vs), 692 (vs), 515 (m), 478 (w), 454 (w).

For **5b**: 1. In a 250 mL flask, to 2.00 g (7.50 mmol) of 18 wt/wt % sodium acetylide slurry in xylenes and 15 mL of THF, 1.529 g (4.87 mmol) of N-dipp-tolyl imidoyl chloride in 30 mL THF was added dropwise over 10 minutes and then refluxed for 4 days. After purification by column chromatography and recrystallization, 0.145 g (5.13% yield, mp: 252 - 255°C) of bright yellow X-ray quality crystals were obtained.

2. In a 250 mL flask, to 0.60 g (6.52 mmol) of lithium acetylide ethylenediamine complex (90%) and 20 mL of THF, 2.01 g (6.40 mmol) of N-dipp-tolyl imidoyl chloride in 40 mL of THF was added drop wise over 15 minutes while cooling the reaction in an ice/salt bath. The reaction mixture was stirred with cooling for an hour and then allowed to warm to room temperature and stir overnight. After purification by column chromatography, 0.857 g (23.1% yield, mp: 252 - 256°C) of bright yellow powder was obtained.

^{1}H NMR ($CDCl_3$, 25°C): δ 7.31 – 7.05 (m, 7 H; aromatic dipp and tol), 2.71 (septet, *J* 6.82, 2 H; dipp isopropyl CH), 2.40 (s, 3 H; tol CH_3), 1.11 (d, *J* 6.90, 6 H; isopropyl CH_3), 1.03 (d, *J* 6.90, 6 H; isopropyl CH_3).

^{13}C NMR ($CDCl_3$, 25°C): δ 151.32 (C=N), 148.60 (ipso dipp), 142.07 (para tol), 136.96 (ortho dipp), 133.03 (ipso tol), 129.44 (meta tol), 128.37 (ortho tol), 124.54 (para dipp), 123.46 (meta dipp), 87.69 or 77.44 (alkyne carbons), 28.56 (CH of isopropyl), 23.53 (isopropyl methyl), 23.36 (isopropyl methyl), 21.78 (tol methyl).

MS m/z: 580 (M+, 39%), 565 (M–Me, 100%), 537 (M–iPr, 40%), 302 (DippNCTol(C≡C)+, 20%), 278 (DippNCTol+, 40%), 160 (Dipp–H, 12%), 77 (Ph^+, 12%).

IR(neat) cm^{-1}: 2956 (m), 2924 (w), 2865 (w), 1608 (w), 1582 (s), 1561 (s), 1506 (w), 1458 (m), 1436 (m), 1406 (m), 1382 (m), 1361 (w), 1326 (m), 1309 (s), 1291 (vs), 1267 (m), 1192 (m), 1175 (m), 1111 (m), 1081 (m), 1059 (m), 1041 (w), 1015 (m), 924 (m), 850 (m), 826 (vs), 794 (m), 779 (vs), 732 (vs), 721 (s), 670 (s), 534 (m), 483 (m), 439 (m), 424 (m).

5.7 Synthesis of Silylated Alkyne 6b

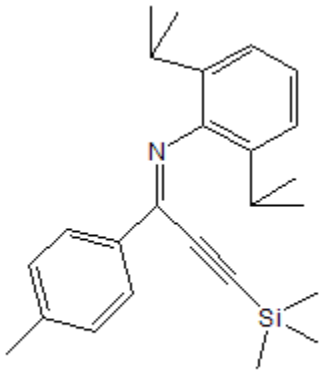

6b

Placed 1.06 g (3.38 mmol) of N-2,6-diisopropylphenyl-tolylimidoyl chloride and 0.575 g (3.37 mmol) of bis-trimethylsilylacetylene were placed in a 100 mL 3-necked flask and 10 mL of methylene chloride was added. While cooling this solution in an ice bath, 0.668 g (5.01 mmol) of $AlCl_3$ was added to the mix. The reaction mixture was then left to warm to room temperature and stir overnight. The reaction was then quenched with 3 mL of concentrated HCl diluted with ice. The organic layer was then washed with concentrated ammonium chloride and dried over $MgSO_4$. After purification by column chromatography (1:1 Hexanes:CH_2Cl_2) and recrystallization in hexanes, 0.346 g (27.2% yield, mp: 91–99°C) of yellow prism X-ray quality crystals were collected.

Anal. Calc. for $C_{25}H_{33}NSi$: C, 79.94; H, 8.85; N, 3.73. Found: C, 79.91; H, 8.56; N, 3.76.

^1H NMR ($CDCl_3$, 25°C): δ 8.11 (d, *J* 8.16, 2 H; ortho aromatic H on tol), 7.30 (d, *J* 8.22, 2 H; meta aromatic H on tol), 7.14 – 7.07 (m, 3 H; aromatic H on dipp), 2.79 (septet, *J* 6.85, 2 H; CH of isopropyl), 2.44 (s, 3 H; methyl on tol), 1.15 (d, *J* 6.81, 6 H; isopropyl methyl), 1.13 (d, *J* 6.75, 6 H; isopropyl methyl), –0.02 (s, 9 H; Me on TMS).

^{13}C NMR ($CDCl_3$, 25°C): δ 151.97 (C=N), 148.78 (ipso dipp), 141.88 (ipso tol), 136.59 (ortho dipp), 133.94 (para tol), 129.35 (meta tol), 128.27 (ortho tol), 123.95 (para dipp), 122.93 (meta dipp), 105.15 (C**C**–TMS), 98.15 (**C**C–TMS), 28.46 (CH of isopropyl), 23.78 (Me of isopropyl), 23.48 (Me of isopropyl), 21.75 (Me on tol), –0.56 ($SiCH_3$).

MS m/z: 376 (MH+, 44%), 375 (M+, 23%), 360 (M–Me, 100%), 332 (M–iPr, 13%), 302 (M–TMS, 25%), 288 ([M–iPr]–iPr, 20%), 174 (NDipp–H, 12%).

IR(neat) cm^{-1}: 2656 (m), 2925 (w), 2867 (w), 1584 (m), 1561 (m), 1459 (w), 1438 (w), 1311 (w), 1286 (m), 1246 (m), 1179 (m), 1103 (w), 1048 (m), 1017 (w), 861 (s), 842 (vs), 824 (vs), 781 (m), 760 (s), 736 (s), 723 (m), 676 (w), 643 (w), 484 (w), 427 (w).

5.8 Synthesis of Desilylated Alkyne 7b

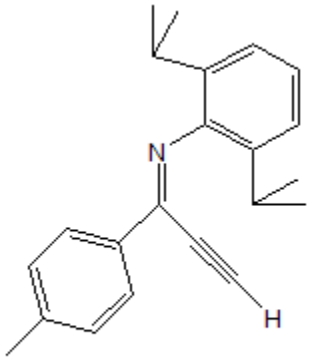

7b

0.534 g (1.42 mmol) of **6b** was placed in a 100 mL flask along with 20 mL of methanol and 20 mL of THF (not dry) and 0.102 g (0.738 mmol) of ground up anhydrous potassium carbonate was added while stirring. Further small amounts of potassium carbonate were added until the reaction was complete as judged by TLC (monitored daily). Once the reaction was complete, 75 mL of slightly diluted saturated ammonium chloride solution and 75 mL of ether were added and mixed. The organic layer was washed 3 times with 100 mL of water and dried over magnesium sulfate. The solvent was removed via reduced pressure on the rotovap resulting in 0.370 g (86% yield, mp: 107–118°C) of a bright yellow crystalline solid.

^{1}H NMR ($CDCl_3$, 25°C): δ 8.13 (d, *J* 8.19, 2 H; ortho aromatic H on tol), 7.30 (d, *J* 8.01, 2 H; meta aromatic H on tol), 7.18 – 7.07 (m, 3 H; aromatic H on dipp), 3.22 (s, 1 H; CH of alkyne), 2.80 (septet, *J* 6.86, 2 H; CH of isopropyl), 2.44 (s, 3 H; methyl on tol), 1.17 (d, *J* 6.87, 6 H; isopropyl methyl), 1.13 (d, *J* 6.84, 6 H; isopropyl methyl).

^{13}C NMR ($CDCl_3$, 25°C): δ 150.80 (C=N), 148.01 (ipso dipp), 142.14 (ipso tol), 136.69 (ortho dipp), 133.96 (para tol), 129.43 (meta tol), 128.24 (ortho tol), 124.27 (para dipp), 123.06 (meta dipp), 85.54

(CH of alkyne), 77.44 (**C**CH of alkyne), 28.50 (CH of isopropyl), 23.54 (Me of isopropyl), 23.38 (Me of isopropyl), 21.74 (Me of tol).

MS m/z: 303 (M+, 10%), 288 (M–Me, 100%), 272 (M–2Me, 41%), 260 (M–iPr, 20%), 174 (Ndipp–H, 24%).

IR(neat) cm^{-1}: 3264 (m), 3254 (m), 2960 (s), 2925 (m), 2867 (m), 2094 (w), 1586 (s), 1561 (s), 1508 (w), 1459 (m), 1438 (m), 1408 (w), 1382 (m), 1362 (m), 1330 (m), 1308 (m), 1277 (s), 1239 (m), 1175 (s), 1101 (m), 1042 (m), 1012 (s), 936 (w), 827 (vs), 774 (vs), 722 (s), 706 (m), 692 (vs), 662 (vs), 434 (m), 424 (m).

References

1. N-dipp-p-tolylimidoyl chloride (N-phenyl-t-butylimidoyl chloride made similarly with substitution of PCl_5 instead of $SOCl_2$): Boeré, R.T.; Klassen, V.; Wolmershauser, G. *J. Chem. Soc, Dalton Trans.* **1998**, 4147.

2. Boeré, R.T.; Bond, A.M.; Chivers, T.; Feldberg, S. W.; Roemmele, T. L. *Inorg. Chem.* **2007**, *46*, 5596-5607.

3. Vitanova, D.V.; Hampel, F.; Hultzsch, K.C. *J. Organomet. Chem.* **2005,** *690,* 5182.

Appendix A
MO's of alkynyl imines and diimines

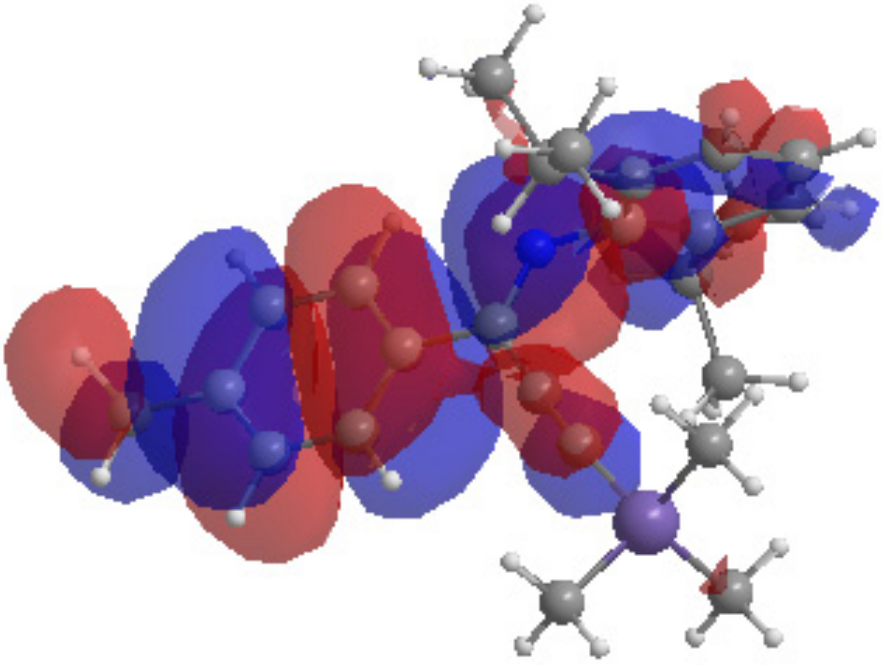

Figure A1 – HOMO-2 for 6b.

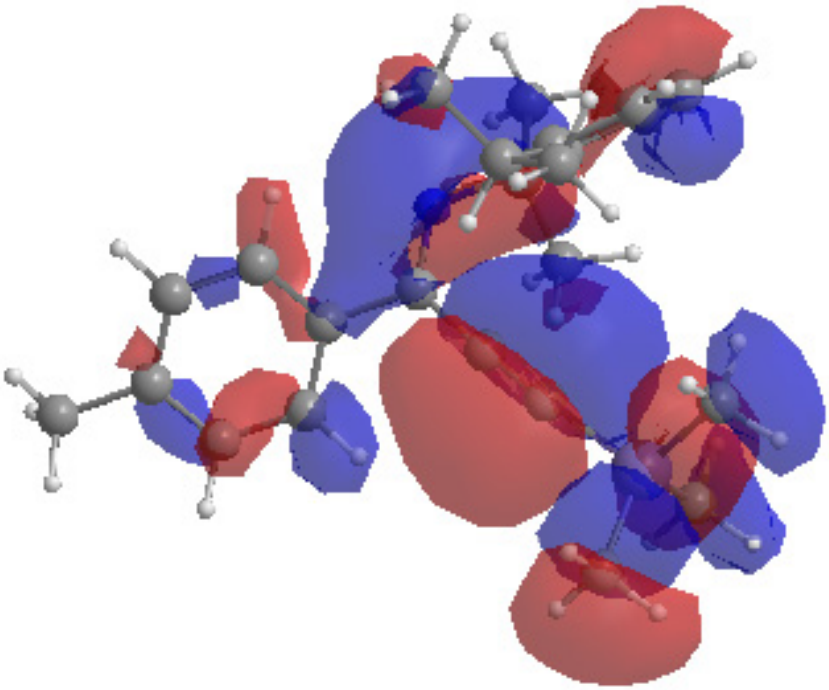

Figure A2 – HOMO-5 for 6b.

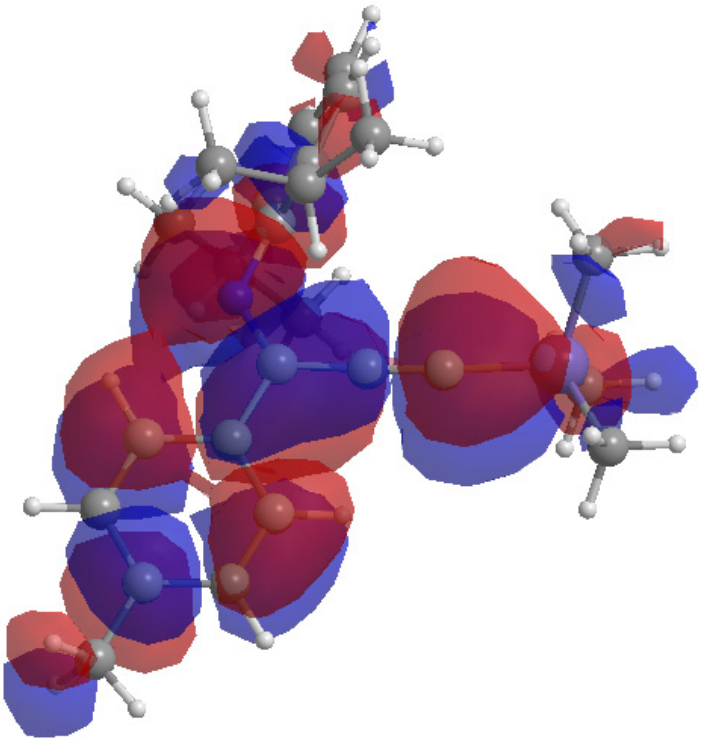

Figure A3 – LUMO of 6b.

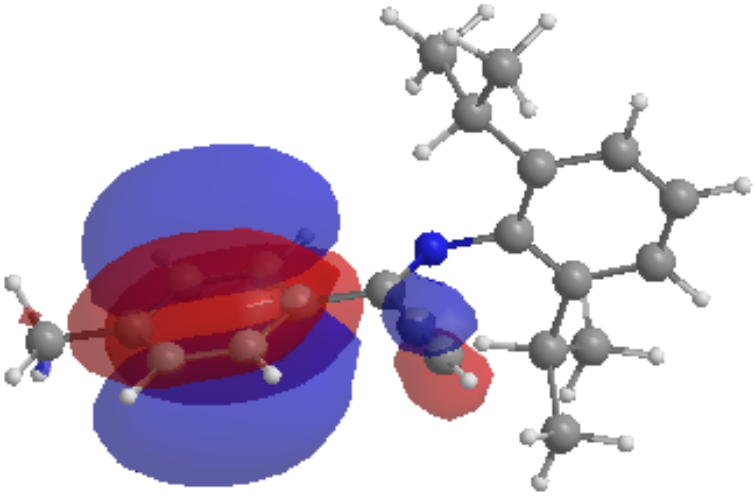

Figure A4 – HOMO-3 for 7b.

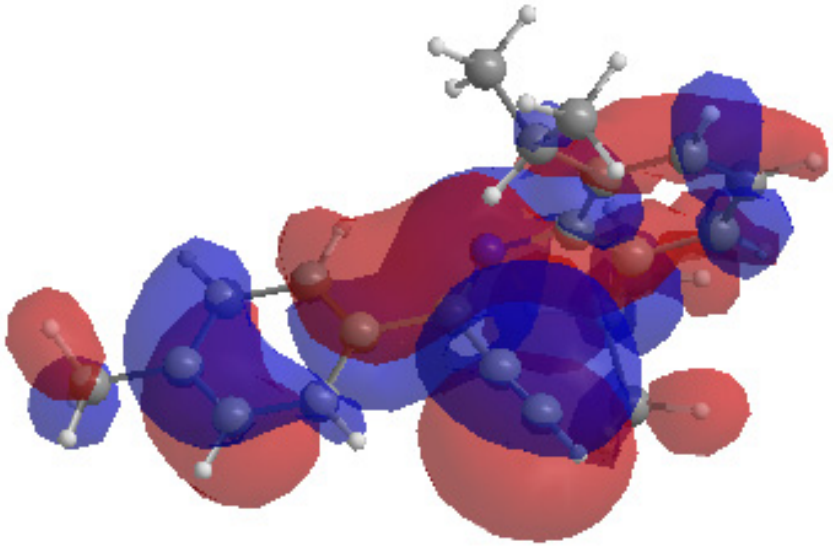

Figure A5 – HOMO-4 for 7b.

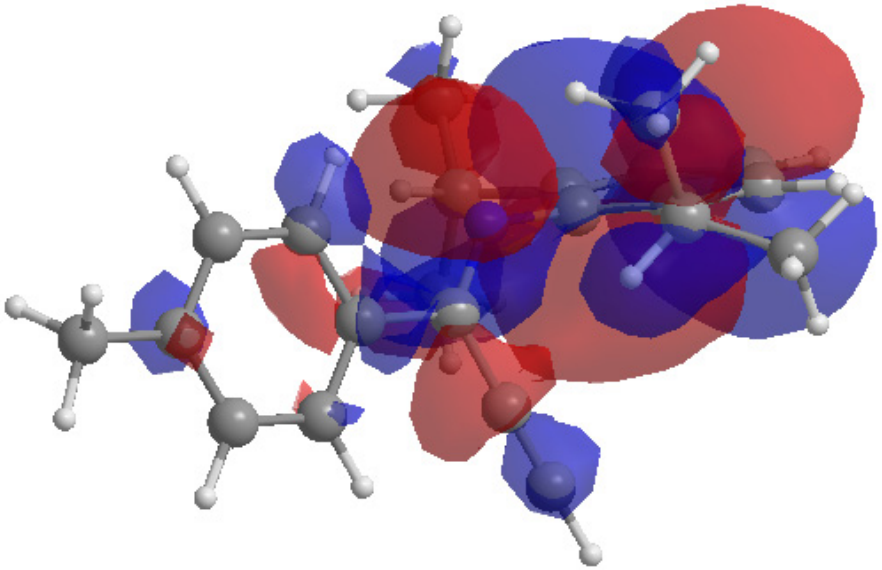

Figure A6 – LUMO for 7b.

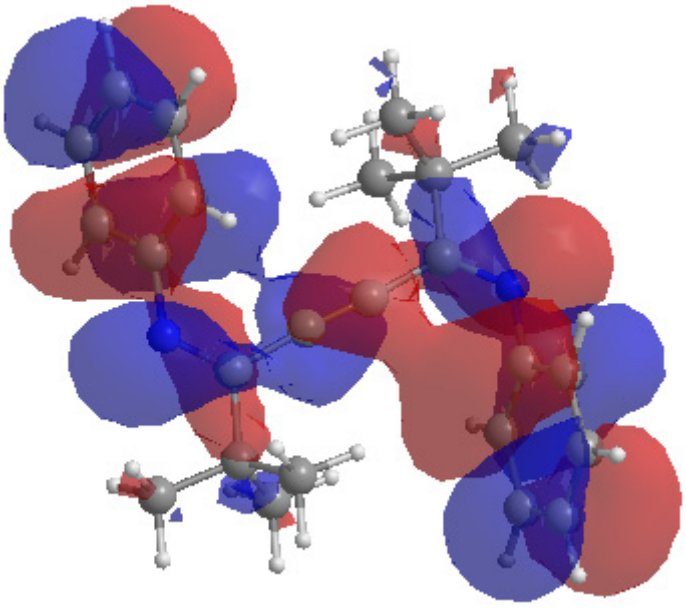

Figure A7 – HOMO for 5a.

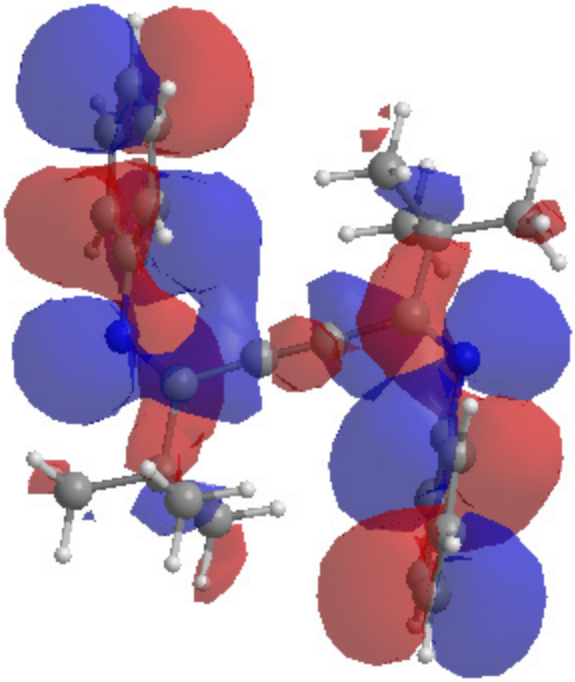

Figure A8 – HOMO-1 for 5a.

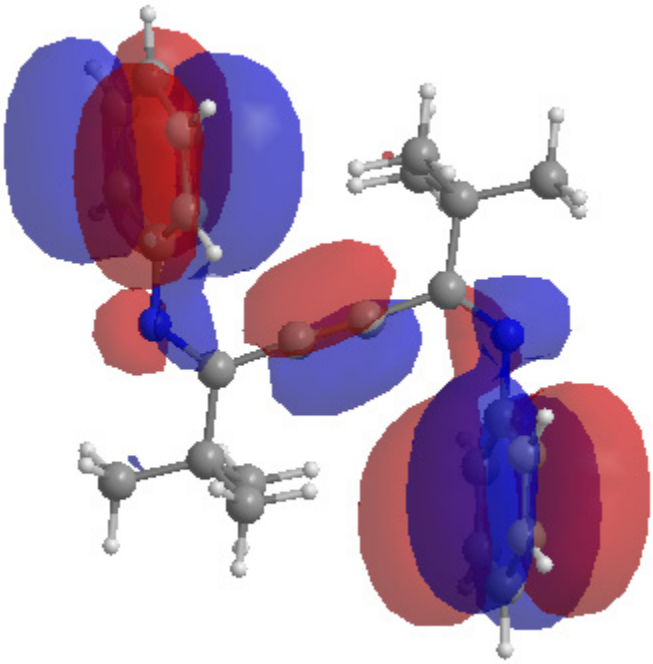

Figure A9 – HOMO-2 for 5a.

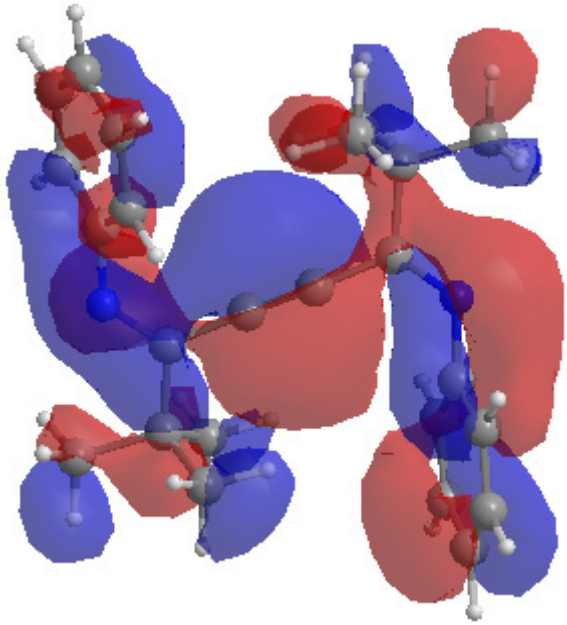

Figure A10 – HOMO-5 for 5a.

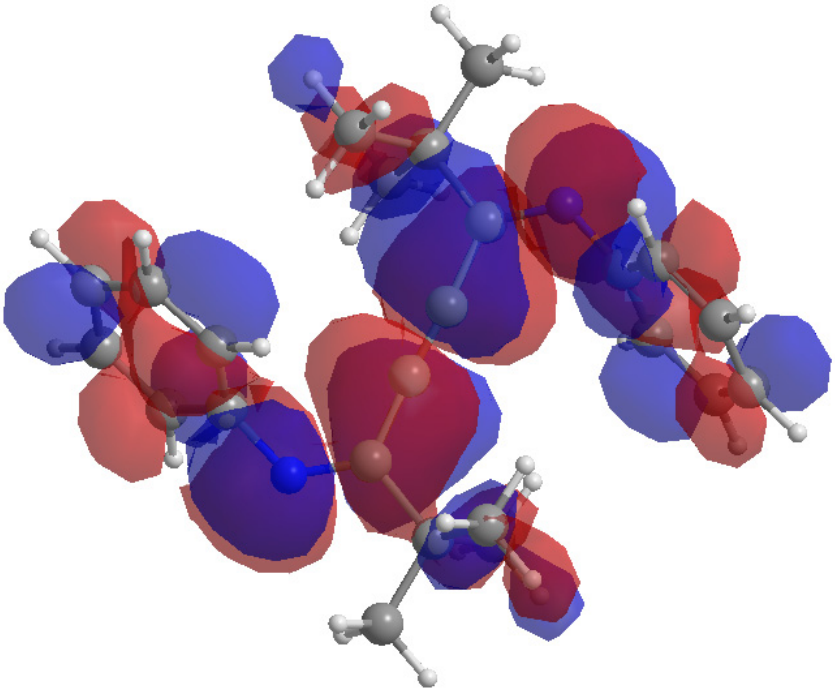

Figure A11 – LUMO for 5a.

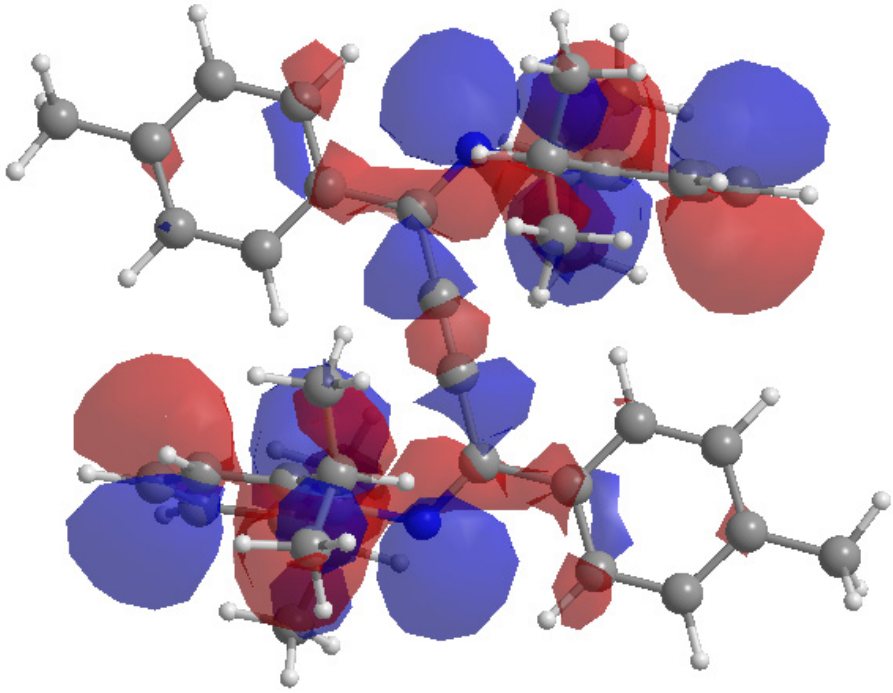

Figure A12 – HOMO for 5b.

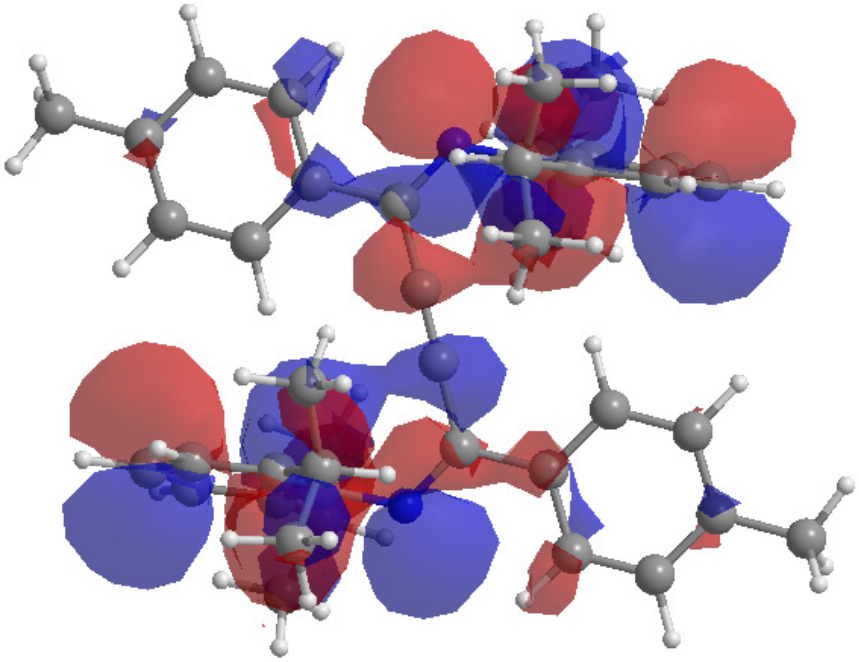

Figure A13 – HOMO-1 for 5b.

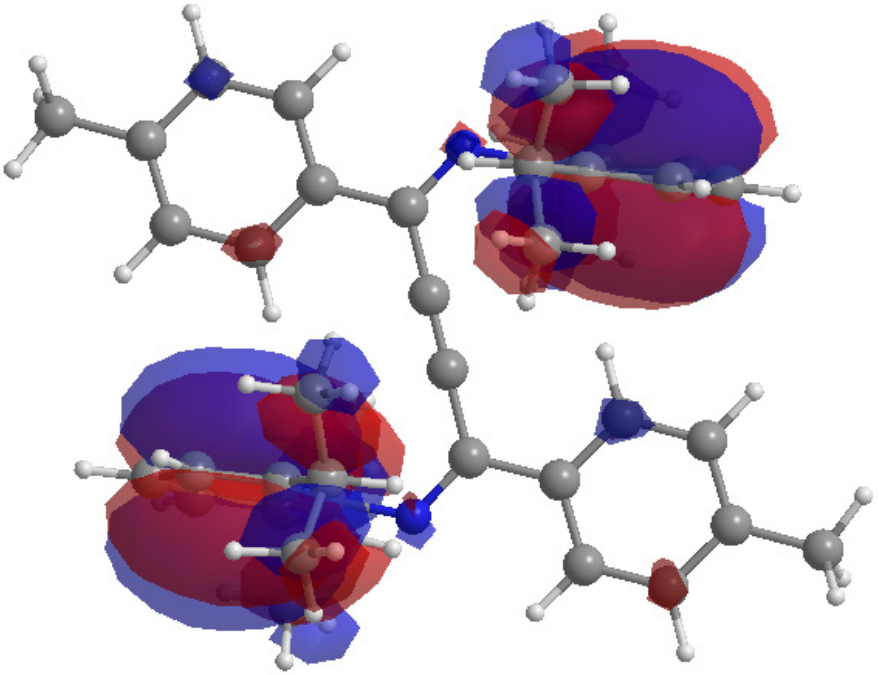

Figure A14 – HOMO-3 for 5b.

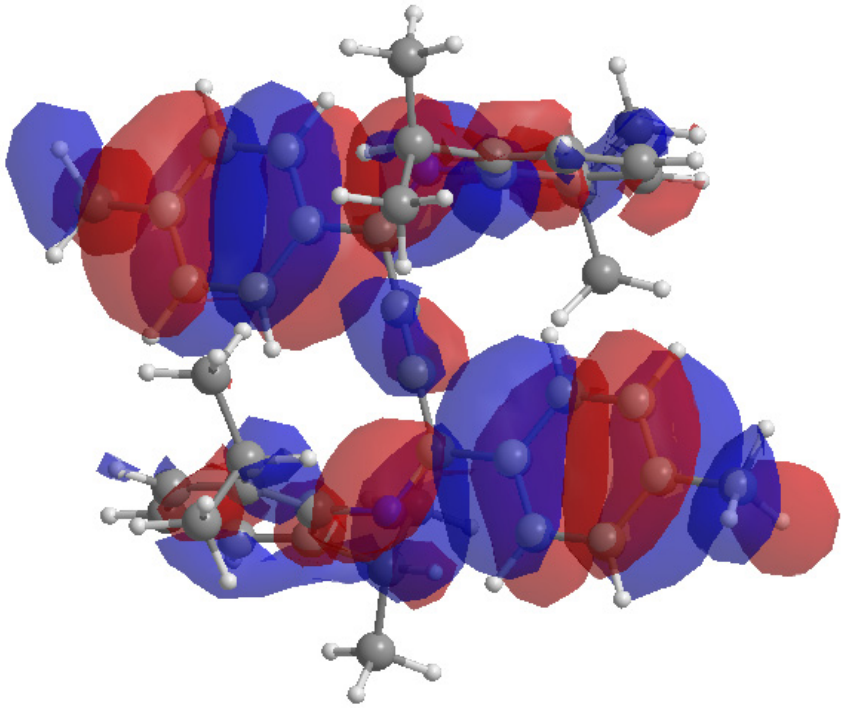

Figure A15 – HOMO-4 for 5b.

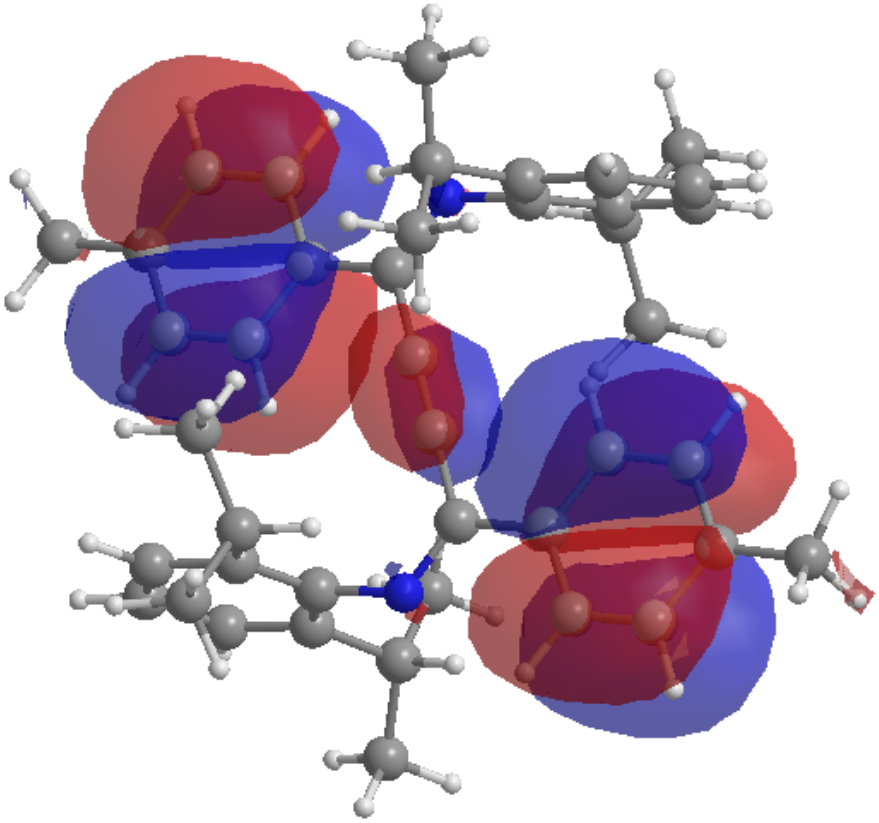

Figure A16 – HOMO-6 for 5b.

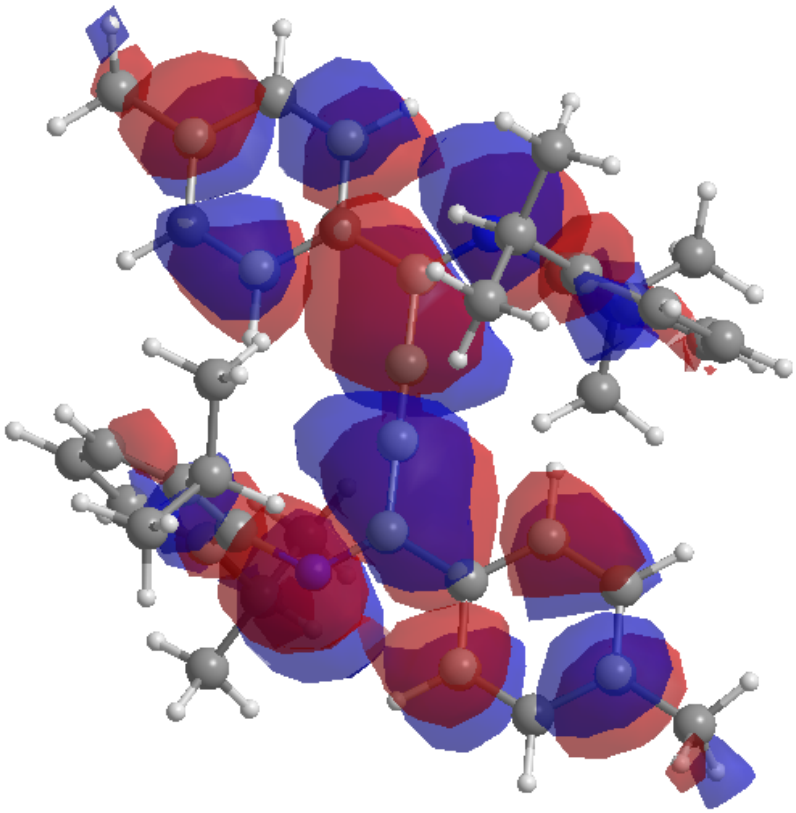

Figure A17 – LUMO for 5b.

Appendix B
2D NMR of 1d and 2c

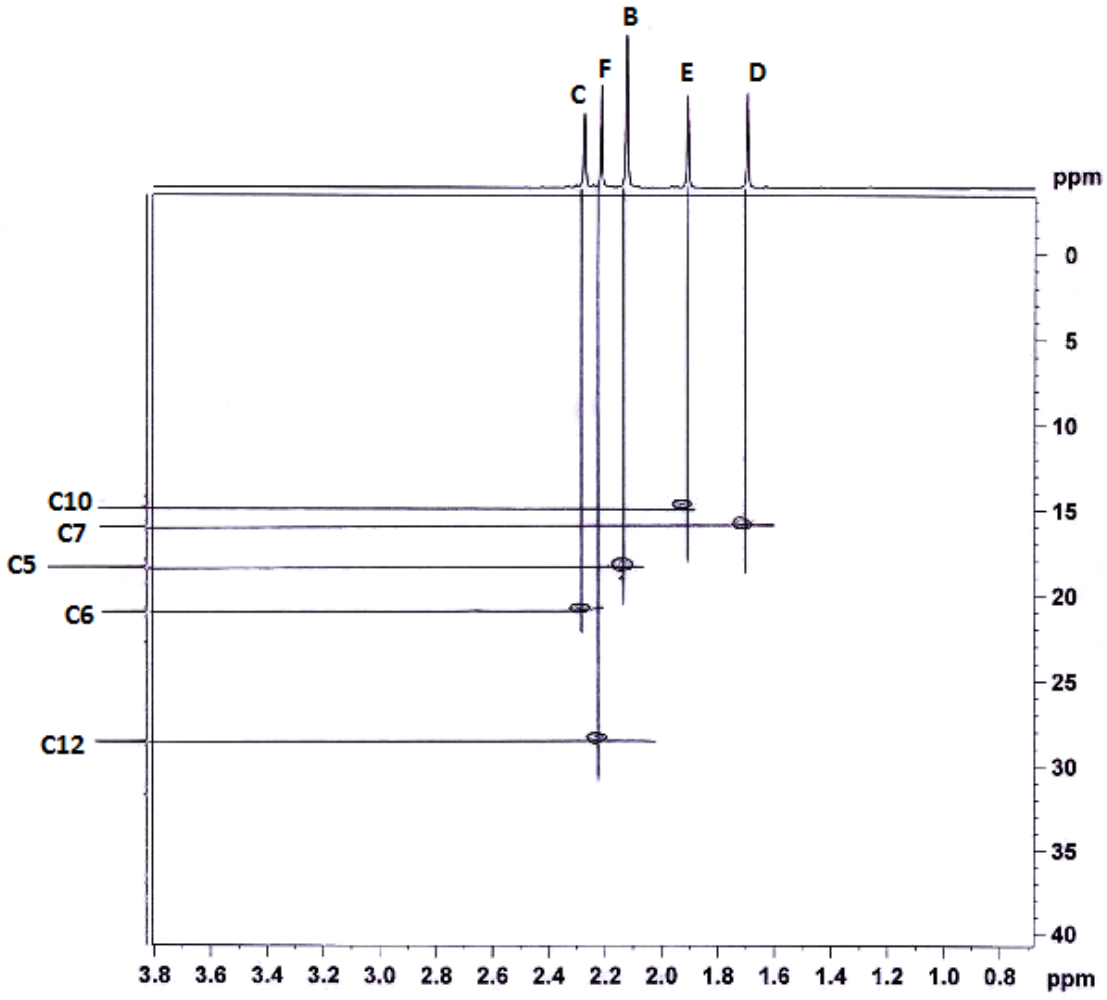

Figure B1 – Portion of the HSQC for 1d. Labeling scheme is found on page 128.

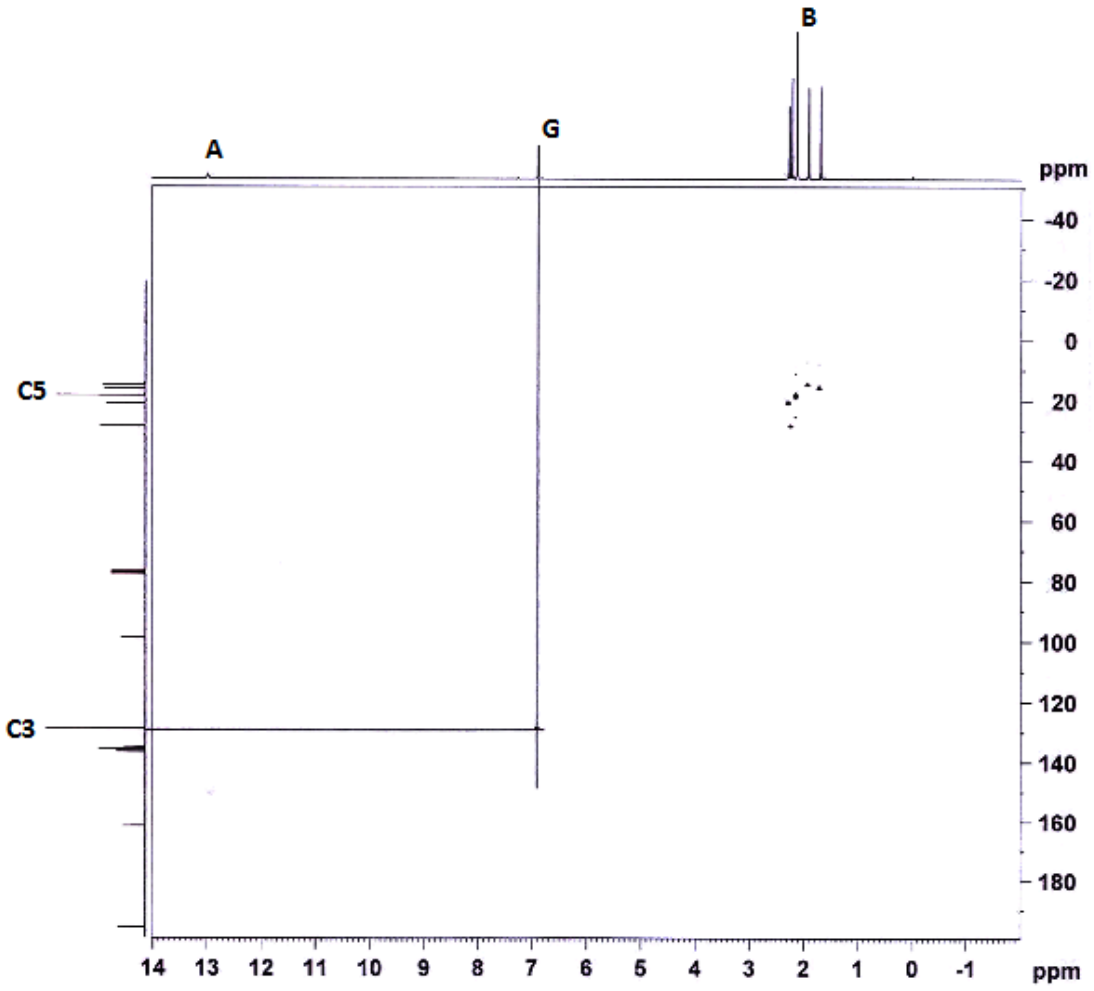

Figure B2 – Full HSQC of 1d. Labeling scheme is below.

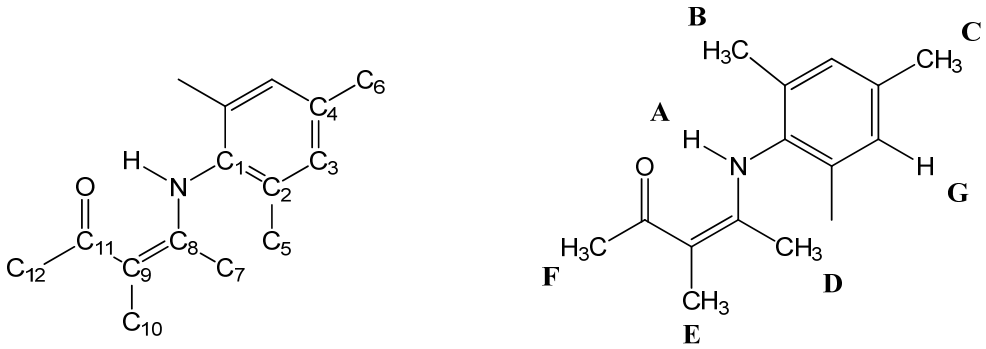

Figure B3 – Labelling scheme for 2d NMR spectra for 1d.

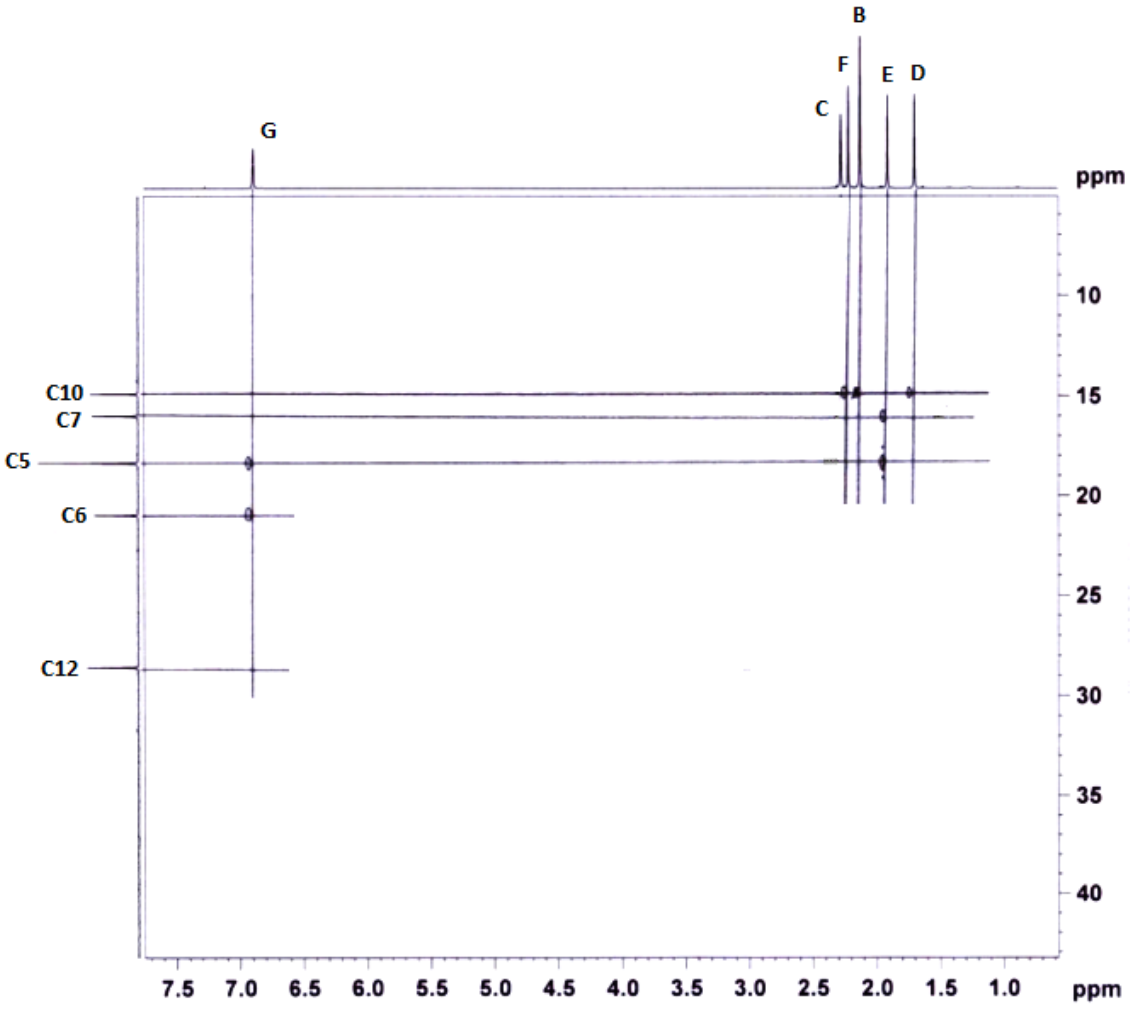

Figure B4 - Portion of HMBC of 1d. Labeling scheme is on page 128.

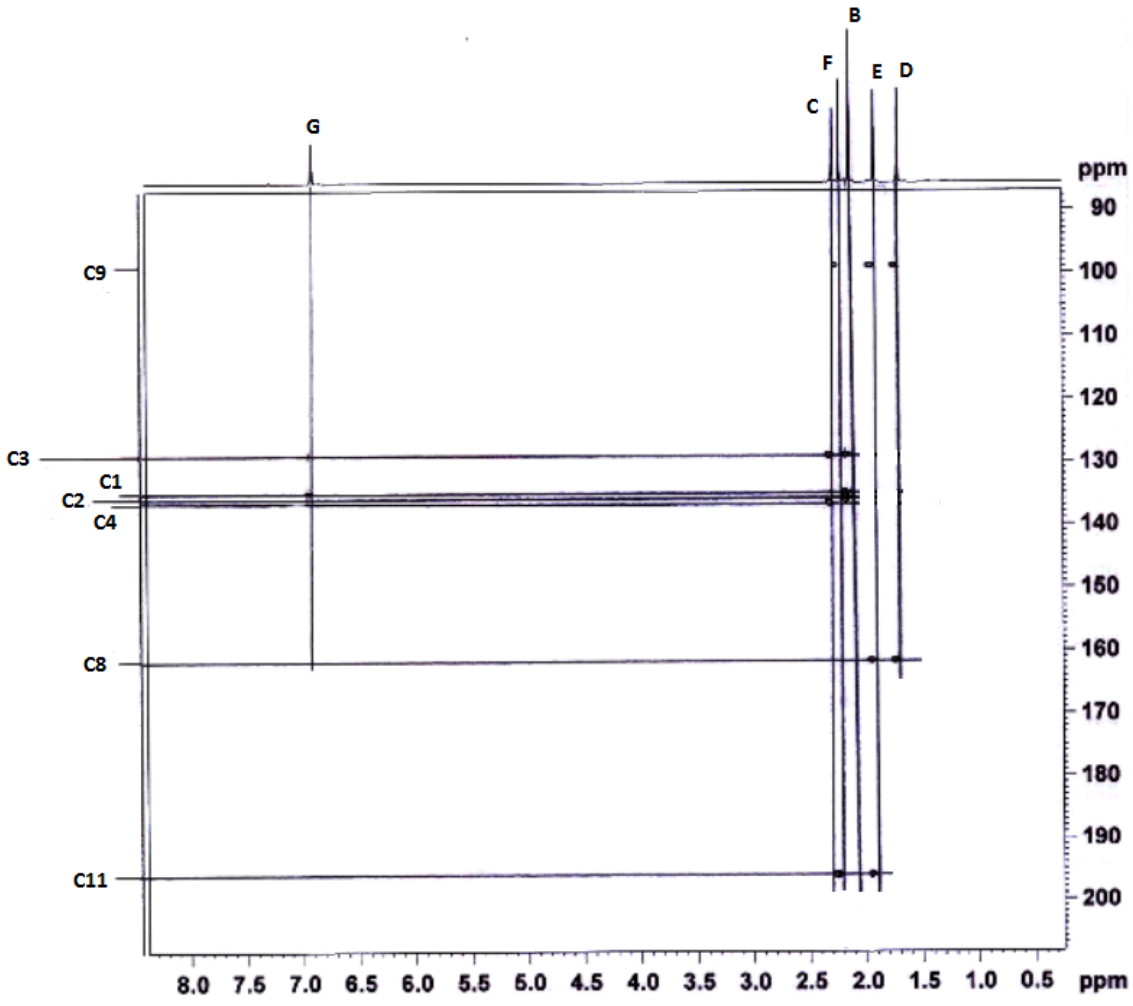

Figure B5 - Second portion of HMBC for 1d. Labeling scheme is on page 128.

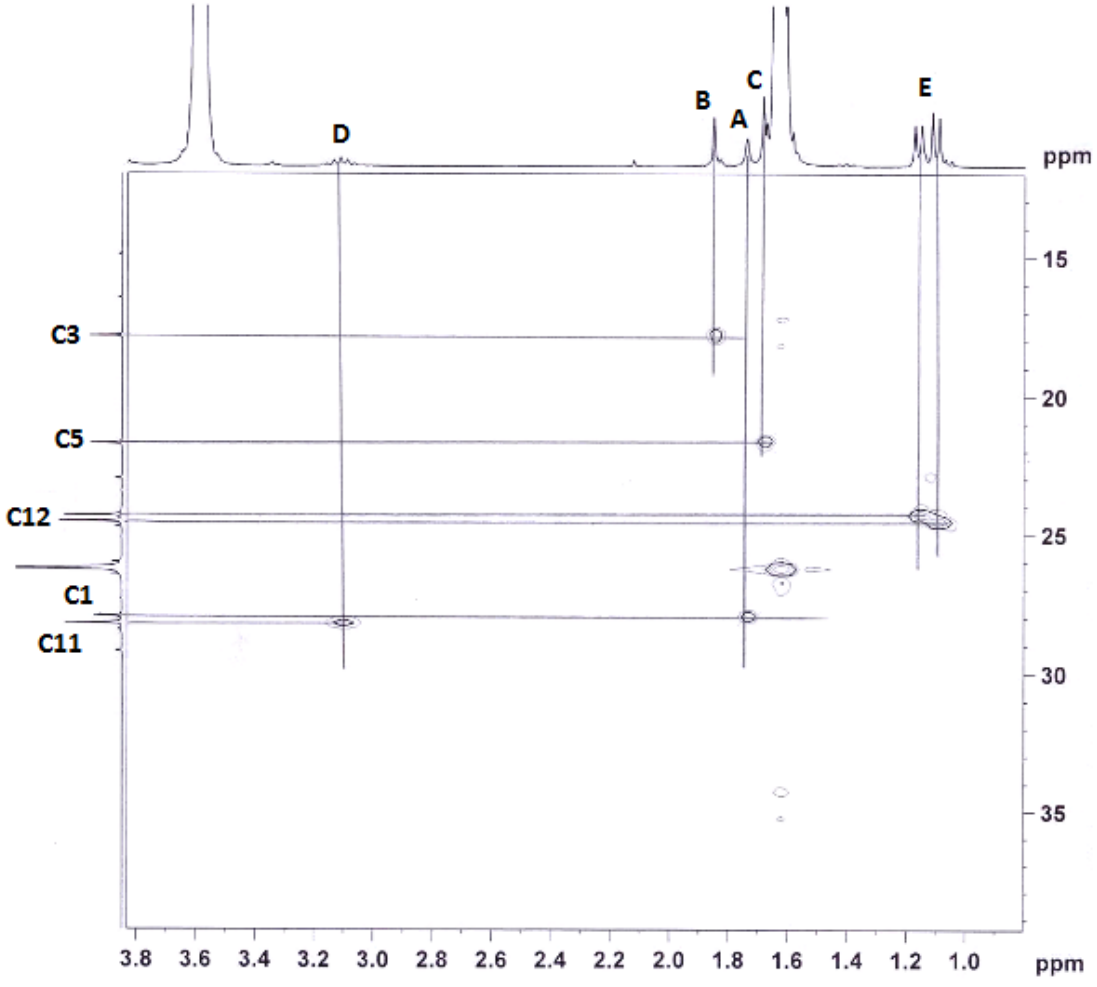

Figure B6 – Portion of the HSQC of 2c. Labeling scheme is below.

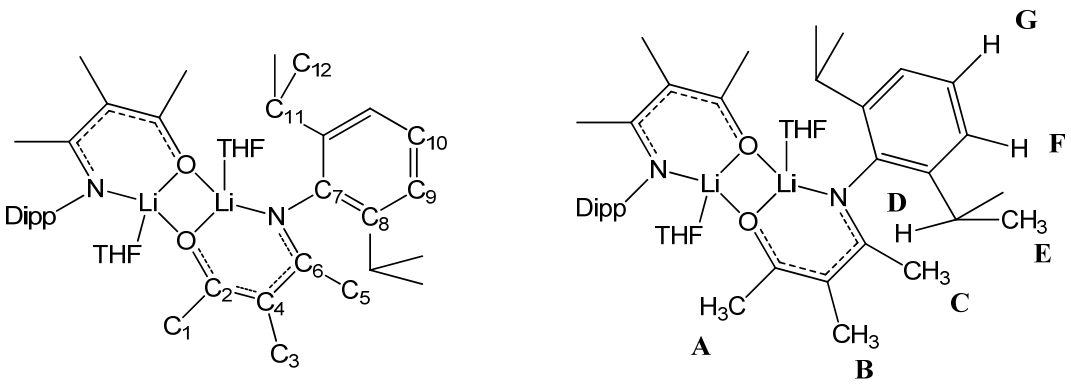

Figure B7 – Labeling scheme for the 2d NMR spectra of 2c.

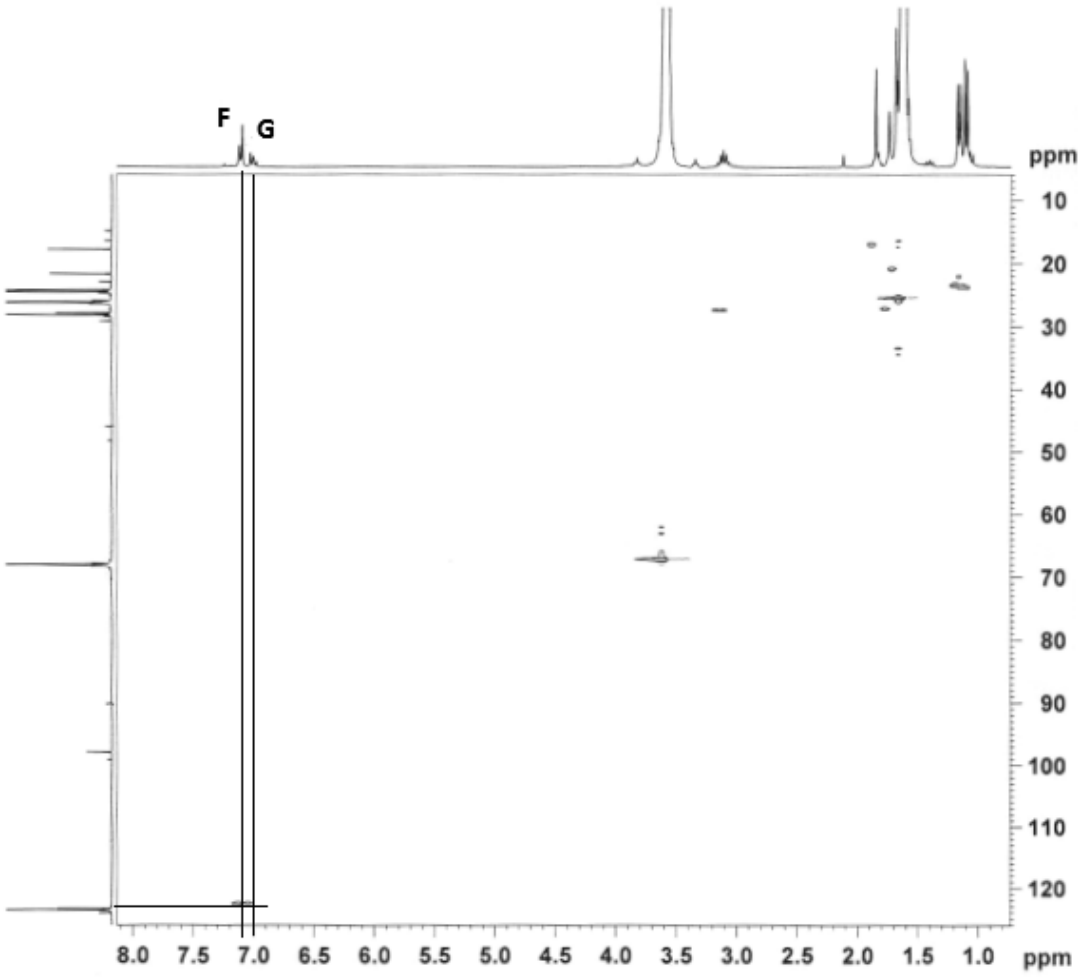

Figure B8 – Full HSQC of 2c. Labeling scheme is on page 131.

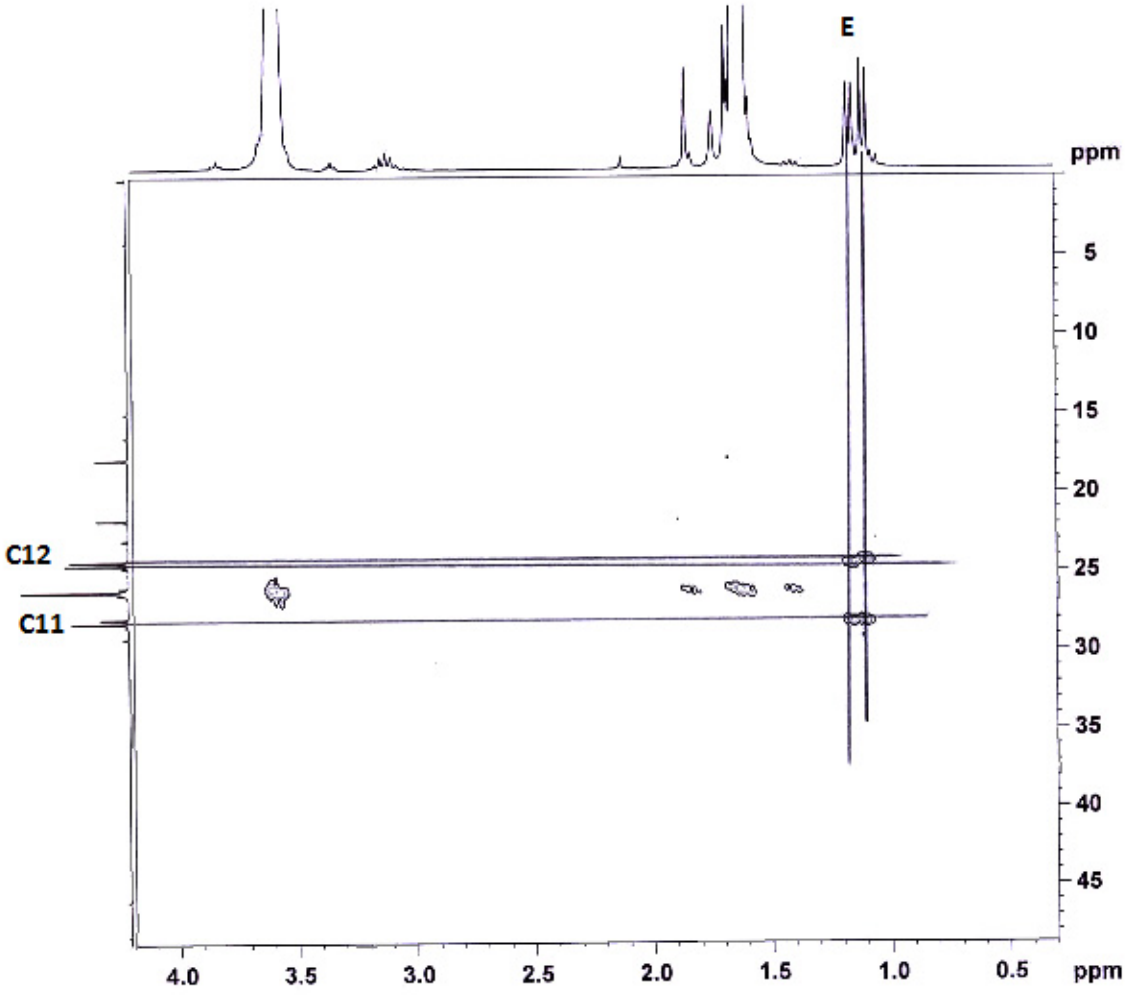

Figure B9 – Portion of the HMBC of 2c. Labeling scheme is on page 131.

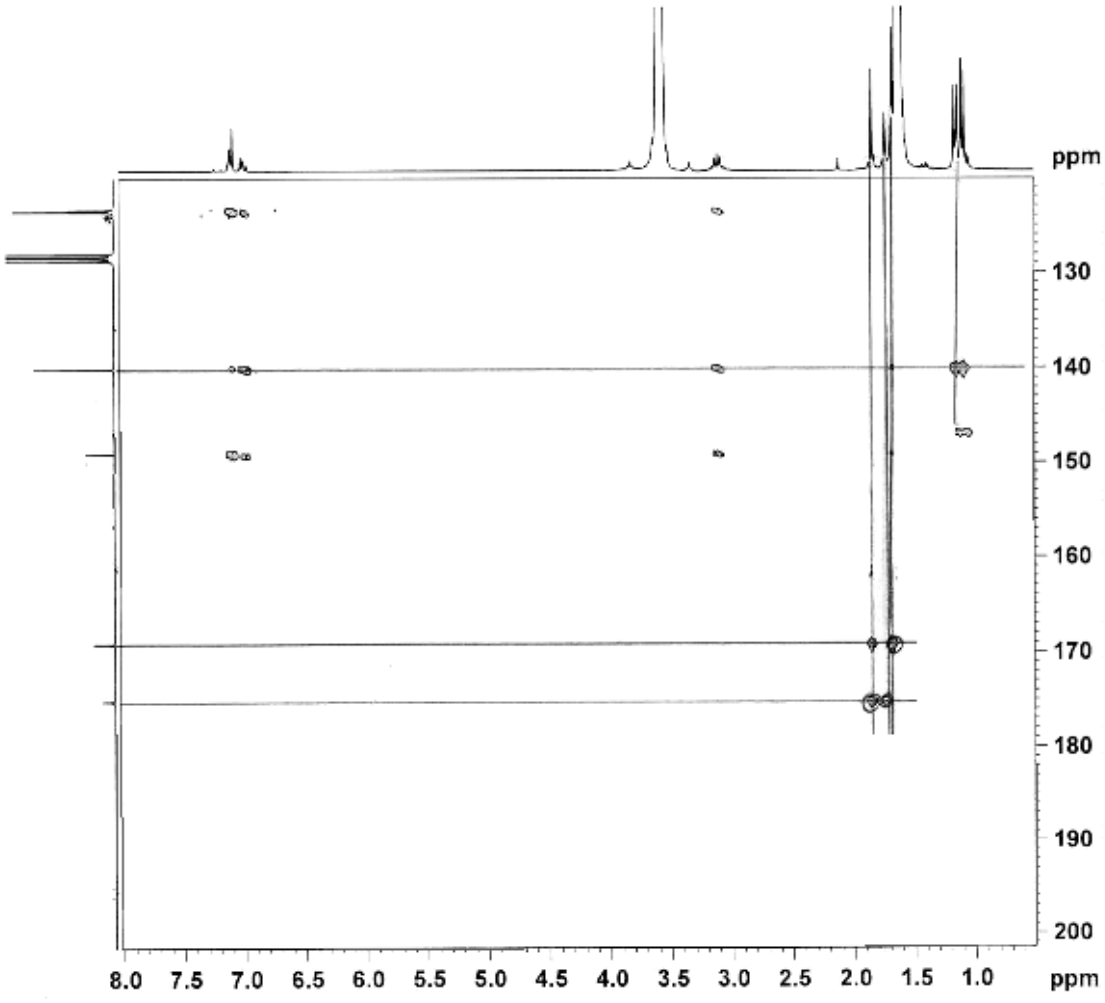

Figure B10 – Second portion of HMBC for 2c. Labeling scheme is on page 131.